INVESTIGATION OF THE IGNITION AND BURNING OF MATERIALS IN SPACE CABIN ATMOSPHERES

PART I: IGNITION AND BURNING OF MATERIAL

H. G. LEW

FINAL REPORT - MARCH 1972
NASA CONTRACT NO. NASW-1874

ESL ENVIRONMENTAL SCIENCES LABORATORY

GENERAL ELECTRIC
Re-entry & Environmental Systems Division

GE TIS 72SD2061

INVESTIGATION OF THE IGNITION AND BURNING OF MATERIALS IN SPACE CABIN ATMOSPHERES

FINAL REPORT - MARCH 1972

PART I: IGNITION AND BURNING OF MATERIAL

NASA Contract No. NASW-1874

Submitted by:

H. G. LEW

Environmental Sciences Laboratory
General Electric Company
Valley Forge Space Technology Center
P.O. Box 8555
Philadelphia, Pennsylvania 19101

TABLE OF CONTENTS

SUMMARY

An analytical study of the theory of ignition and burning of a plastic material immersed in an atmosphere of a space cabin which may be subjected to gravity force changes is considered in this report. The interest is in evaluating the hazardous condition in a space cabin environment where the changes of gravity may affect the combustion process. The model considered the analysis of the coupled gas and solid phases and is based on the premise that material heating leads to the formation of pyrolysis gases from the decomposed solid which then react with the ambient oxidizer to further the combustion process. Moreover, free convection plays a dominant role in transporting these hot gases to the virgin material. A time-dependent study of the coupled gas-solid model as required for ignition processes with emphasis on the surface energy interchange of the gas and solid phases has been made. Detailed distribution of species composition and temperature patterns provide a spatial and time map of the evolving gases from the material combustion.

The numerical method of finite differences has been applied to the analysis. Results have been obtained detailing the importance of the surface energy interchange and giving the dependence of ignition time on gravity and the environmental factors such as pressure and atmosphere composition. The times required for the ignition to spread along the material surfaces by gravity effects have been obtained and are consistent with experiments.

I. INTRODUCTION

Combustible materials exposed to heat ignite when there is a sufficient increase of thermal energy due to exothermic chemical reactions over the energy losses of the system. Upon ignition, a nucleus of a flame appears accompanied by the emission of heat, light, and hot gases. The hot combustion products generated continue the chain reaction and the flame is propagated with finite velocity to the unburnt material. The ignition of the material depends on the environmental conditions and to a large extent on the interaction of the gas phase reactions and their products and with the condensed phase if one is present. The latter affect the conditions which may enhance the flame propagation or extinguishment. It would be useful in considering the elimination of fire hazards in space cabins to be able to predict the critical conditions of ignition for given materials or gases in different cabin environments. These environments are severe since there are the additional effects of acceleration of gravity from low to high values for very oxidizing atmospheres.

1.1 Ignition of Combustible Materials

Ignition or thermal explosion of solids or of gases in a closed vessel originated with the theory of Semenov (1959) who considers the thermal energy of self-heating in a material undergoing exothermic chemical reactions and evaluates it with regard to the cooling losses by conduction through the material and its boundaries. In the case of a gas, the boundaries are the walls of its container. The criterion for ignition is a simple one. Ignition or thermal explosion occurs if the rate of cooling is insufficient to balance the rate of heat generated from

the chemical reaction. Thus, critical dimensions and environmental conditions for ignition can be obtained by this means. In the simplest cases, the theory utilizes the energy equation only but with transient effects dominant through the process.

Further work by Hicks (1954), Adler and Enig (1964), Thomas (1961), Squire (1963) since Semenov has added to the complexity of the model allowing, for instance, other heat sources and reactant consumption during the pre-ignition stage. With the accumulation of experimental data these latter works have led to the consideration of a more realistic evaluation of material behavior. The ignition and the burning of material are known to depend to a large extent on the rate of heat transferred. The effects of different rates of heat transfer are primarily in the temperature gradients established in the material and the resulting pyrolysis products. For example, experimental data by Martin (1965) has assisted in the delineation of these regimes for the burning of cellulosic materials. The high heat rate regime is ablation controlled. The energy is principally deposited near the exposed surface and its pyrolysis products are volatile fragments which then combust in the atmosphere. For low heating rates, the temperature is more uniform through the material but with different pyrolysis products and more carbon remains as char. This char is easily ignited. The diffusion-controlled regime is contained in between these two. The temperature distribution has an appreciable gradient in the material and pyrolysis occurs at some point inside the material emitting flammable gases. Ignition occurs when self-heating is sufficient to continue the increase of thermal energy.

The ignition of rocket solid propellants which are made of plastic-type materials has been considered for some time. A large number of works and several theories have been evolved to predict this phenomenon. A critical review of most

of the work to date has been made recently by Price (1966). Although the effects of many parameters such as environmental pressure, temperature, and oxidizer on ignition have been investigated, most of the theoretical predictions have been compromised by the inadequacies of the simplifying assumptions. Three models are now prevalent for the ignition of solid propellants. The surface ignition theory of Hicks (1954) is a transient surface heating analysis with exothermic chemical heating of the solid. Although this analysis might be an early event in the sequence of ignition in an oxidizing atmosphere it was realized that the gas phase environment effects have to be included. Note that extensions [Adler (1964) and Thomas (1961)] were made to include also the reactant consumption in solid-phase thermal theories with chemical reactivity, but these studies also are not adequate since temporal and spatial variations in the temperature are ignored. The effects of gas-phase environment are included in a gas-phase model, Hermance (1966), composed of a slab of fuel exposed to a hot oxidizing gas; chemical reactions of the fuel vapors and oxidizer and the diffusion of these gases lead to ignition in the gas phase. The study reported by Hermance limits itself to one type of fuel with a number of simplifying assumptions. These assumptions are the use of one-dimensional species equations, mass loss occurring only at the surface, and in the early models the use of a constant wall temperature with respect to time.

Another mechanism for the ignition of materials is that of heterogeneous reactions at the gas-solid interface which can raise the surface temperature. Present evaluation by Price (1966) of ignition by this means is not conclusive since the observed ignition dependency on the gas-phase environment is not included. However, from all indications, it appears to be one ignition mechanism for certain types of material. The burning of Teflon [Fenimore and Jones (1968)]

appears to indicate that both gas-phase and heterogeneous reactions at the surface have a role in the consumption of the polymer. Part of the loss of Teflon material was attributed to fluorine atoms attacking the Teflon directly; the remaining loss came from the depolymerization in depth.

Despite the crudity [Price (1966)] of these theoretical models, their results together with experimental data have delineated some of the important parameters in the ignition of solid material when exposed to heat. Among these parameters are the effects of environmental pressure and chemical composition of the gas phase and the effects of the activation energy of the solid on the ignition delay time. In some cases, the activation energy has been obtained by the simple process of applying the theory to a set of experimental data [Price (1966)] and computing which activation energy best reproduced the data.

1.2 Behavior of Burning Materials

The flammability of materials or gas mixtures is a useful characteristic for evaluating fire hazards. Thus, a material or gas mixture is considered flammable if upon exposure to a heat source sufficient energy is liberated to continue the propagation of the flame into unignited regions of the material. Flammabilities of different fuel-oxidant mixtures have been obtained experimentally [Mullins and Penner (1959)]. For example, Simmons (1957) has obtained these limiting values for a mixture of air, nitrogen and fuel. He has defined the oxygen index as the ratio of oxygen to the mixture of air and nitrogen required to sustain steady burning. For air the index is 0.21; the material or fuel is more flammable for smaller values of n than this. For example, the index for hydrogen is 0.054. This index has been studied mainly in environments of 1-g. Its usefulness is evident since a numerical index is available to evaluate

materials which do not continue burning after being ignited. In the latter case, the index is greater than 0.21 for air mixtures. The effect of different cabin atmospheres can evidently be evaluated.

Fenimore and Martin (1966) have obtained the oxygen index for polymers. Their experiments indicate that the burning of polymers proceeds through a thermal feedback from the flame of the oxygen and pyrolysis products in the gas phase which pyrolyzes the polymer and gives off additional pyrolysis products. These products are usually more combustible. The index reflects the efficiency of this thermal feedback. Thus, index values of 0.95 have been obtained for Teflon since there is some difficulty in pyrolyzing Teflon and, moreover, the monomer is difficult to burn. More recent evidence by Fenimore and Jones (1968, 1966) indicates that a Teflon surface may react directly with the ambient oxygen, as discussed in the previous section. The index for polymers in oxygen and inert gases, such as Ar, N_2, and CO_2, has been further correlated, and Martin (1967) has indicated a linear variation of the index (ratio of oxygen to inert gases with the heat capacity of the inert gas. Some results are shown in Figure 1.1 as obtained by Martin (1967). Only helium indicated a higher oxygen index than the linear relation; Martin attributes this to greater heat losses from the reaction zone due to the additional emphasis of the higher thermal conductivity of helium. A model utilizing an energy balance only was sufficient to correlate predictions with the experimentally determined relation of oxygen index and heat capacity of inert gases, but it does not explain the anomalous index values in the helium-oxygen mixture. The success of the simple model adds reasonable hope that a theoretical model of polymer burning can be formulated to predict the oxygen index. All of this work had been done for a 1-g environment.

1.3 Combustion at Zero-Gravity

The principal effect in the reduction of the acceleration of gravity in combustion is to decrease the free convection in the gas flow. Burning of polymeric materials may differ considerably from the 1-g or higher environment due to this effect. Kimzey (1966, 1968) has performed experiments in burning paraffin, Teflon and other materials at zero-gravity in an aircraft cabin. His findings indicate what might be expected if convection loses its dominant role and diffusion and chemical reaction mechanisms are the rate-controlling processes. The shape of the flame at zero-gravity tends to a spherical one surrounding the fuel mass and Kimzey indicates a much larger reaction-zone thickness with additional accumulation of products and intermediates. Thus, it appears that chemical mechanisms and reactions may change due to the presence of the intermediates. In this way, the burning processes are affected by the absence of gravity. Moreover, the processes prior to ignition may be changed due to the accumulation of the vapors generated by self-heating. In the transition from zero-gravity conditions to 1-g, the burning may be abrupt, since accumulated volatile gases which surround the material will instantaneously burst into flames as convection begins to add oxygen. Therefore, the flame in a zero-gravity environment is diffusion limited and tightly coupled to the chemical reactions, and steady state conditions are not achieved for a long time.

Experimental data have been recently obtained by Cochran and Masica (1970) for the laminar jet diffusion flame (methane-air) in a changing gravity environment. A principal result from this study is that a decrease of normal gravity to zero reduces the height of the flame with a subsequent expansion of the flame and the appearance of extinguishment. The authors attribute this to the lack of

buoyancy at zero gravity and to the accumulation of combustion products surrounding the flame.

1.4 Free Convection of Heat Under Low Gravity

The reduced gravity environment affects a number of heat transfer phenomena. Siegel (1967) has reviewed some of these. Among them, free convection (which is characterized by the Rayleigh number) is controlled by the magnitude of gravity. At the lower gravity level, the Rayleigh number is small and free convection layers forming over solid surfaces are not thin boundary layers as would be expected at one g. Siegel has suggested that boundary layer theory can be applied for values of the Rayleigh number greater than 10^4.

A second and more important effect of reduced gravity is the longer transient time required for re-establishment of the steady state when any changes of thermal boundary conditions occur. Siegel indicates values of transient time inversely proportional to the square root of the acceleration due to gravity, g, for a change in surface temperature of a vertical plate; these are very long for low values of the gravity. This transient time is useful in practical situations, since it delineates the region of usefulness of the steady state heat transfer coefficients. Thus, as noted before, the flame at zero gravity does not tend to steady state conditions.

II. MODEL FOR IGNITION AND BURNING

An analytical study of the theory of ignition and the subsequent burning of a combustible material immersed in a gas (stagnant or flowing) in which the entire system may be subjected to changes in gravity forces ranging from zero to normal atmospheric values is considered in this report. The study is based on experimental results [Hermance, et al (1966)] which demonstrate that polymeric (or for that matter, cellulosic type) material exposed suddenly to a heat source vaporizes and ignition occurs in the gas phase immediately adjacent to the material. Additional experimental data by Fenimore and Jones (1966) indicate that most polymers burn through the pyrolysis products which oxidize in the flame and do not react chemically with the gas surrounding them. The model considered is composed of both the condensed and gas phase and the interaction between them. Ignition processes are, in general, transient by nature and time appears as one of the principal independent variables. In addition, two spatial coordinates are used. Thus, the sets of equations are functions of time and space which interact with each other at their common boundary. Finite rate chemistry for both condensed and gas phase reactions is considered as is diffusion which is dominant at reduced gravity.

The analysis considers ignition of the material with reactant consumption at low temperatures, which subsequently leads to diffusion-limited ignition in the gas phase at the higher gas temperatures. Some consideration is also given to heterogeneous reactions at the gas-solid interface. The burning phase in which a diffusion flame exists in the gas phase appears as the last stage of this analysis. The formulation of the model follows.

The phenomena leading from ignition to the spread of fire involves the gas

phase in the dominant role of providing a heat flux to spread the fire. The model attempts to follow this sequence of events to the time of consumption of the entire material. A solid material exposed to a heat source is vaporized and the chemical reactions of the atmosphere with the fuel (material vapor) leads to a flame. The flame is sustained if there is sufficient fuel and spreads to other parts of the material by free convection with forward radiation and forward heat conduction also playing a role. Vaporization of the unburnt material again leads to gas phase ignition and the fire has been spread. Experimental results substantiate this phenomenological model. Thus the presence of free convection due to gravity plays a major role in the fire spread.

III. EQUATIONS OF MOTION FOR THE GAS PHASE

3.1 Nonequilibrium Unsteady Boundary Layer Equations

For the gas phase, the boundary layer equations are utilized with finite rate chemistry. The flow is time-dependent with the two spatial coordinates x and y along and perpendicular to the material, respectively. Figure 3.1 shows the typical situation. Pyrolysis gases are transferred from the solid material upon exposure to heat and react with the ambient gas, which may be the cabin atmosphere (e.g., a combination of oxygen and inert gases). A temperature profile prior to ignition of the gas phase and a typical concentration of oxygen and fuel species are known. At ignition in the gas phase, the temperature peaks as shown in Figure 3.1, in the gas layer. The orientation of the gravity vector is also shown. Coupling of the condensed and gas phases occur at their boundary where a unique wall temperature and wall mass transfer are obtained from the solution. The equations are given in a surface coordinate system. The equations include the convection terms due to a nonzero mass flux at the material surface and natural convection due to the density changes, although the velocities are generally small. The orientation of the surface material with respect to the direction of the gravity vector determines the velocity field. The equations for momentum and mass balance of a compressible, viscous, heat-conductivity gas are:

Mass Conservation:

$$\frac{\partial}{\partial t}\rho + \frac{\partial}{\partial x}(\rho\, ur_b^j) + \frac{\partial}{\partial y}(\rho\, vr_b^j) = 0 \qquad (3.1)$$

Momentum in x-direction:

$$\frac{Du}{Dt} = \frac{-1}{\rho}\frac{\partial p}{\partial x} + \frac{1}{\rho}\frac{\partial}{\partial y}\left(\mu \frac{\partial u}{\partial_y}\right) + F_x , \qquad (3.2)$$

Momentum in y-direction:

$$\frac{u^2}{R} = -\frac{1}{\rho}\frac{\partial p}{\partial y} + F_y \tag{3.3}$$

where ρ is the mass density, and u and v are the velocity components along x and y respectively, $r_b(x)$ is the radius of the material specimen, j = 0 or 1 for the two-dimensional or three-dimensional case, p is excess pressure over the static pressure, μ is the coefficient of viscosity, and F_x and F_y are the components of body force due to gravity. These equations define the velocity field and are coupled with the temperature field through the density and coefficient of viscosity.

In Equations (3.2) and (3.3) the pressure force is defined as the value above that required to statically balance the body force. Thus, the body force $\bar{F}$ (F_x, F_y) due to gravity has the components

$$F_x = -g\,\frac{(\rho - \rho_\infty)}{\rho}\cos\alpha \quad ,$$

and

$$F_y = -g\,\frac{(\rho - \rho_\infty)}{\rho}\sin\alpha \quad ,$$

where α is the angle of the gravity vector to the x coordinate and the subscript ∞ denotes the value of density of the static fluid. It is seen that a nonzero pressure gradient normal to the boundary layer is created. For the ignition and burning problems, the case of a vertical surface (α = 0) and the case for zero gravity would clearly evaluate the effect of gravity. The flow for the value of $\alpha = \pi/2$ may have adverse pressure gradient. It is noted that most flame studies of droplets [cf. Williams (1965), Isoda and Kumagi (1954)] and theoretical models have been formulated fairly close to that expected at zero

gravity Kimzey (1966, 1968) . It is expected that free convection will play a large part in ignition since hot gases are then brought into contact with virgin material.

The energy equation for the temperature is coupled in a highly nonlinear way to the species equation through the chemical reaction terms. These equations are:

$$\rho \bar{c}_p \frac{DT}{Dt} = u \frac{\partial P}{\partial x} + \frac{\partial}{\partial y} \left(k \frac{\partial T}{\partial y}\right) -$$

$$- \sum_{i=1}^{NI} c_{p_i} j_i \frac{\partial T}{\partial y} - \sum_{i=1}^{NI} h_i \dot{w}_i + \mu \left(\frac{\partial u}{\partial y}\right)^2 \tag{3.4}$$

$$\rho \frac{Dc_i}{Dt} = - \frac{\partial}{\partial y} (j_i) + w_i \tag{3.5}$$

where T is the temperature, c_i is the mass fraction of species, $\bar{c}_p$ is the specific heat at constant pressure, k is the thermal conductivity, c_{p_i} is the specific heat at constant pressure for the i^{th} species, j_i is the diffusion flux of i^{th} species, and w_i is the chemical production of the species i, and NI is the number of species. The operator D/Dt is defined by $\frac{\partial}{\partial t} + u \frac{\partial}{\partial x} + v \frac{\partial}{\partial y}$.

The mass flux j_i is defined by Fick's Law here. This is sufficient in this study because of the species considered herein. The flux j_i is

$$j_i = - \frac{\mu}{P_r} L_e \frac{\partial c_i}{\partial y} \tag{3.6}$$

where the Prandtl number $P_r = \mu \bar{c}_p/k$, the Lewis number is defined by $\rho D_i c_p/k$, and D_i is the diffusion coefficient. In addition, the equation of state is

$$\rho = \frac{P_e}{RT \sum_{i=1}^{NI} \frac{c_i}{M_i}} \tag{3.7}$$

where M_i is the molecular weight of i^{th} species and R the universal gas constant. This equation assumes that the gas consists of a mixture of chemically reacting perfect gases.

These equations are for a heat conducting chemically reacting gas flowing over an arbitrary surface with the body force due to gravity. It is noted that the density has been considered to be variable in the entire field and therefore in all terms including the body force terms. The flow considers effects due to free convection, force convection, and convection due to mass transferred from the material surface. In any case, the flow velocities are expected to be small since application is to the interior of a space cabin. There is no restriction on the magnitude, however.

In these equations the pressure, p, is the excess over the static pressure at hydrostatic equilibrium. The pressure p_e in Equation (3.7) is the total pressure. The principal term for heat generation in the energy equation is that due to exothermic chemical reaction since viscous dissipation is negligible. This term is directly proportional to the heat of combustion of the reaction considered.

As given above the independent variables are the spatial distances x and y and the time t. There are two useful subsets of these equations which have been studied. These are for steady flow where any change with respect to time is zero and for the case of one spatial dimension (normal to the material surface)

and time t (with no change in the lengthwise distance x). The flow is assumed to originate at the beginning of the plate (x = 0). Thus if the body is hotter than the ambient atmosphere the direction of the flow presumed implies that the x-component of the gravity force is in the negative x-direction.

The governing parameter of the field is the Grashof number which is large here.

3.2 Transformation of the Equations

In the above set of equations there are three independent variables x, y, and t; moreover, the gas is considered compressible. It is more convenient to work with boundary layer transformed coordinates ξ and η defined by

$$\eta = \frac{u_e \, r^j}{\sqrt{2\xi}} \int_o^y \rho \, dy \tag{3.8}$$

$$\xi = \int_o^x (\rho \mu)_r \, r^{2j} \, u_e \, dx \tag{3.9}$$

In these equations r denotes the distance of the material surface to the axis of the body and j = 0 for a two-dimensional slab and j = 1 for an axially-symmetric body, $(\rho\mu)_r$ is a constant reference value of the product of density and coefficient of vissocity, and u_e is a reference velocity which is a function of x (in most cases, u_e is a constant).

Equations (3.1)to (3.5) transform to the following set of equations by noting that time is a third independent variable. Thus these equations are:

Mass Conservation:

$$2\xi \left(\frac{\partial f'}{\partial \xi} \right) + \left(\frac{\partial V}{\partial \eta} \right) + f' = 0 \qquad (3.10)$$

Momentum Equation :

$$2\xi f' \frac{\partial f'}{\partial \xi} + 2 \frac{\xi}{\xi_x u_e} \frac{\partial f'}{\partial t} + V \frac{\partial f'}{\partial \eta} = \qquad (3.11)$$

$$- \frac{2\xi}{\xi_x \rho_{u_e}^2} p' + \frac{\partial}{\partial \eta} \left(\ell \frac{\partial f'}{\partial \eta} \right) +$$

$$\frac{2\xi}{\xi_x u_e^2} F_x$$

Energy Equation :

$$\frac{2\xi}{\xi_x u_e} \frac{\partial \theta}{\partial t} + 2\xi f' \frac{\partial \theta}{\partial \xi} + V \frac{\partial \theta}{\partial \eta} = \frac{2\xi}{\xi_x} \frac{p'}{\rho \bar{c}_p T_e} f' \qquad (3.12)$$

$$+ \frac{1}{\bar{c}_p} \frac{\partial}{\partial \eta} \left(\frac{\ell}{P_r} \bar{c}_p \frac{\partial \theta}{\partial \eta} \right) + \frac{\ell}{P_r \bar{c}_p} \sum_{i=1}^{NI} c_{p_i} L_i \frac{\partial \theta}{\partial \eta} \frac{\partial c_i}{\partial \eta}$$

$$- \frac{2\xi}{\xi_x u_e T_e \bar{c}_p} \sum_{i=1}^{NI} h_i w_i / \rho + \frac{\ell e^2}{\bar{c}_p T_e} \cdot \left(\frac{\partial f'}{\partial \eta} \right)^2$$

Species Equations(i = 1, NI)

$$\frac{2\xi}{\xi_x u_e} \frac{\partial c_i}{\partial t} + V \frac{\partial c_i}{\partial \eta} + 2\xi f' \frac{\partial c_i}{\partial \xi} = \frac{\partial}{\partial \eta} \left(\frac{\ell}{P_r} L_i \frac{\partial c_i}{\partial \eta} \right) + \qquad (3.13)$$

$$\frac{2\xi}{u_e \xi_x} \frac{w_i}{\rho} \quad .$$

In these equations the reference velocity u_e and temperature T_e have been taken to be a constant. This is more convenient in free convection flow. Thus the velocity ratio is denoted by $f' = u/u_e$ and the temperature ratio by $\theta = T/T_e$.

The case for the time-dependent flow at a fixed position is obtained by setting the derivative with respect to x to zero and at zero gravity these equations involve only normal velocity due to the mass transfer from the material.

3.3 Boundary Conditions and Initial Conditions

The boundary and initial conditions have been formulated with consideration of the combustion of solid material in a space cabin atmosphere. The initial conditions are that at time zero only the cabin atmosphere gases or any other prescribed gases are present. That is, for t = 0,

$$\left.\begin{aligned} c_i &= c_{i_{INIT}} (x, y, 0) \\ \text{At the temperature} \\ T &= T_{INIT} (x, y, 0) \\ \text{and pressure of} \\ p &= p_{INIT} (x, y, 0) \end{aligned}\right\} \qquad (3.14)$$

The initial flow distribution $u = u_{INIT}(x, y, 0)$ is prescribed.

At the edge of the boundary layer the fuel (material) species concentration gradually becomes zero as one moves away from the solid material surface and the principal gas components remaining are those of the initial cabin atmosphere gases. This implies that for the species, temperature, pressure, and velocity respectively, $c_i = c_{i_e}(x, y_e, t)$

$$\begin{aligned} T &= T_e \\ p &= p_e \\ \text{and} \\ u &= u_e \quad . \end{aligned} \tag{3.15}$$

The boundary condition at the material surface requires some special consideration. This condition is matched with the behavior of the solid material which is losing mass due to the heat transferred from the gas phase. At this surface the tangential velocity is zero, that is,

$$u(x, 0, t) = 0 \tag{3.16}$$

where mass from the solid material is transferred into the gas phase the net mass flux of this species is given by

$$\rho_i v_i = \rho v c_i - \frac{\mu}{P_r} L_e \frac{\partial c_i}{\partial y} \tag{3.17}$$

where the total mass flux transferred to gas phase is denoted by (ρv). This condition (3.17) together with a material and energy balance at the gas-solid interface uniquely determines the mass loss from the solid and the temperature of this interface and the gas species concentration at the interface. This will be considered in a separate section.

3.4 Radiation Effects

Radiation from flames provides additional energy terms to change the temperature distribution and also provides a mechanism for the forward propagation of the flame to non-burning virgin material. The radiation energy is principally due to the species carbon dioxide and water vapor for non-luminous flames. Luminous flames, on the other hand, are the source of more intense radiation and this is derived from hot soot particles. In this section a formulation of the radiative energy terms and the additional radiative flux at the gas-solid interface is given for gaseous radiation; experimental data can be used to modify the emissivity values to account for the effect of particle radiation.

The radiative source term in the gas proper is given by the term $(-\partial q_r/\partial y)$ which is added to the right side of Equation (3.4). The use of this term neglects radiation in the X direction within the gas volume (effect of X variation at the surface is possible in the wall boundary condition) appropriate for the boundary layer approximation. The term q_r is the radiation flux per volume in the y direction normal to the surface. Consider now that the gas is optically thin which is a reasonable assumption for small flames at low temperature, then the radiant heat source per unit volume is given by

$$-\frac{dq_r}{dy} = 2a\,\sigma\,T_e^4\left[\epsilon_w(\theta_w^4 - 1) + 2\,(1 - \theta^4)\right] \qquad (3.18)$$

where a is the absorption coefficient (a function of pressure and temperature), ϵ_w the surface emissivity, σ the Stefan-Boltzmann constant. The subscript w denotes values at the surface. Thus a non-black surface is considered.

The radiative heat flux at the surface is due to contributions from the

free stream edge (ambient conditions), the gas layers immediately above it, and the loss from the surface. Effectively, this net sum is given by

$$q_{rw} = \epsilon_w \sigma T_e^4 (\theta_w^4 - 1) - 2 \sigma \epsilon_w T_e \int_o^{\tau_o} (\theta^4 - 1)\, dt \qquad (3.19)$$

where τ_o is the optical thickness given by $\tau_o = \int_o^L a\, dy$ and L is the thickness of the gas layer at that point along the surface.

In these equations the absorption coefficient of the gas mixture is required as a function of temperature and pressure. This coefficient is also a function of the species concentration. Cess (1964) has derived the absorption coefficient of carbon dioxide and water vapor from the emissivity data of Hottel (1954) for these gases. Thus the absorption coefficient can be obtained from experimental data gas mixture by the combination rules as suggested by Hottel (1954).

In this study it was found appropriate to use the condition that the ratio of the absorption coefficient to the gas density is a constant. This assumption appears reasonable from a selected evaluation of the absorption coefficient in accordance with the previous discussion.

Equation (3.19) forms part of the boundary condition given in Section 4.

IV. EQUATIONS FOR THE SOLID FUEL/CONDENSED PHASE EQUATIONS

In this study consideration is given to the ignition and burning of a solid material which occurs primarily in the gas phase layer directly above the solid. This mechanism for combustion of solid fuel is initiated by some external heating which raises the temperature of the solid such that degradation of the material (polymeric in this instance) occurs and pyrolysis gases leave the solid and enter the gas phase. Ignition occurs then in the gas phase or at the surface if heterogeneous reactions are dominant. Then a continuous consumption of the solid occurs, and the additional heat transferred from the gas phase combustion carries this physical process through to burning until the solid is entirely gone. Consider for our purpose a non-charring burning solid such as Teflon or polymethymethacrylate (Plexiglass) then the energy balance defines the temperature through heat conduction changes and energy loss due to a change in density of the solid. (If a charring solid is considered addition terms containing energy changes through fluid convection through the char must be added and offers no additional complexity to the method of solution). This energy equation for the solid is

$$\rho_s \, c_p \, \frac{\partial T_s}{\partial t} = \frac{\partial}{\partial y_s} \left(k_s \, \frac{\partial T_s}{\partial y_s} \right) + q \, w \, (\rho, T) \tag{4.1}$$

where the subscript s denotes the solid and the coordinate y_s is as given in Figure 4.1 and fixed relative to the gas phase coordinates. Here ρ_s , c_p, k_s, q are the mass density, specific heat, coefficient of thermal conductivity, and the heat of depolymerization. The temperature T_s and the density ρ_s are functions of time t and the distance y_s, whereas k_s, c_p, and q are functions of the local temperature. During the solid degradation process the density changes

in accordance to an Arrhenius rate of the form

$$w\ (\rho_s, T_s) \;=\; -k\ \rho_s^{m} \quad \epsilon^{-E/RT_s} \tag{4.2}$$

as suggested by Madorsky (1964). In this equation k is the frequency factor, E the activation energy for pyrolysis of the polymeric material and m is a constant obtained from experimental data.

The mass flux of solid converted to gas is obtained from summing the integral components of each slice of solid, that is,

$$\dot{m}_w \quad (0,\ t) \;=\; \int_0^{y_{s\ max}} \frac{\partial \rho_s}{\partial t} \quad dy_s \tag{4.3}$$

These three equations completely determine the solid material temperature and density when the solid-gas interface temperature and mass flux are known. In the study herein, the gas phase equations as described in the previous section are coupled to the solid equations and their simultaneous solution leads to the interface quantities.

As suggested by Figure 3.1 the gas and solid coordinates are measured from the phase interface. Since solid material is lost during combustion the solid surface recedes with time and a transformation is needed to meet this requirement of keeping the gas phase coordinates directly next to the solid surface. The transformation of coordinates required is to $(\zeta\ ,\ t)$ coordinates such that

$$\zeta \;=\; \frac{y_s - a}{s\,(t) - a} \tag{4.4}$$

where a is the thickness of the virgin solid and s(t) is the thickness of the solid material lost. Thus the burning surface occurs at $\zeta = 1$ and the for virgin material is at $\zeta = 0$. In terms of (ζ, t) Equations (4.1) and (4.2) become respectively

$$\frac{\partial T_s}{\partial t} - \zeta \frac{\dot{s}}{(s-a)} \frac{\partial T_s}{\partial \zeta} = \frac{1}{\rho \tau_p} \frac{1}{(s-a)^2} \frac{\partial}{\partial \zeta} \left(k_s \frac{\partial T_s}{\partial \zeta}\right) - \frac{h_s}{\tau_{p_s} \rho_s} w(\rho_s, T) \tag{4.5}$$

$$\frac{\partial \rho_s}{\partial t} - \zeta \frac{\dot{s}}{(s-a)} \frac{\partial \rho_s}{\partial \xi} = w(\rho_s, T) \tag{4.6}$$

These equations in this form are utilized in this study.

These equations are highly nonlinear. The receding surface indicated by $\dot{s}$ leads to the additional terms on the left hand side. This quantity is given by a balance of mass through the entire specimen. Thus

$$\rho_{sw} \dot{s} = (s-a) \int_0^1 w(\rho_s, T_s) d\zeta \tag{4.7}$$

where the subscript w indicate quantities evaluated at the surface.

The boundary conditions for the solid equations involve energy balances and mass balances with the gas phase. At time zero if a virgin piece of material is considered then the temperature and density are respectively

$$T_s(y_s, 0) = T_{so}(y_s) \tag{4.8}$$

$$\rho_s(y_s, 0) = \rho_{so} = \text{constant}$$

The initial temperature may be a function of y_s if some initial heating has been applied but not sufficient to cause any change in solid density. Consideration is given to a burning surface on one side of a two-dimensional plane slab of material or to an axially symmetric piece. Thus for these cases the surface $y_s = a$ is at either a prescribed heat flux or temperature. For the latter case, for example,

$$T_s(a, 0) = T_{s1} \tag{4.9}$$

$$\rho_s(a, 0) = \rho_{so}$$

Other conditions can, of course, be used in their place.

At the burning surface the energy balance between the solid and gas phase lead to the net heat flux which enters the surface. This flux is

$$q = - \frac{k_s}{(s-a)} \left. \frac{\partial T_s}{\partial \zeta} \right|_w \tag{4.10}$$

and is related to the gas phase by

$$q_s = -\dot{m}_w \left(\sum_{i=1}^{NI} h_i \, c_{i_{ablat.}} - h_s \right) + \left(k_g \frac{\partial T}{\partial y} \right)_{w,\, gas} \tag{4.11}$$

$$-q_{rad} + B\exp(-E_h/RTw) + F_g$$

and

$$\dot{m}_w = (\rho v)_w \tag{4.12}$$

The energy is partitioned at the wall into several parts. These are the heat of depolymerization, the contribution from the conductive portion of the gas

phase, the loss or gain due to radiation, and finally the energy due to heterogeneous reactions at the surface. In Equation (4.11) the symbol B conveniently contains the surface species for arbitrary order reaction, E_w is the activation energy for this reaction; in addition, F_g is an impressed heat load which is required to initiate the burning of a cooled specimen and can be prescribed as a function of time and distance along the specimen.

V. MATERIAL PROPERTIES

5.1 Solid Material Characteristics

Material properties for two typical polymeric material are given in this section. These materials, Teflon and polymethylmethacrylate(Plexiglass) are polymeric type that can be considered by this model. The properties required for the analysis are the thermal conductivity, specific heat and the enthalpy as a function of the temperature. These characteristics have been compiled from a number of sources. These sources are JANAF TABLE (1966), Jellinek (1955), Madorsky (1964), Ham (1967), Griskey, et al (1966, 1967), Brandrup et al (1966) and Fenimore and Jones (1969). The solid enthalpy distributions with temperature were constructed from specific heat values; these distributions compare well with the values from Wagner & Grisky (1967). The distribution of the solid heat conductivity, enthalpy, and specific heat are given on Table V-1.

5.2 Chemical Model

In this study two representative solid materials have been considered to be burning in an oxygen-nitrogen mixture. These are the thermoplastic resins polytetrafluoroethylene(Teflon) and polymethylmethacrylate (Plexiglass) and are representative of those in usage. These plastics depolymerize under a heat loading and form a monomer at the surface. The plastic polymethylmethacrylate may form a liquid monomer which flashes instantaneously into the gaseous phase. Thus the concern of this section is to formulate the chemical model for the gaseous monomer and its reaction with an oxygen-nitrogen mixture.

5.2.1 Teflon

Teflon burns in oxygen and forms a number of products in an oxygen-nitrogen mixture. The number of species formed are many but only a relatively few major ones together with their global reactions are sufficient for the ignition and burning processes being considered here. Madorsky (1964) indicates that the degradation products from the vacuum pyrolysis of Teflon solid are mostly ($>$ 95%) the monomer. The burning of Teflon in oxygen was considered by Fenimore and Jones (1968) and these experiments indicate the monomer C_2F_4 rapidly decays away from the burning surface. The gas composition along the axis of the Teflon rods burnt were COF_2, CO, CO_2, CF_4 and, of course, the monomer C_2F_4 at 1 atmosphere pressure. Temperatures increase from about 950°K at the surface to about 1500°K Results from diffusion and premixed flame measurement indicate the similar products (Fenimore - 1968) and in addition, that CF_4 increases over COF_2 with an increase of pressure for diffusion flames. The premixed flame results of Fenimore (1968) show that the CF_4/COF_2 ratio decreases sharply with increasing O_2/C_2F_4 mixtures. The gas phase pyrolysis of C_2F_4 has been studied by Bauer, et al (1967) in shock tubes and the lower temperature range covered in these experiments are of interest in the fire problem. The major products obtained from shocking a mixture of C_2F_4 gas, O_2 and the inert gas Argon are COF_2, CO, CF_4. The major oxidation products are COF_2 and CO. One notes that Fenimore (1968) gives evidence from his study that elemental fluorine is present from the burning Teflon rods although this species was not directly measured. Indeed, if equilibrium conditions prevail at the flame the products would include an amount of fluorine atoms which peaks at the mixture ratio of (moles O_2/moles C_2F_4) 1.5 with a flame temperature of 2159°K (at atmosphere pressure) (1965). (See also Fenimore - 1968). Fenimore suggests also that heterogeneous burning occurs

for Teflon and that surface reactions of the F atoms account for some of the burning of Teflon.

The interest in the fire study is to first consider the ignition and burning of material with consideration of the species and chemical reactions which have the major influence on the ignition time and burning velocity.

For this purpose the monomer gas C_2F_4 can be assumed to react with the ambient oxygen-nitrogen mixture to form the species of CF_2, O, F_2CO, CO, CO_2, and F from O_2 and C_2F_4. N_2 is considered inert at this temperature. The global kinetic scheme to form these species has been suggested by Browne and Carabetta (1970).

$$
\begin{aligned}
&(1) \quad C_2F_4 + M_1 \longrightarrow 2CF_2 + M_1 \\
&(2) \quad CF_2 + O_2 \longrightarrow COF_2 + O \\
&(3) \quad C_2F_4 + O \longrightarrow COF_2 + CF_2 \\
&(4) \quad COF_2 + M_1 \longrightarrow CO + 2F + M_1 \\
&(5) \quad CO_2 + O \longrightarrow CO + O_2 \\
&(6) \quad CO + O + M_2 \longrightarrow CO_2 + M_2
\end{aligned}
\qquad (5.1)
$$

Other species such as CF_4 can be added to the group later but would unnecessarily complicate the study. The mechanism for CF_4 has been suggested by Fenimore (1968) through several production reactions involving the additional CF_3 radical. The detailed reactions as given above are useful for determining the detailed species profile over the burning material. For the initial determination of igntion criteria and burning times it is only necessary to select those reactions which give the largest contribution to the exothermic heat of reaction.

For part of the study a one step global reaction suffices for the determination of ignition times and characteristics which do not depend on individual detailed species distributions. A one step global reaction can be partially justified from the system of kinetics as described above by assuming that CF_2 and O radicals are in steady state (cf. Bauer et al - 1969). If this assumption is made, then reactions (1) to (3) can be put into the form:

$$C_2F_4 + O_2 \longrightarrow 2\ COF_2 \tag{5.2}$$

with the production of COF_2 given by the rate ($I = COF_2$)

$$W_I = M_I \rho^{3/2} \left(\frac{C_{O2}}{M_{O2}}\right)\left(\frac{C_{C2F4}}{M_{C2F4}}\right)^{1/2} k_f \tag{5.3}$$

5.2.2 Polymethylmethacrylate

Polymethylmethacrylate rods have been burned in argon-oxygen mixture by Fenimore and Jones (1966). The concentrations of CO_2, CO, H_2 and C_2 were observed with the latter two species about an order of magnitude lower in value than the first pair. Vacuum pyrolysis of polymethylmethacrylate by Madorsky (1964) shows mostly the monomer at 500°C and 800°C (from about 95% to 80%, weight percent of total volatiles). At 1200°C the monomer decomposes with the principal components being CO and CO_2 and the monomer (about 30% CO, 10% CO_2, and 9-16% monomer).

A single step global reaction for the decomposition of the monomer and its reaction with oxygen-nitrogen mixture is suggested by these products. Martin (1967) has considered reactions for the conversion of solid polymer to the gaseous component which are useful for this study. The gaseous monomer reacts with

oxygen to form CO, CO_2, and H_2O. That is,

$$C_5H_8O_2 + 6\ O_2 \longrightarrow 5CO_2 + 4\ H_2O \tag{5.4}$$

or

$$4C_5H_8O_2 + 19\ O_2 \longrightarrow 10\ CO + 10\ CO_2 + 16\ H_2O \tag{5.5}$$

As in the Teflon case more detailed distributions of species can be obtained by resorting to a more elaborate kinetic scheme. Either Equation (5.4) or (5.5) is sufficient for the purpose of energy balance. A typical set has been suggested in the table. The rate constants for this global reaction are considered parametized by values typical of air-hydrocarbon reactions. That is, the pre-exponential factors and the activation energy are part of non-dimensional quantities of which typical values are utilized in the study.

5.3 Thermodynamic and Transport Properties

The thermodynamic properties of the oxygen-nitrogen gaseous monomer, and their reaction products are complicated by the presence of many species. The enthalpy for a multi-species flow is given by

$$h = \sum_{i=1}^{NI} c_i h_i \tag{5.6}$$

where c_i is the mass fraction of species and h_i the individual species enthalpy. The individual species values have been tabulated at G. E. by Browne (1960, 1964, 1965). The thermodynamic properties for the diatomic molecules were obtained by utilizing the second virial coefficient approach utilizing the Morse potential. In addition, at the lower temperature, the diatomic species were considered as rigid rotator harmonic oscillators with corrections for rotational stretching and vibrational anharmonicity. These individual species for Teflon gas

and oxygen-nitrogen mixture are given by Browne (1965). Similar data are available for hydrocarbon species. The mixture of specific heat is given similarly as Equation (5.6) in the form

$$\bar{c}_p = \sum_{i=1}^{N} c_i c_{p_i} \quad . \tag{5.7}$$

The transport properties of the mixture are functions of the individual species and temperature and can be obtained from a combination of these values. The individual species viscosity and heat conductivity are given by the relations

$$\mu_i = 26.693 \times 10^{-6} \cdot \frac{(M_i T)^{1/2}}{\Omega_i^{(2,2)}} \tag{5.8}$$

and

$$k_i = \frac{\mu_i R}{M_i} \left[c_{p_i} \frac{M_i}{R} + 1.25 \right]$$

where the dimensions of μ_i is in units of poises and k_i is in units of g-cal per (cm-sec$^{\circ}$K). The collision integrals required here were evaluated from a number of sources in the literature and numerical evaluation. With these pure species properties the Wilke's mixture rules then give the mixture viscosity and conductivity in the form

$$\mu = \sum_{i=1}^{N} \left(\frac{X_i \mu_i}{\sum_{j=1}^{N} X_j \phi_{ij}} \right) \tag{5.9a}$$

where $X_i = c_i \bar{M}/M_i$

and

$$k = \sum_{i=1}^{N} \left(\frac{X_i k_i}{\sum_{j=1}^{N} X_j \phi_{ij}} \right) \tag{5.9b}$$

$$\phi_{ij} = \frac{\left[1 + \sqrt{\frac{\mu_i}{\mu_j}} \left(\frac{M_j}{M_i} \right)^{1/4} \right]^2}{\sqrt{8} \sqrt{1 + \frac{M_i}{M_j}}} \tag{5.9c}$$

In some instances the Prandtl number has been assumed constant and a value assigned to it.

The diffusion coefficient is also required and the Lewis number is assumed to be a constant with a different value assigned for each species. Multi-component diffusion is not expected to detract from the validity of the ignition times utilizing this assumption.

VI. METHOD OF SOLUTION - FINITE DIFFERENCES

The method utilized for the solution for these coupled equations for the gas phase and the condensed phase to be given in the next section is that of finite differences, in particular, the implicit finite difference method. The essential point of importance in the choice of a method is the computer time requirement; it has been found that the computing time utilizing the implicit method is almost proportional to the number of species, as in the explicit scheme.

The coupled, nonlinear, partial differential equations for both gas and solid phase are quasi-linear with second order derivatives in the y directions only. These equations are parabolic in nature. Moreover, the gas phase equation remains parabolic in the steady state since there exist only second derivatives in the y direction. Thus it appears that the Crank-Nicolson (1947) implicit scheme can be generalized to include the time dependence. Since only second order derivatives in y are present, the finite difference equations following the Crank-Nicolson scheme averages these derivatives in such a way that algebraic equations are tri-diagonal and a simple algorithm can be utilized for their solution. Consider Figure 3.2 and evaluate the finite differences centered on $(k + \frac{1}{2}, m + \frac{1}{2}, n)$ corresponding respectively to the point $(t_k = k\Delta t, \xi_m = m\Delta\xi, \eta_n = n\Delta\eta)$. Let the representative second order equation of either velocity, temperature, or species concentration be given by

$$\phi_{\eta\eta} = F(\xi, \eta, t, \phi, \phi_\xi, \phi_\eta, \phi_t), \tag{6.1}$$

where ϕ is any of the dependent variables. The finite difference representa-

tions are then

$$\Phi_{\eta\eta} = \frac{1}{4}\Delta_\eta^2 \left(\Phi_{k+1,m,n,} + \Phi_{k+1,\ M+1,\ n} + \Phi_{k,m,n,} + \Phi_{k,m+1,n}\right) ,$$

$$(\xi,\eta,\ t) = \left(\xi_{\ m+\frac{1}{2}},\ \eta_n,\ t_{\ k+\frac{1}{2}}\right) ,$$

$$\Phi = \frac{1}{4}\left(\Phi_{k+1,m,n} + \Phi_{k+1,m+1,n} + \Phi_{k,m,n} + \Phi_{k,\ m+1,n}\right) ,$$

$$\Phi_\xi = \frac{1}{2\Delta\xi}\left(\Phi_{k+1,m,n} + \Phi_{k,m,n} - \Phi_{k+1,m+1,n} - \Phi_{k,m+1,n}\right) ,$$

$$\Phi_\eta = \frac{1}{4}\delta_\eta\left(\Phi_{k+1,m,n} + \Phi_{k+1,m+1,n} + \Phi_{k,m,n} + \Phi_{k,m+1,n}\right) ,$$

$$\Phi_t = \frac{1}{2\Delta t}\left(\Phi_{k+1,m+1,n} + \Phi_{k+1,m,n} - \Phi_{k,m+1,n} + \Phi_{k,m,n}\right) ,$$

where by definition

$$\Delta_\eta^{\ 2}\Phi_{k,m,n} = \frac{\Phi_{k,m,n} - 2\Phi_{m,n} + \Phi_{k,m,n-1}}{\Delta\eta}$$

$$\delta_\eta\Phi_{k,m,n} = \frac{\Phi_{k,m,n} - \Phi_{k,m,n-1}}{2\Delta\eta}$$

These are applied to each equation in both the gas and condensed phase. In this formulation, the equation of continuity gives directly the transformed vertical velocity. In fact the equation is evaluated at the point $(k + \frac{1}{2},\ m + \frac{1}{2},\ n - \frac{1}{2})$ and the vertical velocity at the line $(k + 1)$ is obtained following the solution of the other equations.

This finite difference scheme leads to a tri-diagonal system of algebraic equations of the form:

$$A_n w_{n+1} + B_n w_n + C_n w_{n-1} = D_n . \tag{6.3}$$

The solution of this system of equations is obtained by the simple algorithm of

$$w_n = E_n w_{n+1} + e_n , \tag{6.4}$$

where

$$E_2 = -(B_2 + C_2 H)^{-1} (A_2 + C_2 F) ,$$

$$e_2 = (B_2 + C_2 H)^{-1} (D_2 - C_2 H) ,$$

$$E_n = -(B_n + C_n E_{n-1})^{-1} A_n ,$$

$$e_n = (B_n + C_n E_{n-1}) (D_n - C_n e_{n-1}) ,$$

for $3 \leqq n \leqq N-1$. The boundary conditions are given in the form of

$$w_1 = H w_2 + F w_3 + h ,$$

$$w_N = g ,$$

where F, H, h, g are given functions. The equations are solved in sequence proceeding from the velocity, temperature, to the species equations of the gas phase and then to the two equations for the condensed phase.

In formulating the difference equations, the concept of quasi-linearization is used wherever necessary. For example, the chemical production terms in the species equation and energy equation are linearized in this manner. This has been found to be of considerable assistance in obtaining stable solutions for fairly large step sizes.

VII. IGNITION DELAY RESULTS

7.1 Ignition of Gas Mixture with Uniform Composition of Fuel and Oxidizer

Ignition is studied first for the gas phase with uniform composition and fixed wall conditions. That is, a combustible gas mixture is heated by a hot wall until it ignites. The surface temperature and gas composition are given quantities. This example will give an understanding of the gaseous exothermic reactions causing ignition. In this situation the energy equation for a given mixture of fuel and oxidizer (as discussed in the previous sections) of fixed composition is sufficient to determine its combustion characteristics. The problem is posed as follows. A cool stationary gas mixture typical of zero gravity condition is supposed to be in contact with the hot surface which is to remain at a given temperature. Fuel is injected from the surface of the body so that a normal mass flux of fuel gas exists at the body surface; this mass flux is prescribed (its magnitude is suggested by the coupled gas-solid analysis to be considered later). A time dependent gas model with one spatial dimension normal to the surface is considered in this section. Due to the hot surface a thermal wave travels outward from the surface into the gas and raises its temperature. The increase of gas temperature with time releases heat energy from the exothermic reaction in the gas and leads to a sharp temperature rise and a subsequent ignition. The governing equation for the thermal energy balance of a compressible gas under these conditions is obtained from Equation (3.12). This equation is

$$\frac{\partial \theta}{\partial t} + V \frac{\partial \theta}{\partial \eta} = \frac{1}{C_p} \frac{\partial}{\partial \eta} \left(\frac{\ell}{P_r} C_p \frac{\partial \theta}{\partial \eta} \right) - \sum \frac{h_i}{C_p T_e} \frac{W_i}{\rho} \qquad (7.1)$$

where θ is the temperature ratio T/T_e, t and η are the time and transformed normal coordinate respectively, C_p the coefficient of specific heat at constant pressure, P_r the Prandtl number, and ℓ the ratio of the product of density and viscosity coefficient, h_i the enthalpy specific heat, ρ the mass density, W_i the rate of production per volume of mass from the chemical reaction, T_e the ambient gas temperature, and the summation is over all the species.

In this section the boundary conditions for Equation (7.1) are explicitly given in terms of the surface and ambient temperature. Thus these conditions are:

$$\eta = \eta_{max}: \quad \theta = 1 \tag{7.2}$$

$$\eta = 0 : \quad \theta = \theta_W$$

An additional relation is required for the V function. This relation can be supplied by the conservation of mass. For a nonsteady compressible flow and one normal spatial coordinate the mass conservation equation is given by V = constant along this coordinate where V is defined by

$$V = \rho v + \frac{\partial}{\partial t} \int_o^y \rho \, dy \tag{7.3}$$

Since V is constant along the normal coordinate it can be evaluated at the surface y = 0. At the surface fuel can be injected with a prescribed mass flux of $(\rho v)_w$. Thus one has that:

$$V = (\rho v)_w \tag{7.4}$$

In place of the physical coordinate y it is convenient to use a trans-

formed coordinate η as suggested by Equation (7.3). For this problem the coordinate η is proportional to the stream function at constant time. Thus η is given by

$$\eta = \left(\frac{\rho_r}{\mu_r} \right)^{1/2} \int_o^y \frac{\rho}{\rho_r} \, dy \tag{7.5}$$

where μ is the viscosity coefficient and the subscript r denotes a constant reference value.

To recapitulate, the system of equations from (7.1) to (7.5) is valid for a one spatial dimensional nonsteady compressible heat conducting gas flow with non-zero mass flux prescribed at the surface (y = 0) with a distributed internal energy source due to exothermic chemical reactions. The problem to be studied here is the thermal ignition of combustible gas mixtures when the energy flux for heating is provided by the hot wall. The study of the thermal ignition of gases posed in this manner is not a new one. This problem has been studied for constant density assumption and for zero mass flux at the surface. A summary of these investigations has been made recently by Merzhanov (1971) for the hot wall-cool gas case. Some of the older studies are discussed in the text by Frank-Kamenetskii (1969). As pointed out in the Introduction the situation of the gas phase ignition for a hot gas-cool wall condition which exists in a rocket motor or in the shock-reflected regions of a shock tube has been considered by Hermance, et al (1966) and Hermance, et al (1967-1971). In the latter works assumptions such as equal molecular weight, constant Prandtl number, and sometimes a constant gas density are made in addition to the ones quoted above.

For the particular consideration of any gas mixture the chemical energy term on the right side of Equation (7.1) must be formulated. A gas mixture characteristic of that discussed in Section (5.2) is utilized in this portion of the study. A further reduction is made of those reactions to that of a fuel, oxidizer, and inert diluent mixture. The chemical reaction following Section (5.2) can be symbolized by

$$F + nO_x \rightarrow (n + 1)\ P \tag{7.6}$$

where the symbols F, O_x, and P denote the fuel, oxidizer, and product respectively. This reaction occurs between active species which are immersed in an inert gas bath. The chemical energy in Equation (7.1) can be written for the reaction (7.5) in the simple form of

$$-\sum \frac{h_i W_i}{C_p \rho} = \frac{Q \rho^n}{C_p} \left(\frac{C_{ox}}{M_{ox}}\right)^n k_{fr} \tag{7.7}$$

where Q is the heat release per unit mass for fuel, C_F and C_{OX} are the fuel and oxidizer concentrations in units of mass fraction, M_{OX} is the molecular weight of the oxidizer, and k_{fr} is the rate of reaction of the combustion process. In this form, the power (n + 1) is the order of the reaction. The rate of reaction is a function of temperature only and has the form of

$$k_{fr} = a\ T^c \exp\left(\frac{-E}{RT}\right) \tag{7.8}$$

where the symbol E is the activation energy of the reaction, a and c are constants, and R is the universal gas constant. Usually the pre-exponential factor is a constant. In Equation (7.7) the mass density appears explicitly so that Equation (7.1) is not entirely independent of density despite the transformation

of coordinates.

Thus an additional equation is required to close the system and this is the equation of state given by

$$p = \rho \frac{R}{M} T_e \theta \tag{7.9}$$

where p is the pressure, M the mixture molecular weight, and T_e the ambient temperature.

The system of equations is now complete for the determination of $\theta(\eta, t)$. The solution of this system is obtained by using a fully implicit finite difference scheme.

Characteristic Time

In the constant density case Equation (7.1) can be written in a non-dimensional form such that the system is dependent on two characteristic parameters. One of these dimensionless parameters is the ratio of activation energy to the wall temperature and the second is a characteristic time t_o. This characteristic time is useful here and is defined for a second order reaction by

$$\frac{1}{t_o} = \frac{E}{RT_w} \frac{Q}{C_p T_w} (\rho_e a) \frac{C_F C_{OX}}{M_{OX}} \exp\left(-\frac{E}{RT_w}\right) \tag{7.10}$$

The parameter t_o characterizes the behavior of the thermal ignition times of gas mixture in terms of its physical parameters. Thus it is inversely proportional to the heat release of combustion, the product of mass density of the mixture and pre-exponential factor of the rate constant, and the product of the fuel and oxidizer mixture. Moreover, (t_o^{-1}) is proportional to $\frac{E}{RT_w} \exp\left(-\frac{E}{RT_w}\right)$

which has a maximum at $\frac{E}{RT_w} = 1$ so that t_o decreases with $\frac{E}{RT_w}$ for $\frac{E}{RT_w} < 1$ and increases with increasing $\frac{E}{RT_w}$ for $\frac{E}{RT_w} > 1$. This parameter t_o is a useful means of extrapolation to unknown gas mixture from a given condition. Comparison with an actual solution is shown on Figure 7.1.

Numerical Results

The results for this special case considered in this section are summarized in Figures 7.1-7.6 compiled from a large number of numerical solutions of Equation (7.1) and its boundary conditions. The gas mixture is considered to be initially at room temperature and typical of the polymethylmethacrylate gas in Section 5.2. Furthermore, most of the results are for a pressure of 1/8 of an atmosphere. The pre-exponential factor a was taken to be equal to 10^7 cm^3/ mole sec and the exponent C is zero. Other data utilized in this section are given on the figures. The subscripts for the wall and ambient temperature T are w and e respectively. The ℓ function and the Prandtl number have been set to unity for this set of numerical results.

In the first two figures, Figures 7.1 and 7.2, the concentration of fuel has been kept constant and the inert and oxidizer concentrations have been varied. The results for the hot wall-cold gas are given on Figure 7.1 and the reverse case on Figure 7.2. Both figures show the ignition times as a function of the ambient concentration of oxidizer. It is remembered that ignition times can be defined in several ways. Two of the more useful definitions are utilized here. One definition is the time of occurrence of the first maximum in the gas temperature which gives a wall heat flux close to that of an adiabatic wall where no heat is transferred between the wall and the gas. A second definition is the time required for the peak gas temperature (after the

temperature has peaked within the gas) to achieve a prescribed ratio to the wall temperature. Results for both definitions are shown on Figures 7.1 and 7.2. The results show that as physically expected the ignition times vary inversely with the oxidizer concentration. In fact, this variation is given by the relation

$$t_{IG} \sim \frac{1}{C_{Ox}^{n}} \tag{7.11}$$

A least squares fit of the results indicate that n varies between 1.079 to 1.27 for the second order kinetics considered in this example. Equation (7.10) show that t_o, the characteristic time, varies inversely with the oxidizer concentration to the first power of n. The variation of t_o for the same conditions is also shown on these figures. The ratio of the ignition time to the characteristic time is almost a constant except for a slight variation due to the variable density and the V function. The quantitative effects of non-zero values of V are relatively small for the two values of V utilized in the computation. In the latter part of this report it will be seen that V can have an appreciable effect at other conditions. Thus the term in Equation (7.1) containing V has only a small effect for the results on Figures 7.1 and 7.2. A study of the magnitude of each term as time progresses indicate that initially the chemical energy production is small so that the initial solution is governed by the usual heat conduction equation and then increases to values comparable to the other terms as the temperature peaks. For very long times a steady state may develop whereby the chemical energy production is more or less in equilibrium with the heat conducted away from the source. The temperature does not run away to a large value due primarily to the decrease of density when the temperature rises. This can be seen from Equation (7.7) where the multiplicative density factor damps

any increase of the entire term with increasing temperature. In many of the variable density results this steady state has occurred for time of the order of 100 sec.

Figure 7.3 shows the variation of the ignition time with fuel concentration for a fixed oxidizer concentration. As expected, the ignition time is also inversely proportional to the fuel concentration. This variation of ignition time can also be represented by the relation

$$t_{IG} \sim \frac{1}{C_F^{\,n}} \tag{7.12}$$

where n is approximately 0.9. This value is close to the variation of t_o with the fuel concentration.

These results together with the proper values of t_o can be utilized in estimating the ignition times of gas mixtures at other conditions at fixed wall temperatures.

For contrast some results for a constant density assumptions are given in the next two figures. For constant density the equation can be scaled to contain only two parameters as given in Figure 7.4. The behaviors of the temperature with time and within the gas are given on the next two figures, Figures 7.4 and 7.5, for the hot wall-cold gas case. Figure 7.4 shows the development of the peak values with time. Since the gas is initially cold with respect to the wall an increment of time and energy flux from the wall is required to heat the gas to the point when the chemical energy generated starts to increase the temperature. The temperature peaks by this mean and starts to run away and tends to approach very large values for the constant density case

shown here. As mentioned before the effect of a variable density is to tend to level the peak temperature with time so that a steady state is developed. The effect of increasing the wall temperature is shown on Figure 7.4 resulting in an increase of the temperature in the gas layer. A typical set of temperature profiles is given on Figure 7.5 indicating the development of the peak temperature with time. This figure is characteristic of all the temperature behavior across the gas and with time. The normal coordinate across the layer has been scaled with respect to the square root of the time coordinate; thus there is a movement of the peak temperature away from the wall with increasing time. A correlation of ignition time results for constant density is given on Figure 7.6. The curve is valid for a constant value of the parameter (E/RT_w). This variation is typical for a constant density gas. Since the parameter (E/RT_w) is constant this curve can be interpreted as the effect of wall temperature on the ignition time. One notes that the ordinate θ_o is bounded above by the value of E/RT_w for very large wall temperature ratio. The two principal parameters for the constant density case are the activation energy of the reaction in the gas phase and the wall temperature ratio.

7.2 Ignition of Gas Mixture for Non-Uniform Mixture of Fuel and Oxidizer With Full Consumption and Diffusion

A fuel-oxidizer gas mixture with chemical reaction does not remain uniform with increasing time. Fuel consumption will change the concentration at each point of the mixture. Moreover, diffusion of each of the gas species will destroy the uniformity of the mixture. These effects are considered in this section for a stationary mixture for given wall conditions. The system of equations valid for this case has been given already. The energy equation was given in the last section as Equation (7.1) with the boundary conditions (7.2).

The species concentration equations for the three species of fuel, oxidizer, and reaction product are given by Equation (3.13). The corresponding boundary conditions are prescribed species concentration since V is set to zero for this section. The general case of $V \neq 0$ is treated in the following chapter where coupling of the gas and solid are accounted for. Thus the species boundary conditions are:

$$\eta = \eta_{max}: \qquad C_F = 0, \qquad C_{OX} = C_{OX\infty} \tag{7.13}$$

$$\eta = 0: \qquad C_F = C_{F_w}, \qquad C_{OX} = C_{OX_w}$$

As before, an inert species is contained in the formulation. The species equation from Equation (3.13) is simply written in the form:

$$\frac{\partial C_i}{\partial t} + V \frac{\partial C_i}{\partial \eta} = \frac{\partial}{\partial \eta}\left(\frac{\ell}{P_r} L_e \frac{\partial C_i}{\partial \eta}\right) + \frac{W_i}{\rho} \tag{7.14}$$

One notes that V is set to zero. As in the previous section the numerical results are obtained for constant values of the ℓ, P_r, and L_e functions. Appropriate values are 1 for ℓ and P_r and 1.4 for L_e. The chemical rate of production of mass from chemical reactions has already been given in the previous section. There are now sufficient equations and boundary conditions to consider the problem posed at the beginning of this section. This problem has been solved by the use of an implicit finite difference scheme. The solution involves the coupling of the temperature and species equation together with the subsidiary relations from chemical reactions. A sufficient number of cases has been solved to obtain expressions for the variation of ignition time with oxidizer concentration.

Numerical Results

Numerical results are again obtained for an ambient gas at room temperature at a pressure of 1/8 of an atmosphere. Chemical parameters are typical of the gas considered in the last section. Consider the cool gas with a hot wall first. The ignition times as defined before vary inversely with the oxidizer concentration as before. These variations with oxidizer concentration is shown on Figure 7.7. These curves bear some similarity to those on Figure 7.1. In fact, for the combination of activation energy of the gas reaction and fuel concentration the curves for $T_w/T_e = 1.5$ are almost the same. The variation of ignition times with oxidizer concentration can be represented approximately with a least square fit by the relation

$$t_{IG} \sim C_{OX}^{-1.2} \tag{7.15}$$

One notes that the ambient value of oxidizer concentation is used. The first peak variation shown on the same figure is almost the same as that given by Equation (7.15). The exponent in Equation (7.15) is about the same as that obtained for a uniform mixture. A hot gas-cold wall case is also given on Figure 7.7 for a gas only slightly hotter than the wall. As expected, ignition can occur more rapidly when the gas has a higher average temperature.

The development of the concentration profiles and the temperature profiles across the layer is given on Figure 7.9 for the hot wall-cold gas example. The growth of the peak temperature with time until ignition occurs shows a movement of the peak location away from the wall. The heat pulse will eventually pass through the entire layer. The peak temperature with fuel consumption and variable gas density does not appear to run away as time increases. For the

cases calculated a steady state is almost approached (but has not quite been attained - Figure 7.8). However, this aspect will be considered in detail in the next chapter when the solid is coupled with the gas phase activity.

7.3 Ignition of Gas Mixture of Uniform Composition of Fuel and Oxidizer Coupled With Pyrolyzing Solid

A gas mixture under the influence of fixed wall conditions has been considered in the last section. It was seen from the results that indications of ignition are that the temperature tends to run away as time progresses; a tendency for the temperature to approach a horizontal asymptote occur when fuel consumption is allowed. Thus it is expected that the behavior of gas mixtures with other heat loss mechanisms may be quite different. That is, the peak temperature may approach an asymptote so that sustained combustion occurs. In this section the next step in the complexity of this ignition and burning of solid material is taken. The gas mixture is assumed to be of a uniform composition and interacts with a combustible solid (typical plastic as discussed in the previous section) which is heated until it pyrolyzes and injects fuel into the ambient atmosphere of the gas mixture. The fuel reacts chemically with the oxidizer and releases heat back to the solid. Ignition is assumed to occur at some defined point; this can be considered as the point when a sustained and equilibrated peak gas temperature occurs for the interacting gas-solid system. Steady burning occurs when sufficient heat energy is generated to maintain the solid decomposition.

The energy equation for the temperature of the gas mixture of uniform composition has been given in Section 7.1 with the addition of the energy exchanges due to radiation as discussed in Section 3. It remains to consider

the equations involving the solid and its interaction with the gas.

The solid equations have been given by Equations (4.1) and (4.2). These two equations describe the temperature distribution of the decomposing plastic and the degradation rate. The interaction of the solid and gas is made at their common interface and the condition has been given by Equation (4.11). In this section only homogeneous gas phase chemical reactions are considered so that $B = 0$ in Equation (4.11). Thus there are two equations for the gas temperature and solid temperature which are related by the interface energy exchange. The method of solution utilized is the implicit finite difference one for both equations; the solutions are matched at each point along their interface to satisfy the condition (4.11).

In summary, the gas equation involves the two dimensions of time and the normal distance away from the solid surface and the solid equation is dependent on the time coordinate and the normal distance within the solid. This system of coordinates is depicted in Figure 3.1.

Numerical results have been obtained for one set of material constraints. The characteristics of the gas mixture have been assumed to be that in the last section so as to afford some basis for comparison. Results have been obtained for both solid materials in Table VI - only those for the Teflon solid are shown. Initially, the gas and solid are at the uniform temperature of $90^{\circ}F$. An external heating is imposed on the solid and the solid temperature (and the gas layer temperature next to the solid) starts to rise. Appropriate initial conditions for this situation before decomposition of the solid begins are derived in closed form for the finite difference method utilized for subsequent

times. With the progress of time the surface temperature of the solid rises to cause decomposition of the solid material. At this point fuel is injected into the ambient gas atmosphere and reacts with the oxygen there. Gas phase reaction rates increase with temperature and heat is released to cause a temperature peak within the gas layer. The creation of a gas temperature greater than the solid imposes an additional heat load on the solid. Subsequently, when this additional heat flux is sufficient to maintain the chemical reaction in the absence of the external heating the process is then in sustained combustion. An example of the development with time of the profiles of the gas and solid temperatures is shown on Figure 7.10. At early times the wall temperature is higher than any gas values and the gas mixture is being heated by the hot wall. Later, the release of chemical energy in the gas phase maximizes the distribution of the gas temperature as can be seen from the Figure. It is noted in most solid and gas combinations the transfer of heat is more rapid in the gas than in the solid. This can be seen also from the Figure.

Results of the history of peak gas temperature are shown on Figure 7.11 and 7.12 for different values of the atmosphere pressure and two compositions of the gas mixture. One notes the S shape of all these results; that is, a flat initial rise at early times with an occurrence of an inflection point and then an approach to a constant asymptote with increasing time. Thus it is seen that the heat transfer to the solid indeed limits the growth of the peak gas temperature with time. In two cases on Figure 7.12 the external heating was set to zero and the solution continues for a time duration of about 10 sec in one case and 25 sec for another. A constant peak temperature was maintained for this time indicating a possible sustained burning. The behavior of the wall

temperature with time follows that of the peak gas temperature except for a slight dip at the heat shutdown point to a second asymptote (cf Figure 7.13). Figure 7.14 shows the same behavior except that the wall temperature has not quite reached its second level for the time duration considered. It is interesting to note the behavior of the heat flux of gas mixture at the wall. This flux is shown on Figure 7.14 increasing with external heating and maintaining its value when external heat is shut down.

The effect of pressure on the ignition time has been obtained by determining the time of occurrence of a temperature ratio of 1.5 or by obtaining the first time the peak temperature has achieved a constant value. Both of these definitions are shown on Figure 7.15 together with the behavior of the peak temperature at the asymptote condition with pressure. The ignition time at the asymptotic temperature can be represented by the equation

$$t_{IG} = 1.3\ p^{-.9994} \tag{7.16}$$

where t is in sec and p in atmospheres. That is, t_{IG}, is inversely related to pressure by (-1) power. The ignition time obtained from the intersection of the asymptote with the rising temperature slope yields almost the same constants. Similarly, the peak temperature can be represented by

$$(T/T_e)_{PEAK} = 12.7\ p^{.265} \tag{7.17}$$

It is remembered that the constants are a function of the other parameters of the system.

For a given value of external heating and fuel-oxidizer composition the peak value of the temperature varies as $p^{.265}$. These two relations give

useful scaling factors for other conditions.

VIII. IGNITION AND BURNING OF MATERIAL WITH FUEL CONSUMPTION AND GAS PHASE DIFFUSION

In this section the results are given for the ignition and burning of one material typical of that of polymethylmethacrylate. The set of equations to be considered is given in Sections 3, 4, 5, and 6. As in the previous cases the material is heated from a low temperature to the point where ignition can occur and burning is initiated. The principal mechanisms for the propagation of heat to the virgin material that have been considered may be convection, heterogeneous reactions, internal heat conduction, and forward propagation of radiative flux from the flame. The two latter effects are not important when small elements of material are considered. Numerical results for the example of one mechanism of propagation, free convection, is used as an illustration.

The difference in the magnitude of gravity from zero causes free convection flow to be established along the material surface which sweeps the pyrolyzed products away and also convects heat energy downstream to be transferred into the solid.

8.1 Time Variation Without Spatial Changes

Consider first the development of the phenomenon at a given point on a piece of material at conditions for which there is no streamwise variation in any quantity. This case corresponds to that given in the last section but with the presence of free convection flow. The development of the surface and the gas peak temperatures (greater than the wall value) with time is given on Figure 8.1. The solid is being heated with a flux of 8.76 watts/cm^2. Both material and gas are at room temperature.

In the case shown on Figure 8.1 the atmosphere is oxygen gas with gas phase reaction constant such that $E/RT_e = 6.55$. As seen from the Figure the solid temperature rises and decomposition of the solid is gradually initiated. The difference in gravity does not effect the wall temperature at these times to any great extent. The gas temperature rises due to the exothermic gas phase reaction and the principal effect of the presence of free convection or gravity is to sweep the hot gases away resulting in a lower peak temperature than the zero gravity case (there is no streamwise variation). One notes that there is mass transfer from the surface material in all cases when any pyrolysis of the material occurs. The times at which the local peak temperature achieves the arbitrary defined ignition of 1.5 the wall temperatures are indicated on the Figure. They have the values of 18 and 26 sec for the zero gravity and normal gravity respectively. One notes from this Figure also that the rise in the peak temperature is more rapid at zero gravity than the normal gravity case and that an indication of a sustained burning is beginning to form. The effect of pressure with free convection flow is given on Figure 8.2. The gas phase reaction is increased by the larger pressure and therefore a larger peak value of the gas phase temperature is obtained. At atmospheric pressure the peak temperature ratio approaches a value of 9 and the corresponding value at a pressure of 1/8 atmosphere is only 5 at the time of 40 sec. The mass flux of the decomposed solid is about the same for this variation in presure. The variation of mass flux from the solid surface is shown next on Figure 8.3. In the cases which have been continued for a longer time all characteristics approaches an asymptote with time and a steady state is obtained. Indications of this is given by the leveling off of the peak temperature, the mass flux, and the surface values of the species concentration with time for the zero

gravity case.

The behavior of the species concentration at the surface of the material is given on Figure 8.4. As time progresses the oxygen concentration disappears at the surface and is replaced by the solid material pyrolysis products. The typical trend for all conditions is shown on this Figure. In the one case (one gravity, one atmosphere) where an approach to an asymptote is indicated the oxygen concentration forms an S-shaped figure. The layer of gas next to the surface is mostly fuel although diffusion has permitted oxygen to penetrate near to the material surface. A typical distribution of concentration profiles is shown on Figure 8.5. Thus fuel and products of chemical reactions dominates the region next to the material surface but drops off rapidly within a small distance from the surface. The corresponding temperature profiles in both the gas and solid are given on Figure 8.6 together with the corresponding velocity profile. The surface of the material is at the zero point as indicated on the Figure. The peak values of both the free convection velocity and the temperature are noted to occur at about the same location together with the peak in the concentration of reaction products. One notes that only a small layer of the plastic near the surface is affected by the decomposition at any given instant of time as evidenced from this Figure. It is remembered that the solid coordinate is non-dimensionalized by the virgin material thickness.

A number of cases were obtained for these conditions and these solutions appear to give a variation of ignition time with pressure as shown on Figure 8.7. Ignition time was defined by the gas peak temperature achieving a value of 1.5 of the wall temperature; thus ignition time as defined is a decreasing function of pressure and is least squares fitted by

$$t_{Ign} \sim p^{-.11} \tag{8.1}$$

with the constant of proportionality for the one gravity case of 47.3.

8.2 Spatial and Time Variation

The general case of the ignition and burning of a piece of material with spatial variations along the material surface in addition to the normal variation to the surface in both the gas and solid and with time variation in both the gas and solid phases is now considered. The solid material is oriented as described in the first section in such a way that the free convection gas flow proceeds upward along the surface for the gravity pointing down. The origin of coordinates is at the lower edge of the material. The region near X = 0 is heated externally and as the solid temperature rises a free convection flow is generated which flows in the positive X direction in the opposite direction of gravity. Thus any pyrolysis products in the gaseous form which react chemically with the ambient oxidizer are convected to the virgin material by this arrangement. A recapitulation of the method of analysis is made here. As mentioned in the first sections an implicit finite difference scheme is utilized for the time-dependent free convection gas flow and for the solid decomposition and temperature change. A matching at the gas-solid interface accounts for the various energy fluxes from mass transfer and chemical reactions to give a unique temperature there. As pointed out before the procedure involving the solution of the set of difference equations with the three independent variables is to sweep along the physical coordinates X and up and down the y coordinate for an increment of time t.

The numerical example selected for discussion is as considered in Section 8.1. A piece of solid material of length 7.63 cm and thickness of 2.54 cm typical of those selected for laboratory experimental investigations is considered. A uniform heat loading of 29.2 watts/cm^2 is imposed over half of the material surface starting from X = 0. Thus the latter half of the material surface, X > 3.81 cm, is not heated externally. The gas is at the ambient room temperature at the initial time, whereas the solid has been heated uniformly to 850°R. With this heat loading at the front end of the material and the difference in gas-solid temperature, a free convection flow is immediately generated. This initial phase involves heating of the cool gas layer by the solid and a slow decomposition of the solid (mostly at the surface); subsequently, there is a mass transferred of combustible pyrolysis products to the gas phase. Chemical reaction of these products with the oxidizer lead to additional gas temperature rises. Free convection plays an important role in convecting the hot gases downstream to heat the virgin material. The development of the surface temperature with time is shown on Figure 8.8 at several locations of the surface. As is to be expected, the temperature is highest at the front end of the material where the imposed heat flux is located and lowest toward the back end. The back end is heated primarily by the exothermic reaction of the fuel and oxidizer gases. For the length of time considered in the example this generated heat flux is only a fraction of the imposed value and this is reflected in the different rates of surface temperature rise at the various spatial locations.

With continuous chemical reactions between the fuel and oxidizer the gas temperature begins to rise and overshoots the material temperature. One notes

that the gas temperature is affected not only by the local conditions at the material surface but also by the heat energy convected from upstream. The peak temperature in the gas is shown on Figure 8.9 for the spatial locations indicated; its value is a number of time higher than the surface temperature. The point where the peak gas temperature is 1.5 times the local wall temperature is indicated by the cross. The heat flux causing the temperature rise toward the back end of the material is shown on Figure 8.10 as a fraction of the imposed heat flux. It is seen that the gas is receiving heat energy from the heated solid at the early time and subsequently returns energy to the solid with increasing time and distance. The amount of material loss due to depolymerization of the solid is given by Figures 8.11 and 8.12. The values of the mass flux are within the usual boundary layer limits. Figure 8.12 shows the linear rate of loss of material with the inverse of surface temperature. This is a useful quantity indicative of the burning rate of the material normal to its surface. Due to the heat transfer characteristics and the activation energy of the decomposition process of the plastic, only a relatively thin layer of the solid near the surface is heated. Thus its mass density changes mostly at the surface. Some idea of this change is given on Figure 8.13.

The variation of species concentrations at the surface of the material is shown on Figure 8.14. It shows the same form as in the previous section. Oxygen rapidly disappears with increasing time as more pyrolysis product enter the boundary layer. Since the mass flux of material transferred is relatively small a thin layer of material species and their products formed from reaction with the ambient oxidizer is contained in the immediate region of the surface.

The peak convection velocity is given on Figure 8.15 and increases with

time with the changes in surface temperature. The local free convection velocity is established by the difference of the local and the ambient temperatures and by its upstream value. Since the front portion of the material is at a higher temperature relative to the back part a free convection flow is established there and driven forward.

An idea of the flame spreading rate is a useful criterion for the comparison of the burning characteristics of different materials. Flame spread rate depends on the sum of the individual processes such as thermal response of the system, chemical reactions, etc., occurring in the coupled gas-solid system. However, it is controlled by the slowest process, that is, the one which requires the longest time. As mentioned in the last section the flame spreading mechanism of prime importance is the heating of the material surface ahead of the flame [Tarifa et al (1967)]. For small flames in the environment considered herein the dominant process of flame spread is due to convection and can be given by the condition that a characteristic such as the surface temperature or peak gas phase temperature reaches a pre-defined value at a given location when the flame has spread to that point [Tarifa et al (1967,1969), McAlevy (1969)]. Experimentally, the spread rate is determined in most cases by visual observation of the speed of travel of the flame, e.g., the flame's light emission. In the time and spatial analysis as considered herein the combustion phenomenon is a continuous one and one useful definition for the measure of the flame spread rate is that corresponding to the observation of the gas phase ignition occurrence at a given location. With this criterion the flame spread rate for this case is found to be 12.2 in/sec remembering that the material is burning upward in the opposite direction to the gravity vector. Experimental data

by Kuchta (1967) reports a difference in the flame spread rate in burning upward or burning downward; burning upward flame spread is about a factor of 40 higher than the burning downward rate. If consideration is given to this fact then the value as calculated is of the same order of the experimental values determined by McAlevy (1969).

It is remembered that flame spread rate is usually observed as a steady state condition when the system has approached a sustained combustion. The ignition times as defined by the latter condition would decrease the spread rate slightly. Results for a value of acceleration of gravity 3 times the normal value of 32.2 ft/sec^2 shows that the ignition times occurs at an earlier X and at an earlier time but only slightly.

IX. CONCLUDING REMARKS

An analytical model of the ignition and burning of plastic material for the coupled gas and solid phases subjected to free convection currents and in an environment of a space cabin atmosphere has been formulated and reduced to a form susceptible to numerical treatment. Combustion in the gas phase together with pyrolysis of the solid material is considered in the model with finite rate chemical reactions dominating the behavior of the phenomena considered. A time-dependent problem with two spatial coordinates is treated. The solution to the problem is obtained by the implicit finite difference method. Energy transfer between the gas and solid at the interface govern the behavior of the time dependent problem; in particular, radiation of the gas phase is included.

The principal premise of this study is that ignition and burning of plastic material is due to the exothermic energy release in the gas phase coupled with its interaction with a pyrolyzing solid. This energy release is governed by the heat conducting diffusing oxidizer and fuel species characteristics including that of convection currents due to temperature differences. Results from the study confirm the important role of the coupled interaction of the gas and solid in establishing the ignition of the system and the subsequent development to a steady burning process. By defining the ignition time as that required for the peak gas phase temperature to achieve a multiple of the material surface temperature the combustible quality of a gas-solid system becomes determinable. It is shown by this study that the ignition times are much longer (correctly) when the early time gas-solid interaction is accounted for.

The effect of free convection on the ignition and burning has been

shown. Free convection currents due to gas density differences is an effective means of moving hot gases to and away from the vicinity of the virgin material. Thus the parameter of importance in determining the ignition of material at a given location is the ratio of the flow time to the chemical time. A number of cases with no streamwise variation along the surface of the material have been studied in detail. Physical consideration imply that these cases correspond to the behavior of the gas-solid system in which each point along the surface remains identical to any other one. These results show that under this condition the ignition times increase with increasing values of the ratio of actual acceleration to normal gravity. Relations between the ignition times and environmental parameters such as pressure and gas composition have been obtained. These results are a function of the important material parameters such as the activation energy of the gas phase reaction and the activation energy of the solid depolymerization process. Secondary influences are the thermodynamic properties of the gas and solid and the transport characteristics of the gas. The continuance of these solutions with time have uncovered an interesting feature. The development has led to a steady state condition whereby a sustained burning persists without assistance from external heating. Comparison of the times of this occurrence with ignition times shows a close relationship and behavior with environmental parameters. Thus a unique ignition time can be defined as that corresponding to the point of sustained buring at steady state conditions. These new times are much longer.

For the general case in which streamwise variations along the surface coordinates are permissible, results show the effectiveness of the flow due to buoyancy in convecting the hot gases downstream and pre-heating the virgin

material. That is, these hot gases ignite downstream and subsequently heat the solid there; the time for the gas to ignite downstream has been obtained. The times for the occurrence of each phenomenon, as such mass transfer and heat penetration are obtained and can be used for the determination of an overall flame spread rate. In addition the distributions of species concentration show the extent of the motion of the combustion products away from the material surface. The study is capable of mapping and quantifying other species concentration which may be of importance for other uses, for example, the distribution of toxic gases.

REFERENCES

Adler, J. and Enig, J. W., "The Critical Conditions in Thermal Explosion Theory with Reactant Consumption", Combustion and Flame 8, 97-103, June 1964.

Bauer, S. H., How, K. C., and Resler, Jr., E. L., "Single-Pulse Shock-Tube Studies of the Pyrolysis of Fluorocarbons and of the Oxidation of Perfluoroethylene", Phys. of Fluid Supplement 1 (1969).

Browne, W. G., "Thermodynamic Properties of Some Ablation Products From Teflon Heat Shields in Air", GE TIS 65SD5315 (1965).

Browne, W. G., "Thermodynamic Properties of Some Diatoms and Diatomic Ions at High Temperatures", G.E. Memo 8 (1962).

Browne, W. G., "Thermodynamic Properties of Some Ablation Products From Plastic Heat Shields in Air", G.E. Memo 11 (1964).

Browne, W. G., and Carabetta, R., Private Communication, 1970.

Brandrup, J. and Immergut, E. H., eds., Polymer Handbook, Chaps. V-1 and V-5, Interscience (1966).

Cess, R. D.,"The Interaction of Thermal Radiation with Conduction and Convection Heat Transfer", Advances in Heat Transfer, Volume 1 (1964).

Colwell, J. E. and Wachi, F. M., "An Investigation of the Tetrafluoroethylene-Oxygen Flame", Aerospace Corp. Report No. TDR-469 (5250-40)-16 (1965).

Cochran, T. H., Masica, W. J., "An Investigation of Gravity Effects on Laminar Diffusion Flames", Thirteenth Symposium on Combustion, August 1970.

Crank, J. and Nicolson, P., "A Practical Method for Numerical Evaluation of Solutions of Partial Differential Equations of the Heat Conduction Type", Proc. Camb. Phil. Soc., Volume 43, p. 50 (1947).

Fenimore, C. P. and Martin, F. J., "Flammability of Polymers", Combustion and Flame 10, 135-139, 1966.

Fenimore, C. P. and Jones, G. W., "Modes of Inhibiting Polymer Flammability", Combustion and Flame 10, 295-301, 1966.

Fenimore, C. P. and Jones, G. W., "Decomposition of Burning Teflon, Polytetrafluoroethylene", GE TIS 68-C-138, 1968, J. of Applied Polymer Science (1969).

Fenimore, C. P., "Stability of CF_4 and Its Yield in C_2F_4 Flames", GE TIS 68C231, GERDC Schenectady (1968).

Frank-Kamenetskii, D. A., "Diffusion and Heat Transfer in Chemical Kinetics", Plenum Press (1969).

Griskey, R. G., Din, M. W., et al, "Thermodynamic Properties of Polymers. Part 5, Polymethyl methacrylate", Modern Plastics, Volume 43, 103-105 (1966); also, Volume 44, 134-138 (1967).

REFERENCES (Continued)

Ham, G., ed., "Vinyl Polymerization", Chap. 8, Heats of Polymerization and Their Implication. (R. M. Joski and B. J. Zwolinski), M. Dekker, New York (1967).

Hermance, C. E., Shinnar, R., and Summerfield, M., "Ignition of an Evaporating Fuel in a Hot, Oxidizing Gas Including the Effect of Heat Feedback", Astro. Acta 12, 95-112, 1966.

Hermance, C. E. and Kumar, R. K., "Gas Phase Ignition Theory for Homogeneous Propellants Under Shock Tube Conditions", AIAA Journal, Volume 8, No. 9, Sept., pp. 1551-1558 (1970).

Hicks, B. L., "Theory of Ignition Considered as a Thermal Reaction", J. Chem. Phys., 22, 414-429, 1954.

Hottel, H., "Radiant Heat Transmission", Chap. 4 of Heat Transmission by McAdams, McGraw Hill (1954).

Isoda, H. and Kumagi, S., "New Aspects of Droplet Combustion", 7th International Symposium of Combustion, 523-531, 1959.

JANAF Table, 1964.

Jellinek, H., "Degradation of Vinyl Polymers", Academic Press (1955).

Kimzey, J. H., et al, "Flammability in Zero-Gravity Environment", NASA TR-R-246, 1966.

Kumar, R. K. and Hermance, C. E., "Ignition of Homogeneous Solid Propellants Under Shock Tube Conditions: Further Theoretical Development", AIAA Journal, Volume 9, No. 8, August, pp. 1615-1620 (1971).

Madorsky, S., Thermal Degradation of Organic Polymers, Interscience, 1964.

Martin, F. J., "A Model for the Candle-like Burning of Polymers", GE Report No. 67-C-006, 1967.

Martin, S., "Diffusion-Controlled Ignition of Cellulosic Materials by Intense Radiant Energy", 10th Int. Symp. of Combustion, 877-896, 1965.

McAlevy, R. F. and Magee, R. S., "The Mechanism of Flame Spreading Over The Surface of Igniting Condensed-Phase Materials", 12th Symposium on Combustion, The Combustion Institute (1969).

Merzhanov, A. G. and Averson, A. E., "The Present State of the Thermal Ignition Theory", Combustion and Flame, Volume 16, No. 1, Feb. (1971).

Mullins, B. P. and Penner, S. S., Explosions, Detonations, and Flammability and Ignition, Pergamon Press, 1959.

REFERENCES (Continued)

Price, E. W., et al, "Theory of Ignition of Solid Propellants", AIAA Journal, 4, 1153-1181, 1966.

Semenov, N., Some Problems in Chemical Kinetics and Reactivity, Volume II, Part IV, Princeton University Press, Princeton, 1959.

Simmons, R. F. and Wolfhard, H. G., "Some Limiting Oxygen Concentrations for Diffusion Flames in Air Diluted with Nitrogen", 1, 155-161, 1957.

Squire, W., "A Mathematical Analysis of Self-Ignition", Combust. Flame, 7, 1-8, 1963.

Siegel, R., "Effects of Reduced Gravity on Heat Transfer", Advances in Heat Transfer, Volume 4, 1967.

Tarifa, C. S. and Torralbo, A. M., "Flame Propagation Along the Interface Between a Gas and a Reacting Medium", Eleventh Symposium Combustion, The Combustion Institute, 1967.

Tarifa, C. S., et al, "On the Process of Flame Spreading Over the Surface of Plastic Fuels in an Oxidizing Atmosphere", 12th Symposium of Combustion, The Combustion Institute, 1968.

Thomas, P. H., "Effect of Reactant Consumption of the Induction Period and Critical Conditions for a Thermal Explosion", Proc. Roy. Soc. (London) 262A, 192-206, 1961.

Wagner, W. H. and Griskey, R. G., "Thermodynamic Properties of Polymers. Part 9, Polytetrafluoroethylene", Modern Plastics, Volume 44, 134-138 (1967).

TABLE V-1.

	TEFLON	POLYMETHYMETHACRYLATE
Mol. Wt.	100.022	100.11
Density	2.162 g/cm^3	1.185 g/cm^3
ΔH_f, monomer gas	-154.179 (JANAF) kcal/mole	- 82.2 (HAM) kcal/mole
ΔH_f, solid	-193.5 (JANAF) kcal/mole	-103.6 (HAM) kcal/mole
Degradation Rate		
Order	1	1
Frequency	3.24×10^{20} sec^{-1} (MADORSKY)	2.82×10^{9} sec^{-1} (JELLINEK)
Activation Energy	80.5 kcal/mole	31. kcal/mole

TABLE V-2.

TEFLON SOLID PROPERTIES (GRISKEY, GE, WAGNER)

Heat Conductivity, k, ft.lb/ft.sec^{o}R

Heat Capacity, C_p ft.lb/lb^{o}R, and

Enthalpy, h, ft.lb/slug

T (^{o}R)	k	C_p	h
400	.032	140	-9×10^{7}
600	.0358	186.5	-8.87×10^{7}
800	.0420	204	-8.75×10^{7}
1000	.0506	218	-8.62×10^{7}
1200	.0587	249	-8.45×10^{7}
1400	.0666	272	-8.28×10^{7}
1600	.077	292	-8.08×10^{7}
1800	.0831	311	-7.88×10^{7}
2000	.0885	334	-7.68×10^{7}

LIST OF FIGURES

LIST OF FIGURES

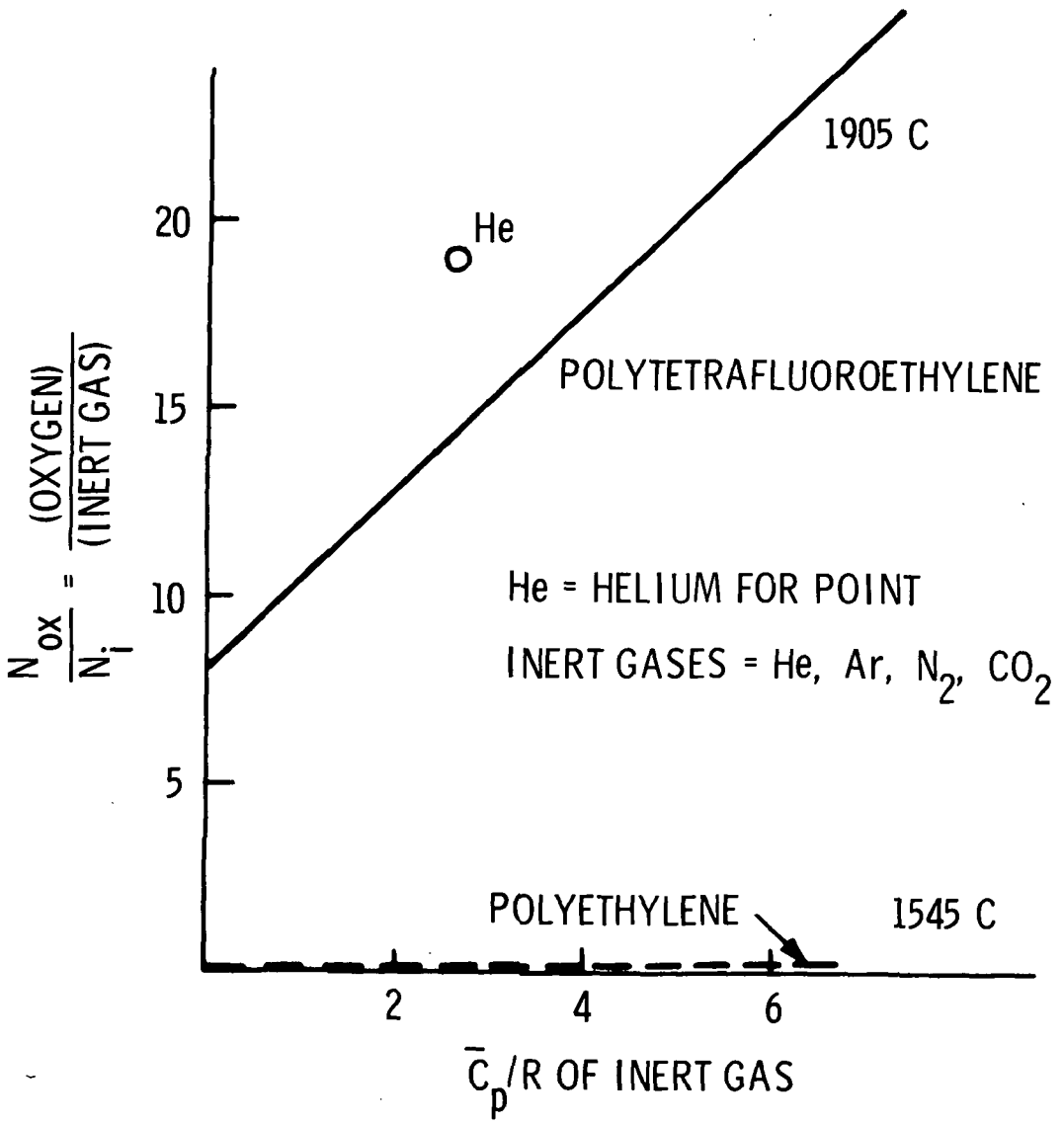

FIGURE 1.1 OXYGEN INDEX FOR SUSTAIN BURNING FOR TWO PLASTICS

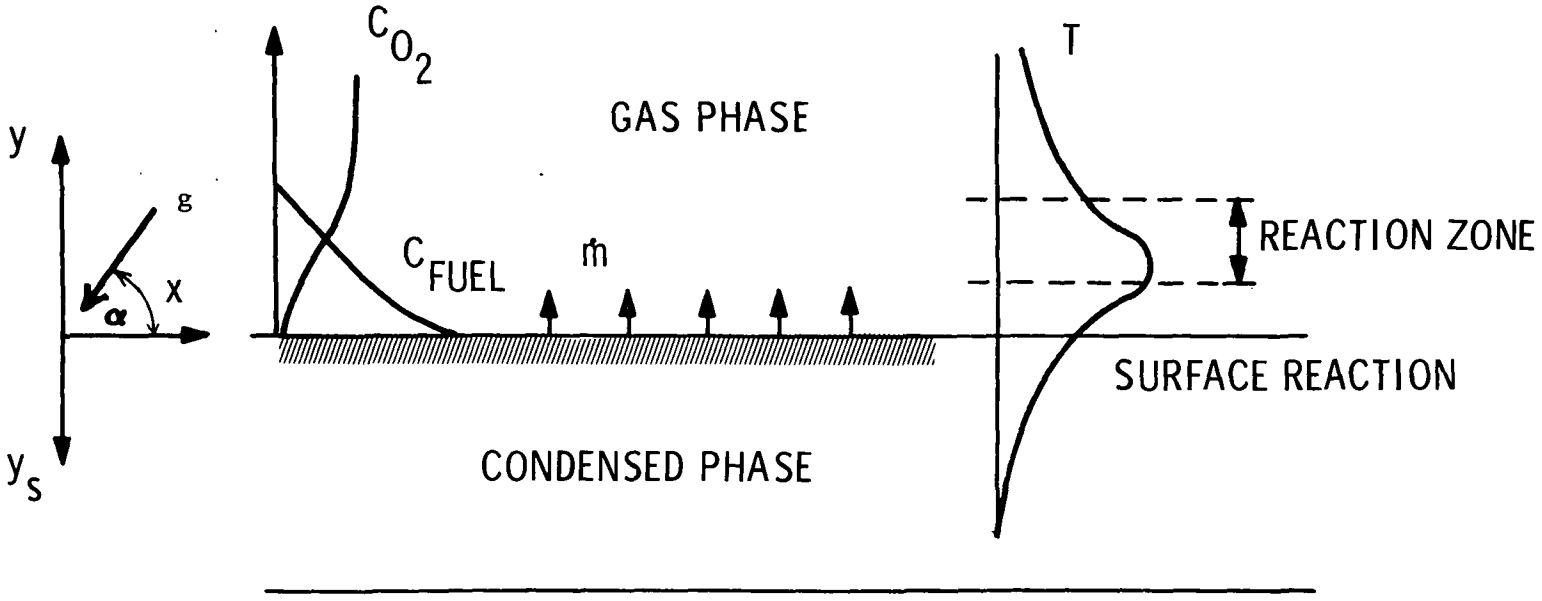

FIGURE 3.1 GAS PHASE AND CONDENSED PHASE MODEL FOR IGNITION AND BURNING OF COMBUSTIBLE MATERIAL

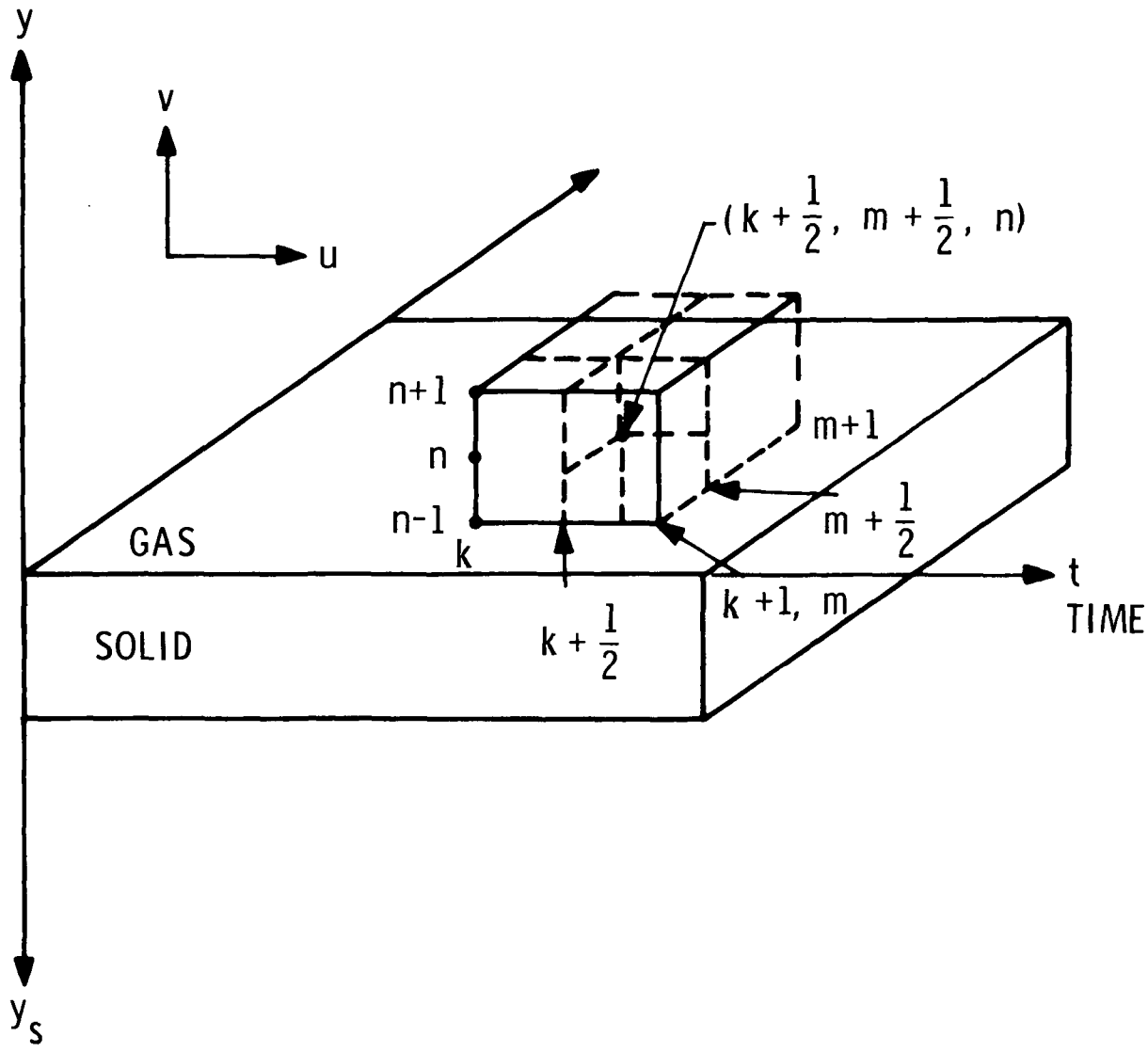

FIGURE 3.2 GRID FOR FINITE DIFFERENCE SCHEME

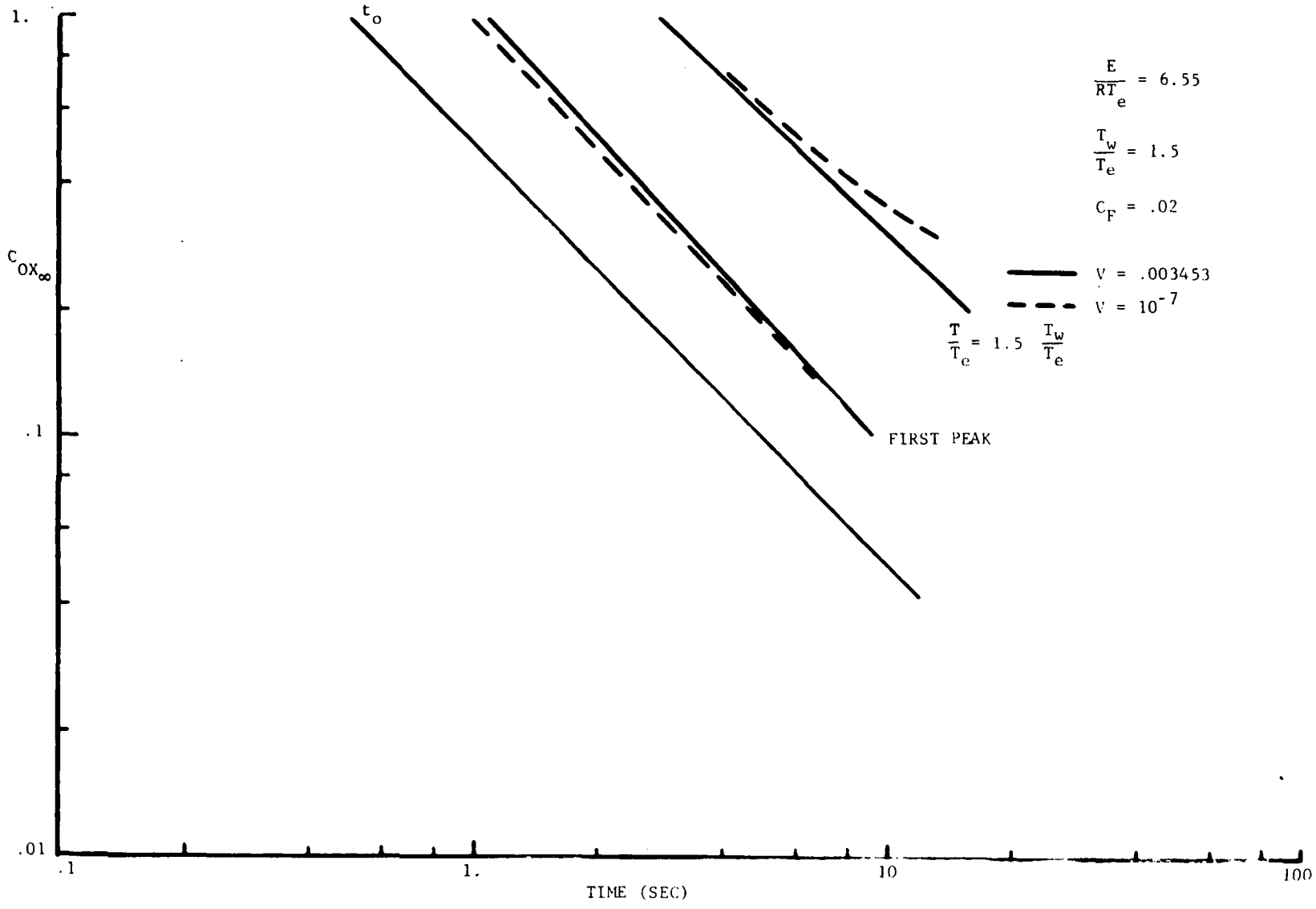

FIGURE 7.1 IGNITION TIME OF GAS MIXTURE OF OXYGEN, FUEL AND INERT DILUENT

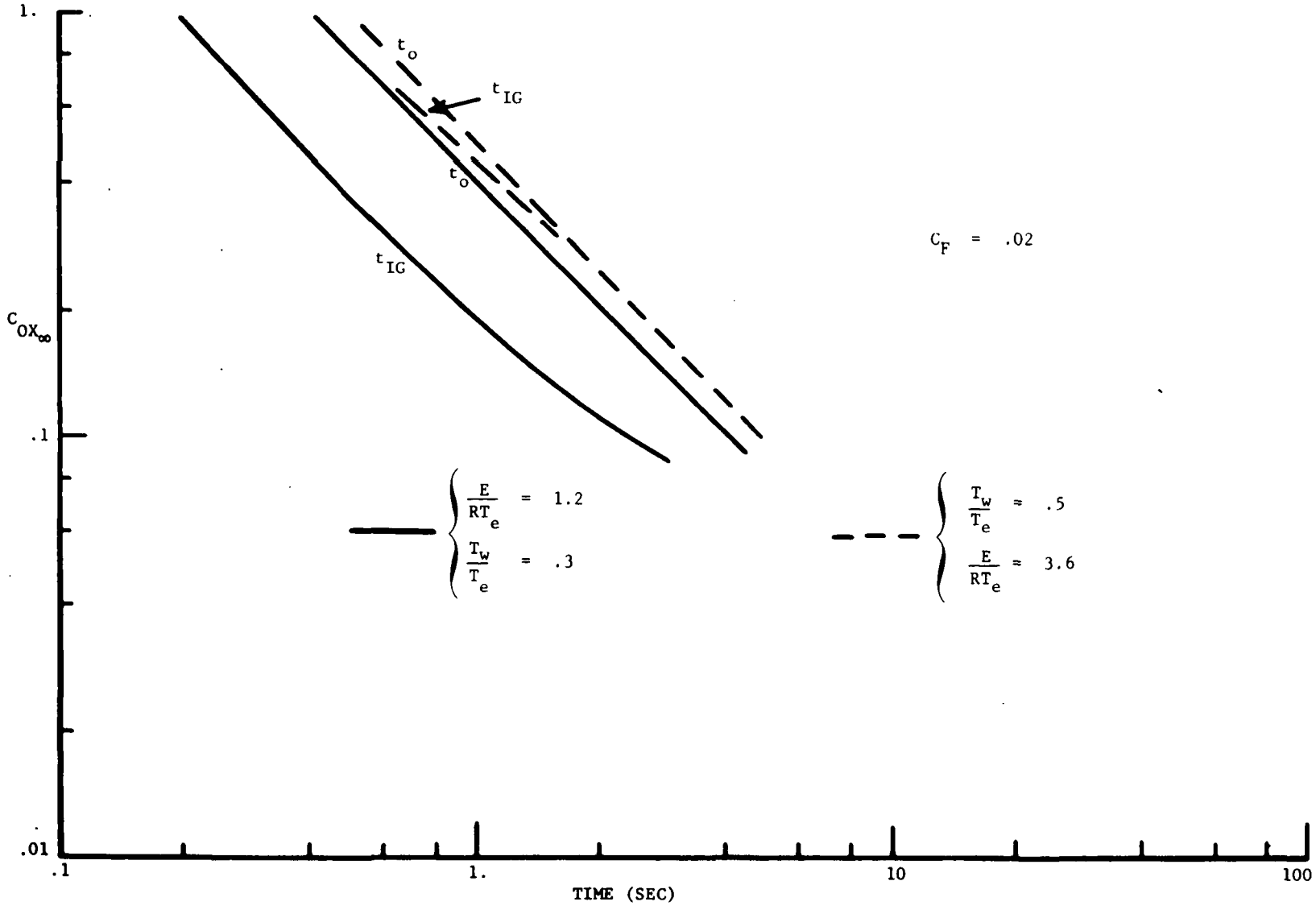

FIGURE 7.2 IGNITION TIME OF GAS MIXTURE OF OXYGEN, FUEL AND INERT DILUENT

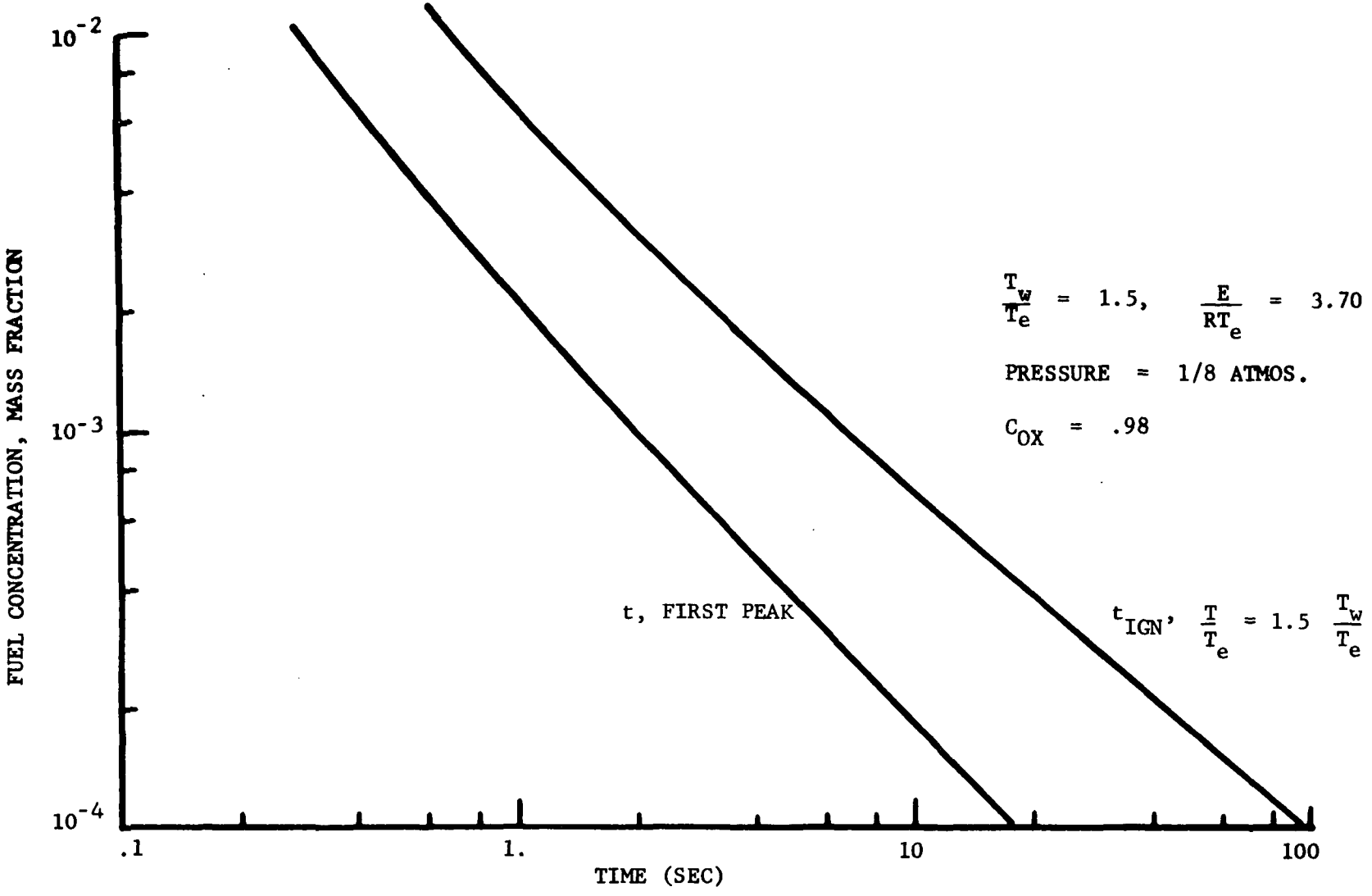

FIGURE 7.3 IGNITION TIME VARIATION WITH FUEL CONCENTRATION

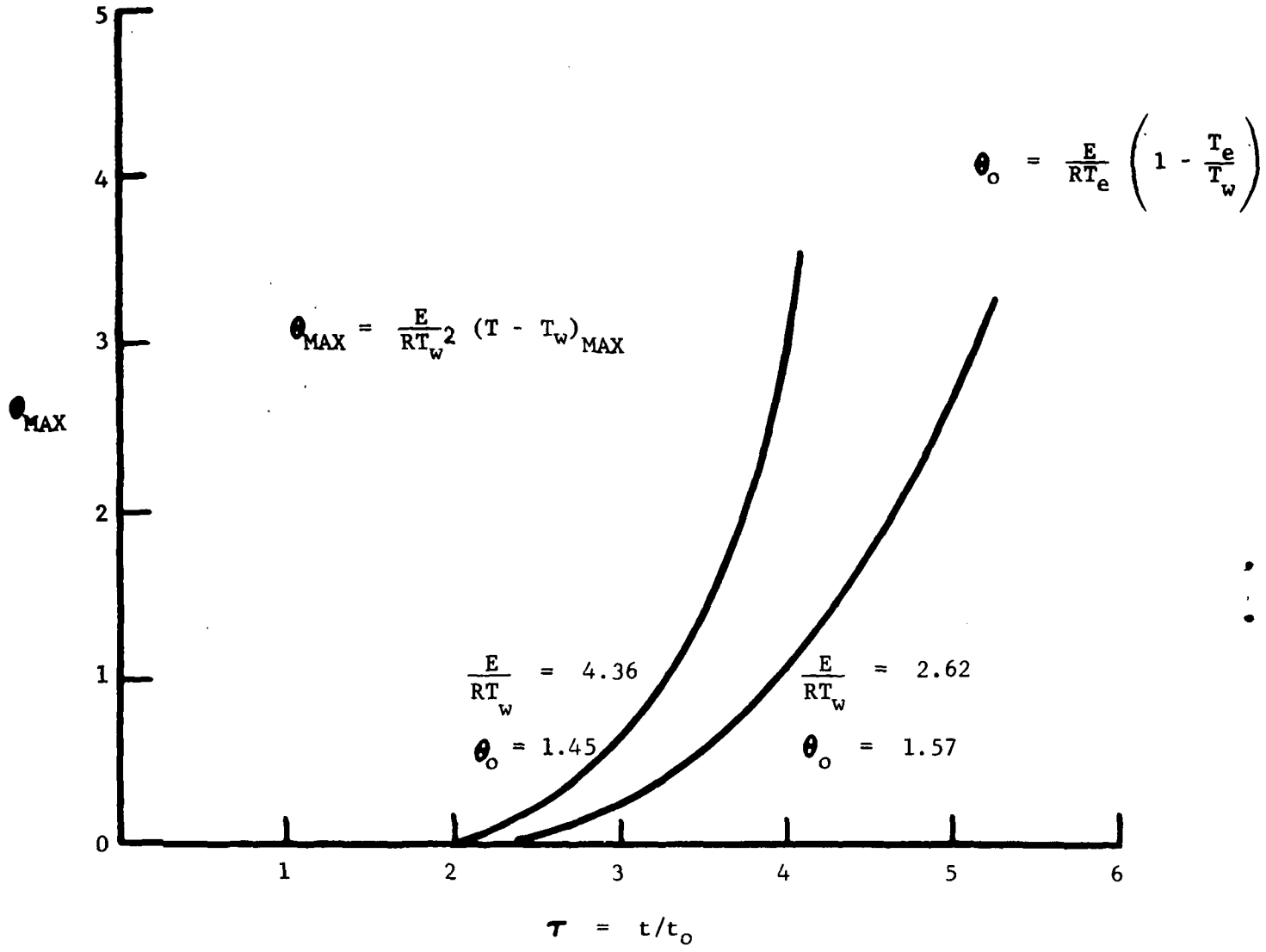

FIGURE 7.4 PEAK VALUE OF TEMPERATURE RATIO DEVELOPMENT WITH TIME, CONSTANT DENSITY

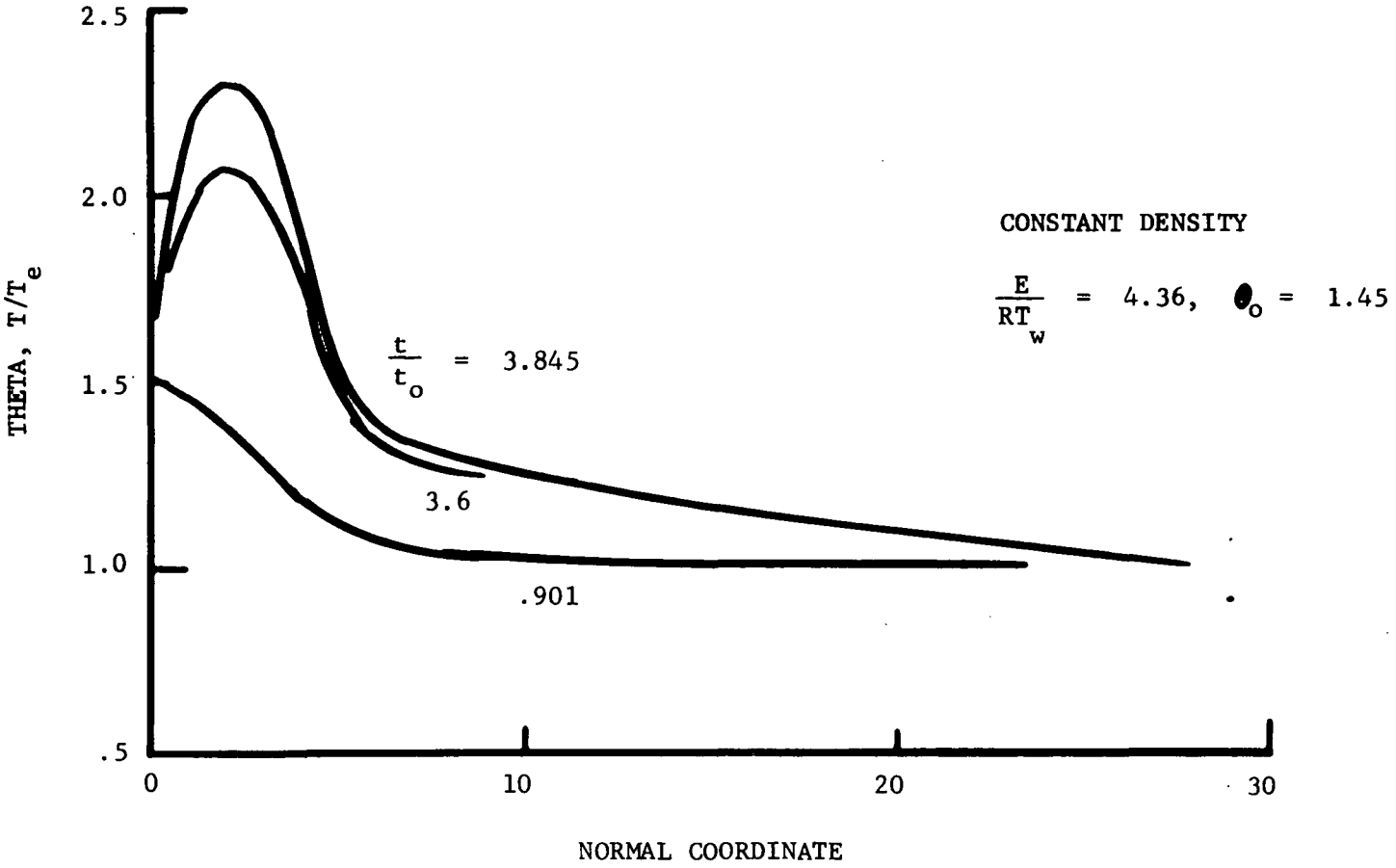

FIGURE 7.5 TEMPERATURE PROFILES DEVELOPMENT WITH TIME

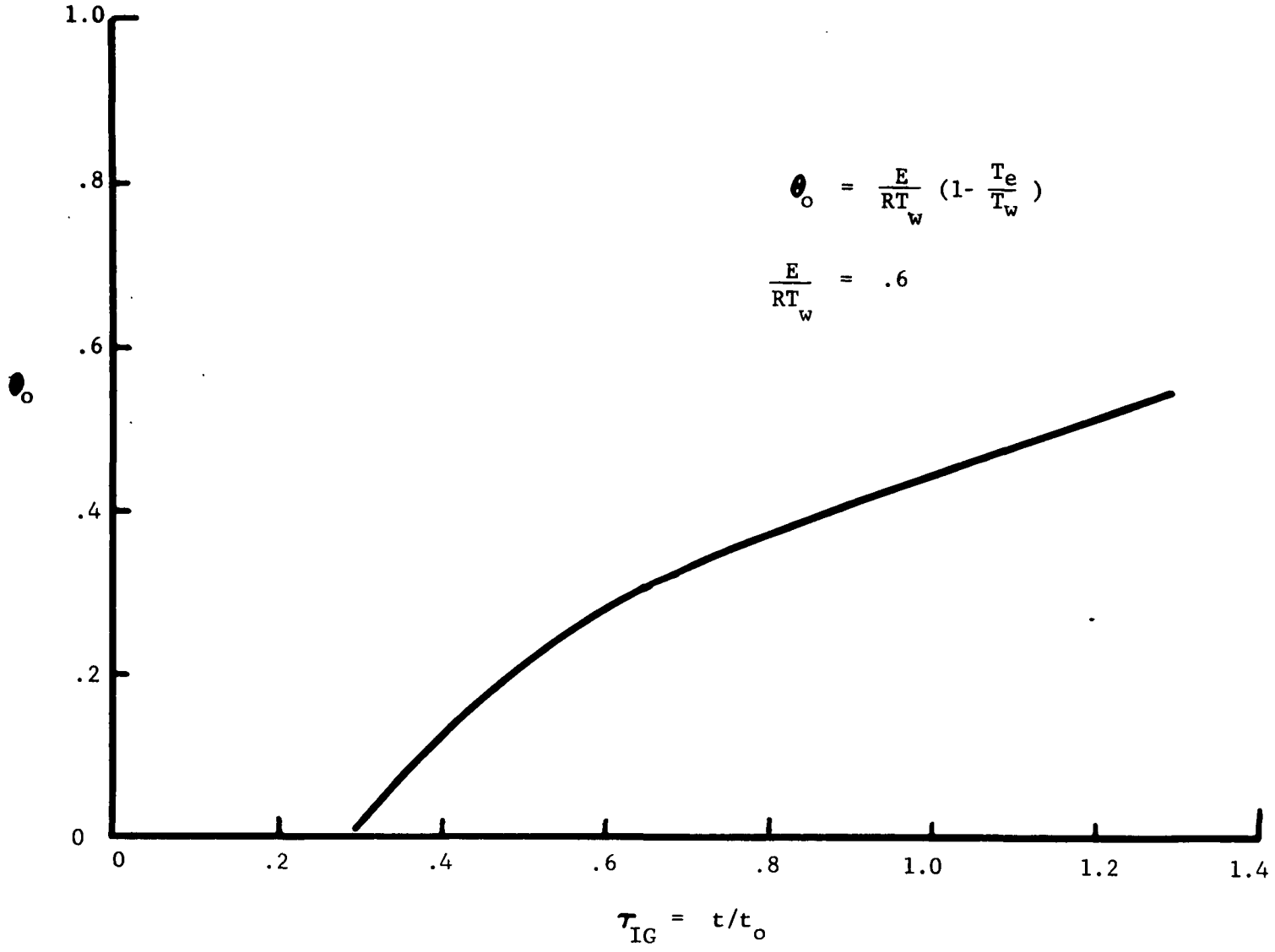

FIGURE 7.6 IGNITION TIME FOR FUEL-OXIDIZER MIXTURE, CONSTANT DENSITY

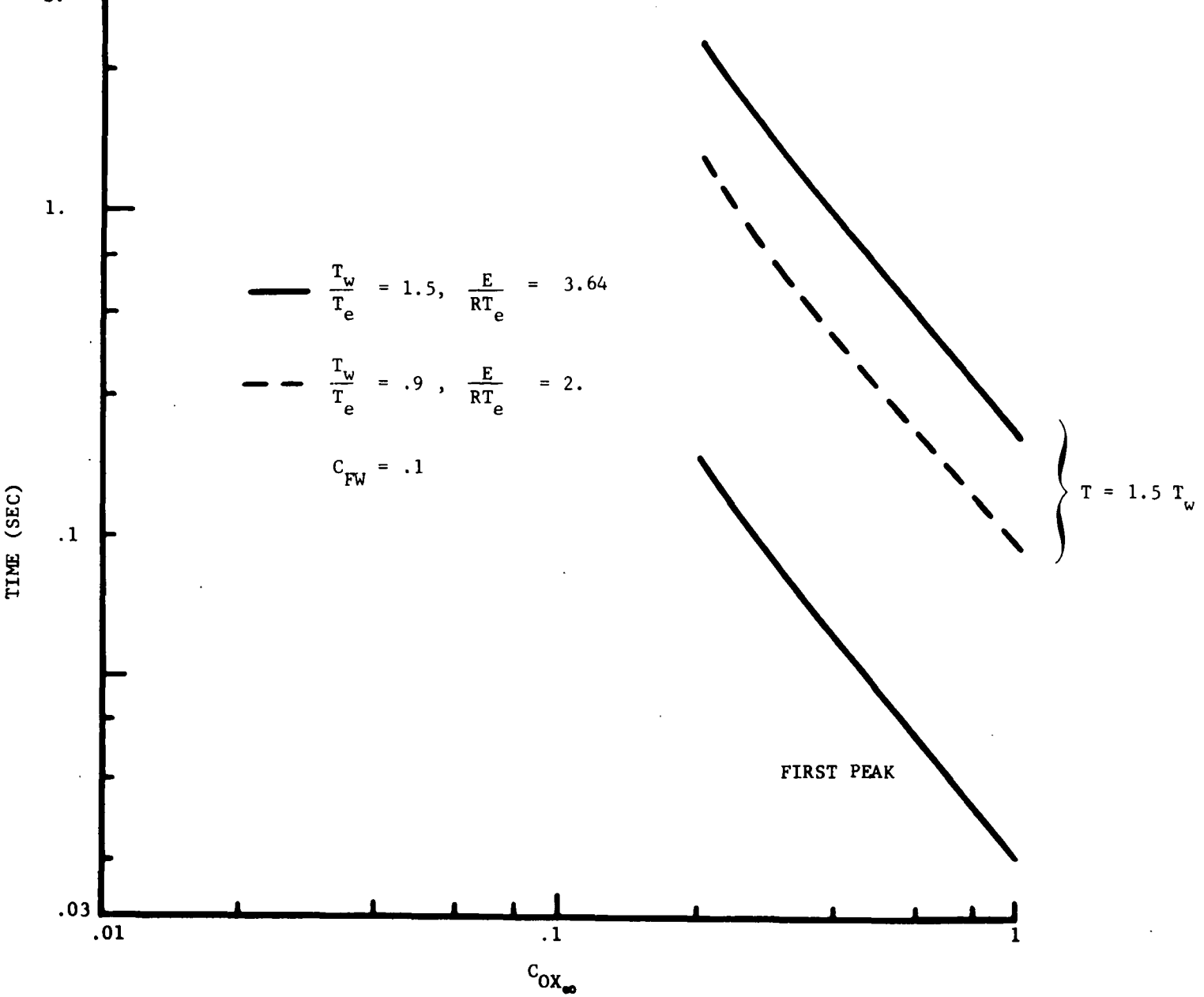

FIGURE 7.7 IGNITION TIME OF NON-UNIFORM GAS MIXTURE FOR DIFFERENT OXIDIZER CONCENTRATION

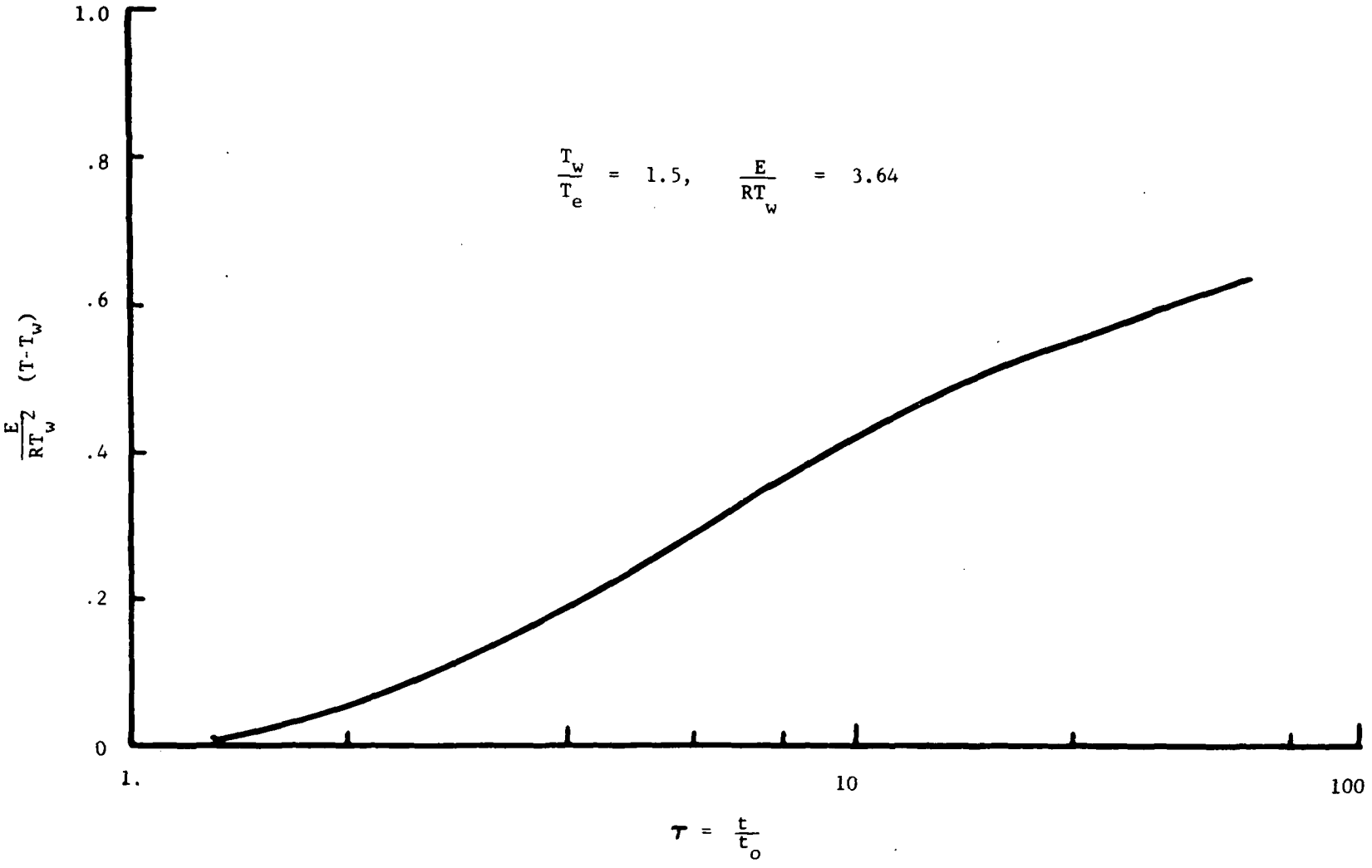

FIGURE 7.8 PEAK TEMPERATURE DISTRIBUTION WITH TIME

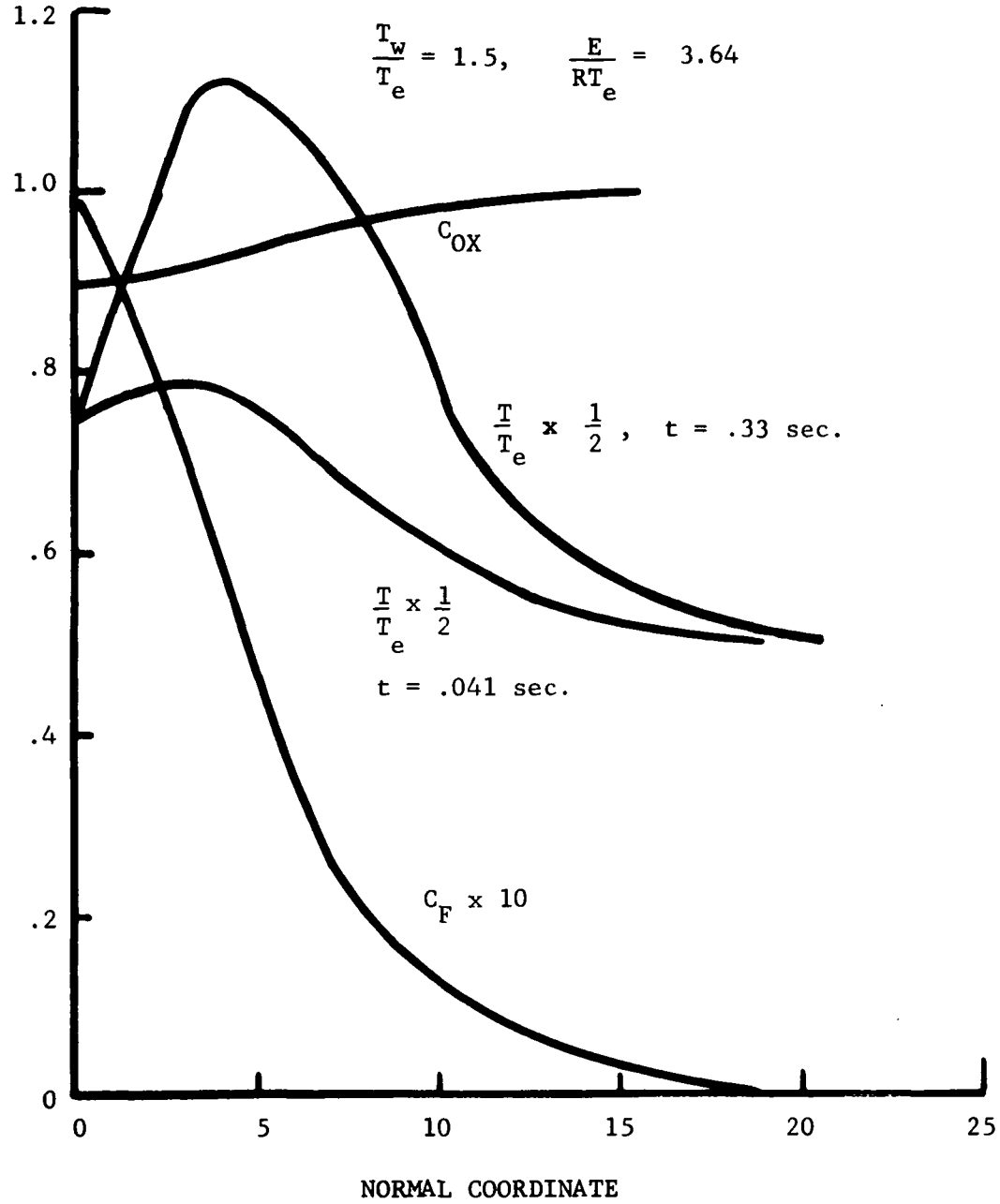

FIGURE 7.9 TEMPERATURE AND CONCENTRATION PROFILES FOR NON-UNIFORM GAS MIXTURE

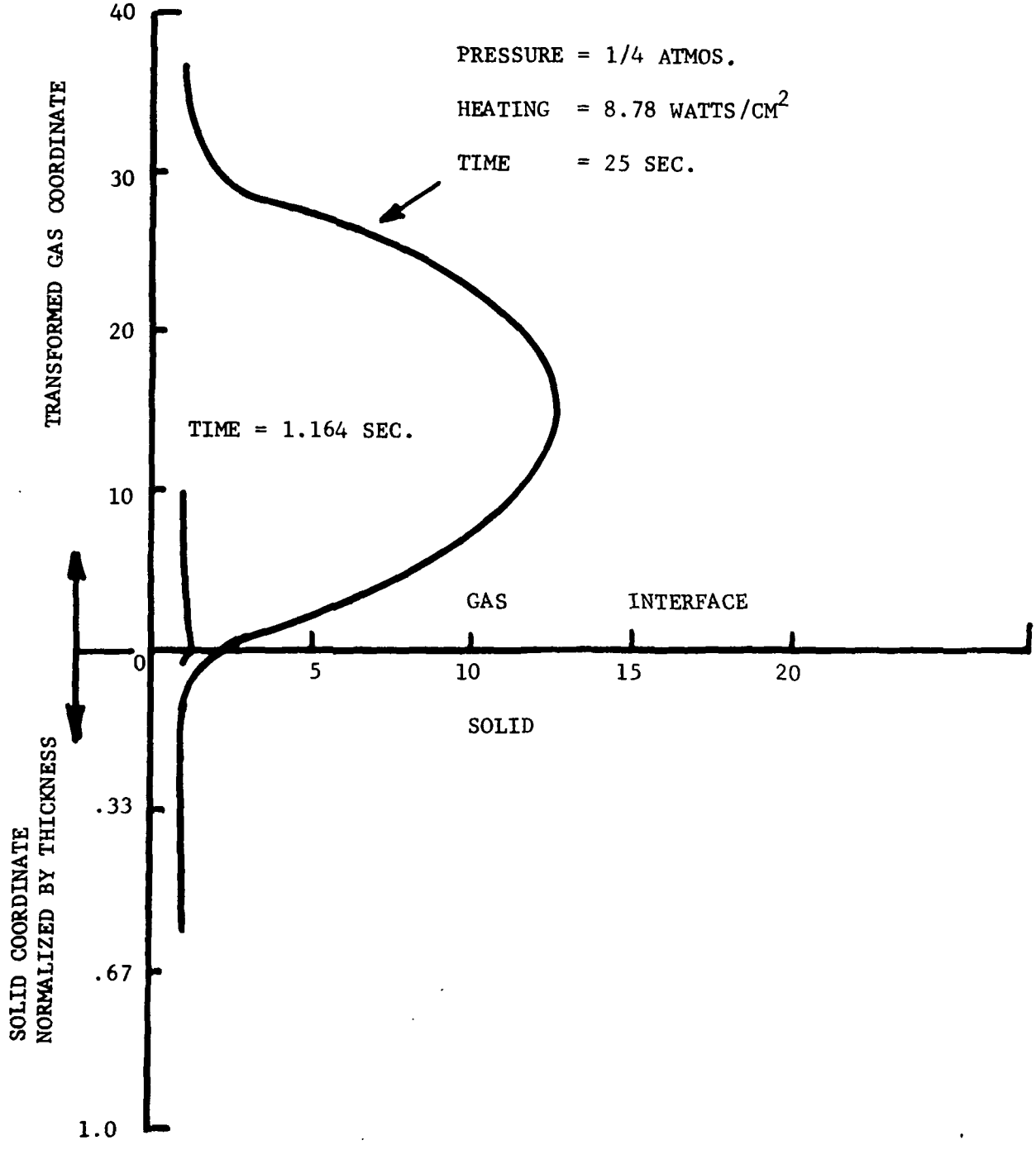

FIGURE 7.10 TEMPERATURE PROFILE DEVELOPMENT WITH TIME

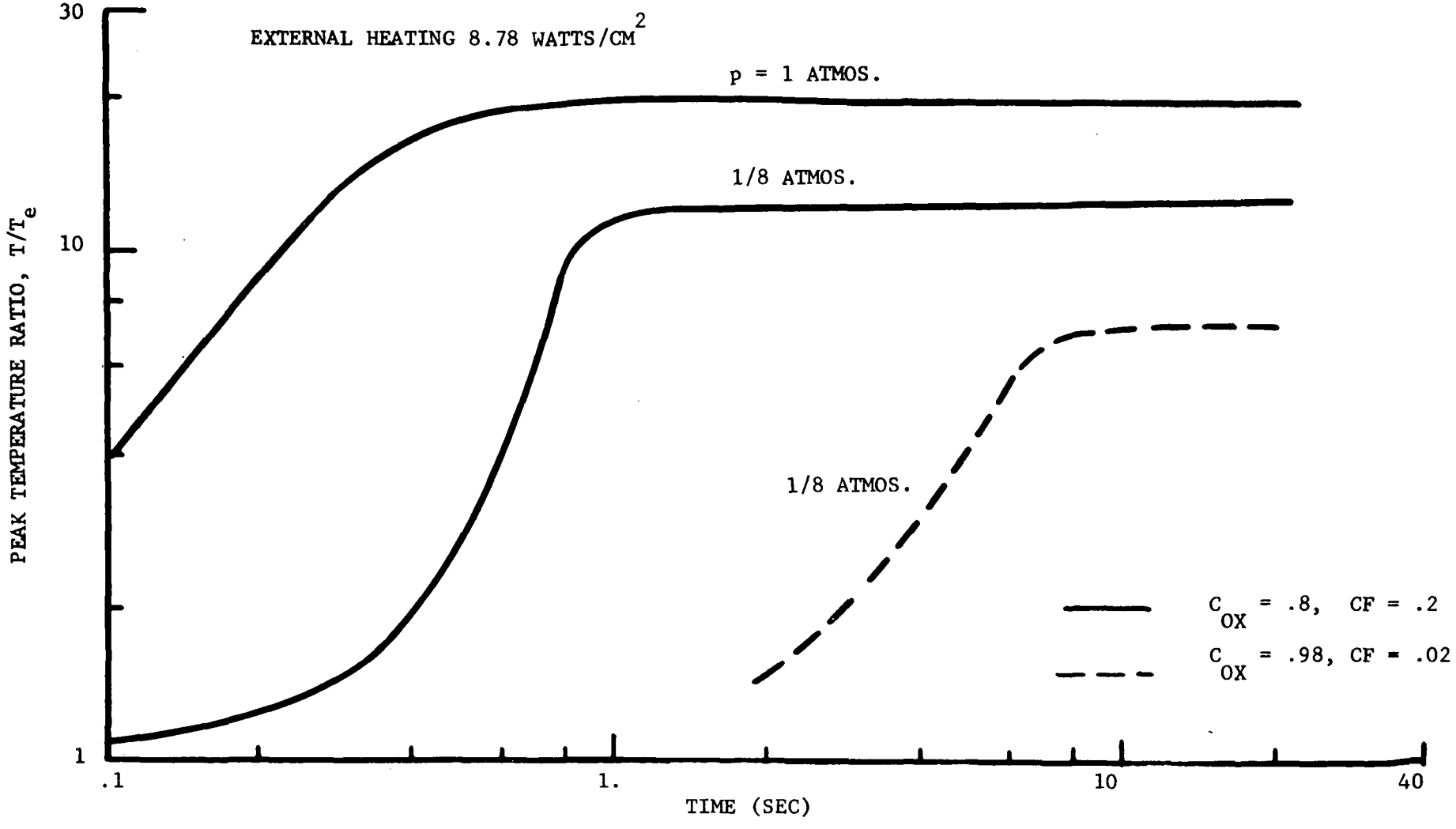

FIGURE 7.11 PEAK TEMPERATURE DEVELOPMENT WITH TIME

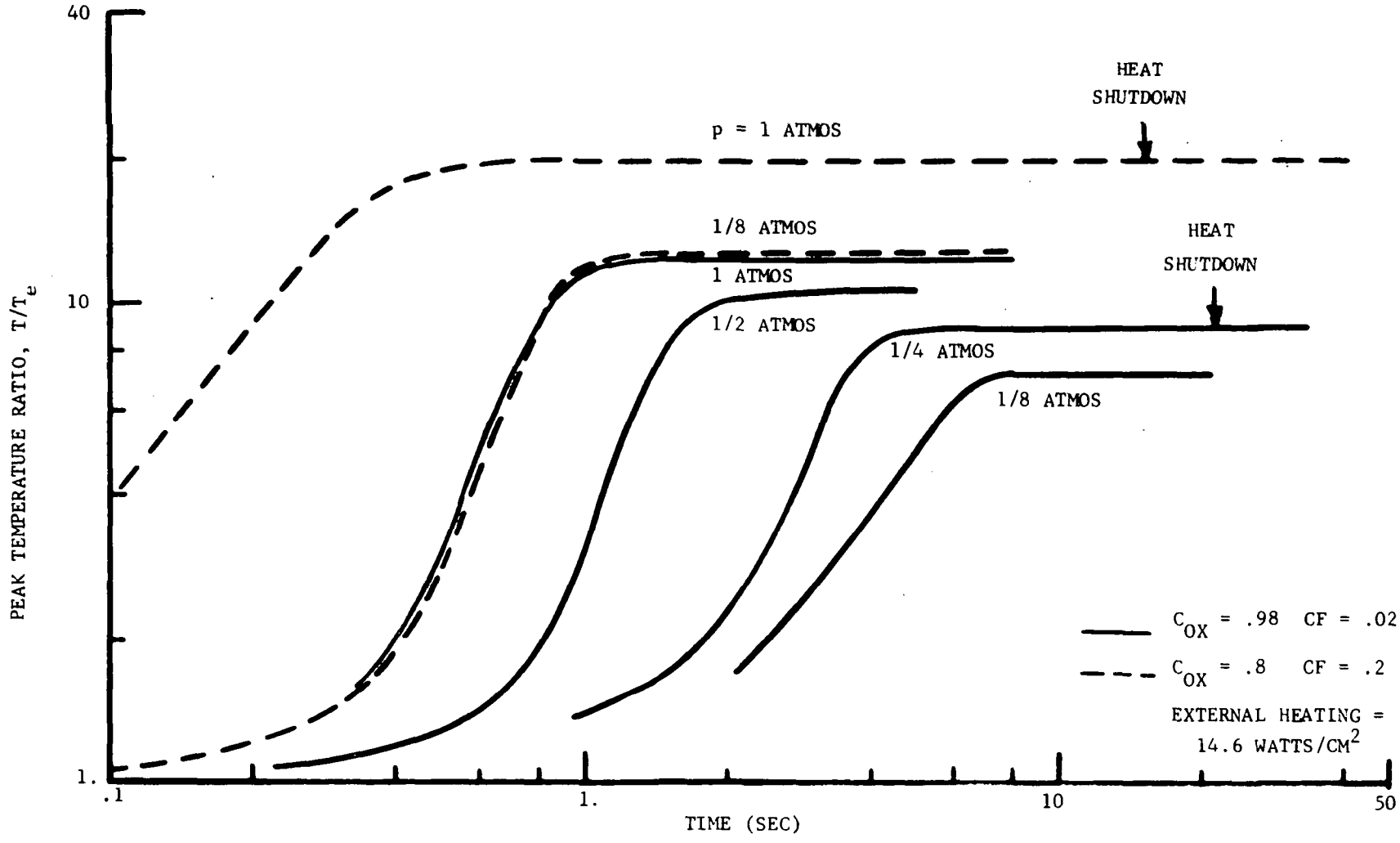

FIGURE 7.12 PEAK TEMPERATURE DEVELOPMENT WITH TIME

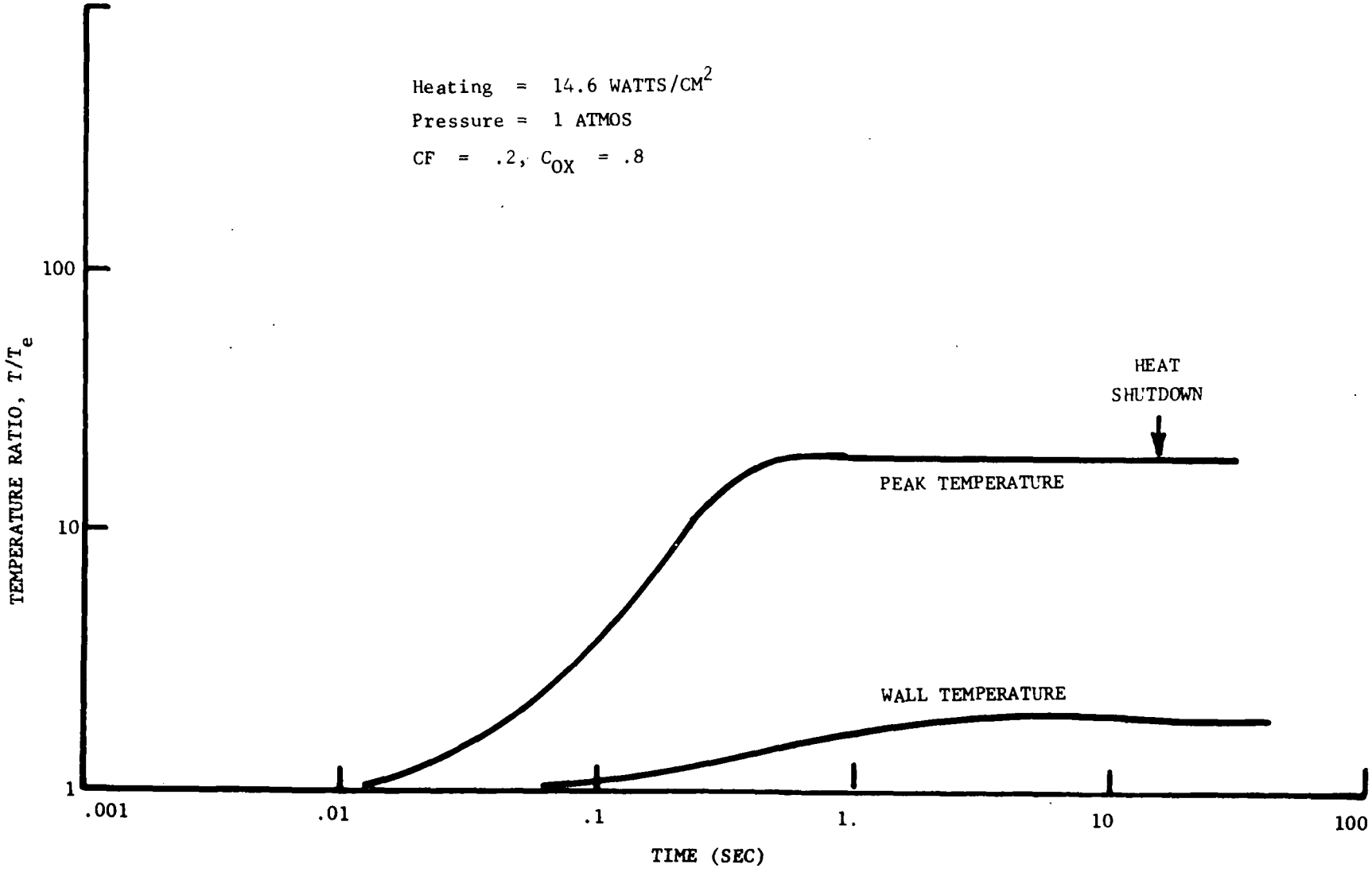

FIGURE 7.13 PEAK TEMPERATURE AND WALL TEMPERATURE APPROACH TO SUSTAINED BURNING

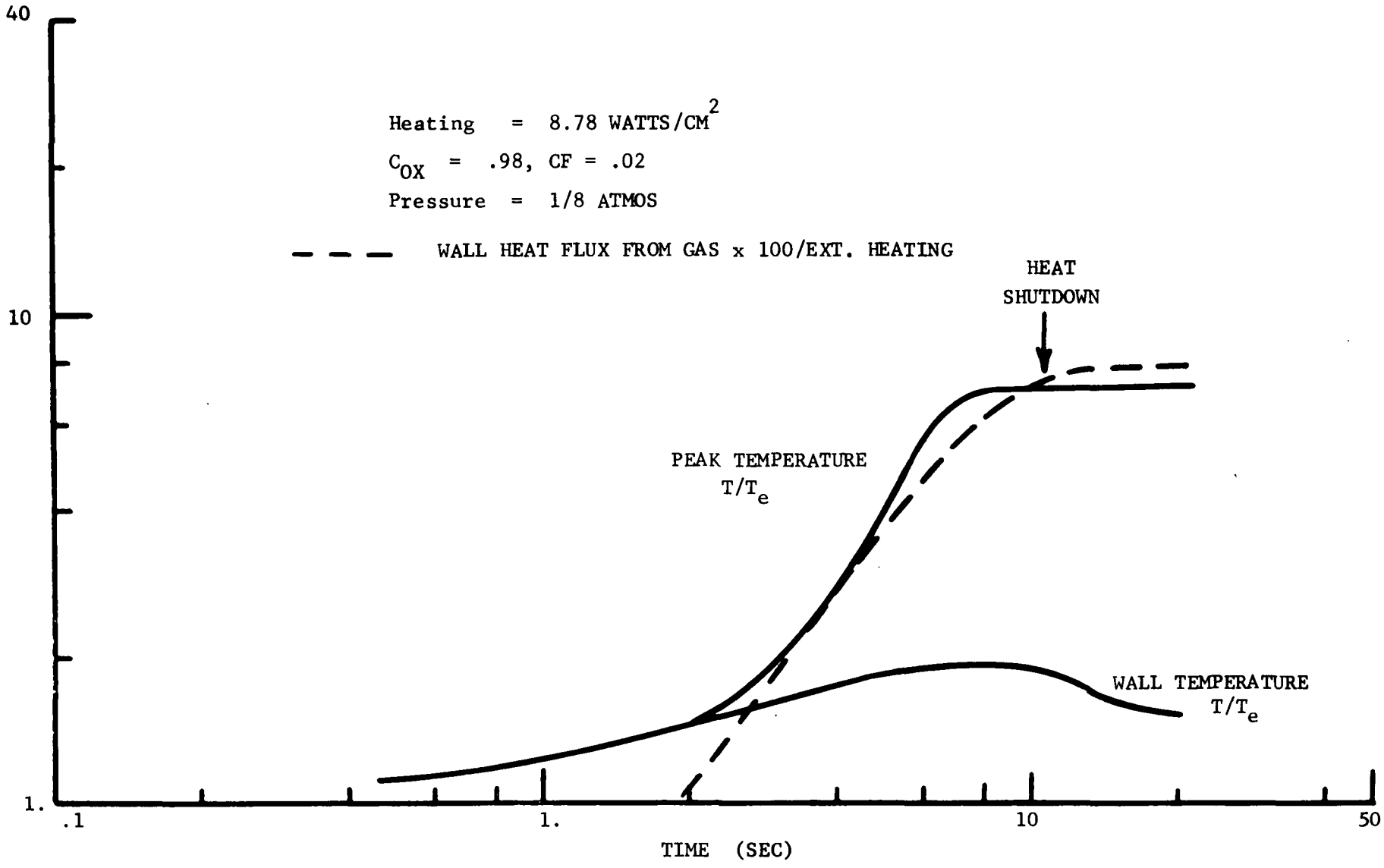

FIGURE 7.14 HEAT FLUX DUE TO CHEMICAL ENERGY RELEASE

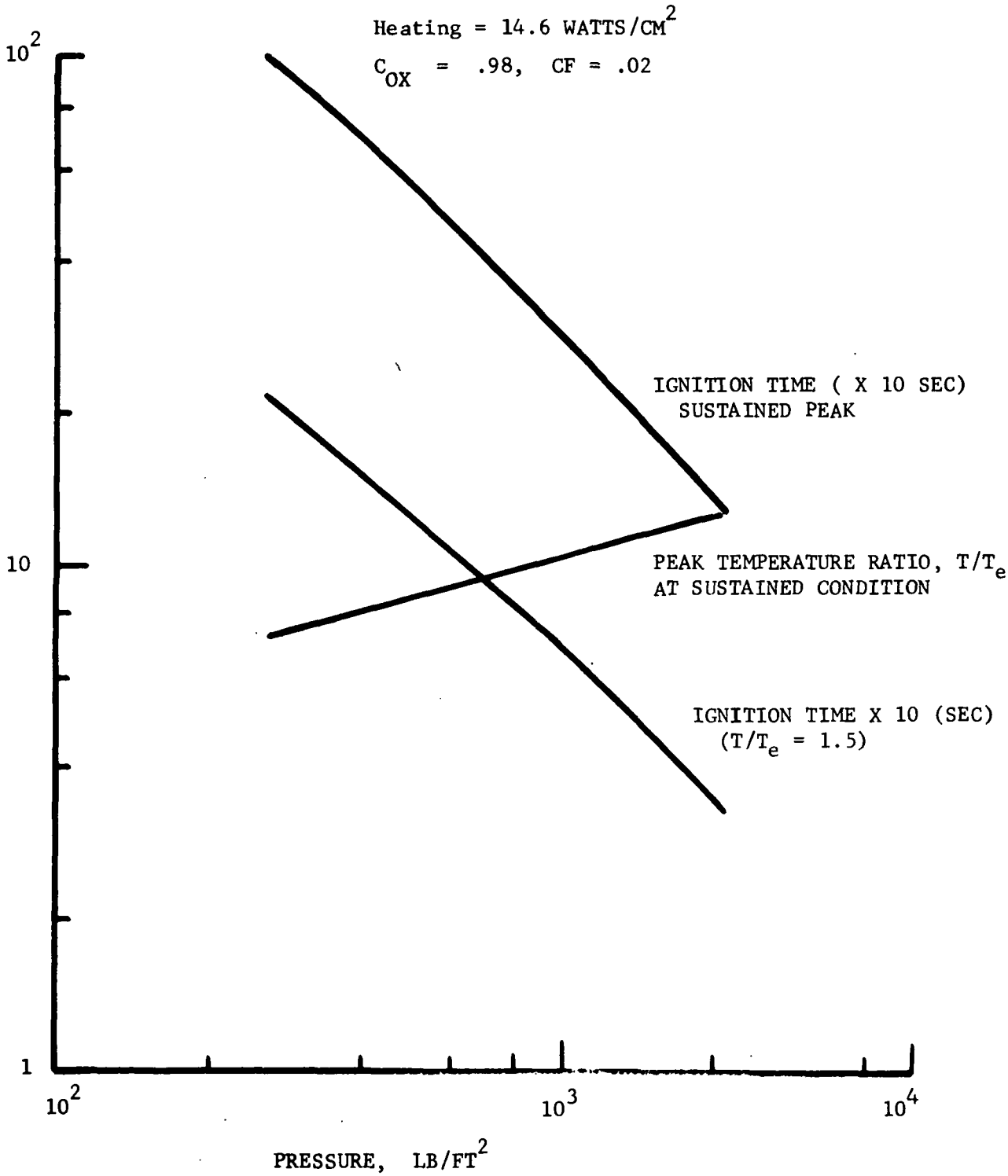

FIGURE 7.15 PRESSURE EFFECT ON IGNITION TIME AND PEAK TEMPERATURE

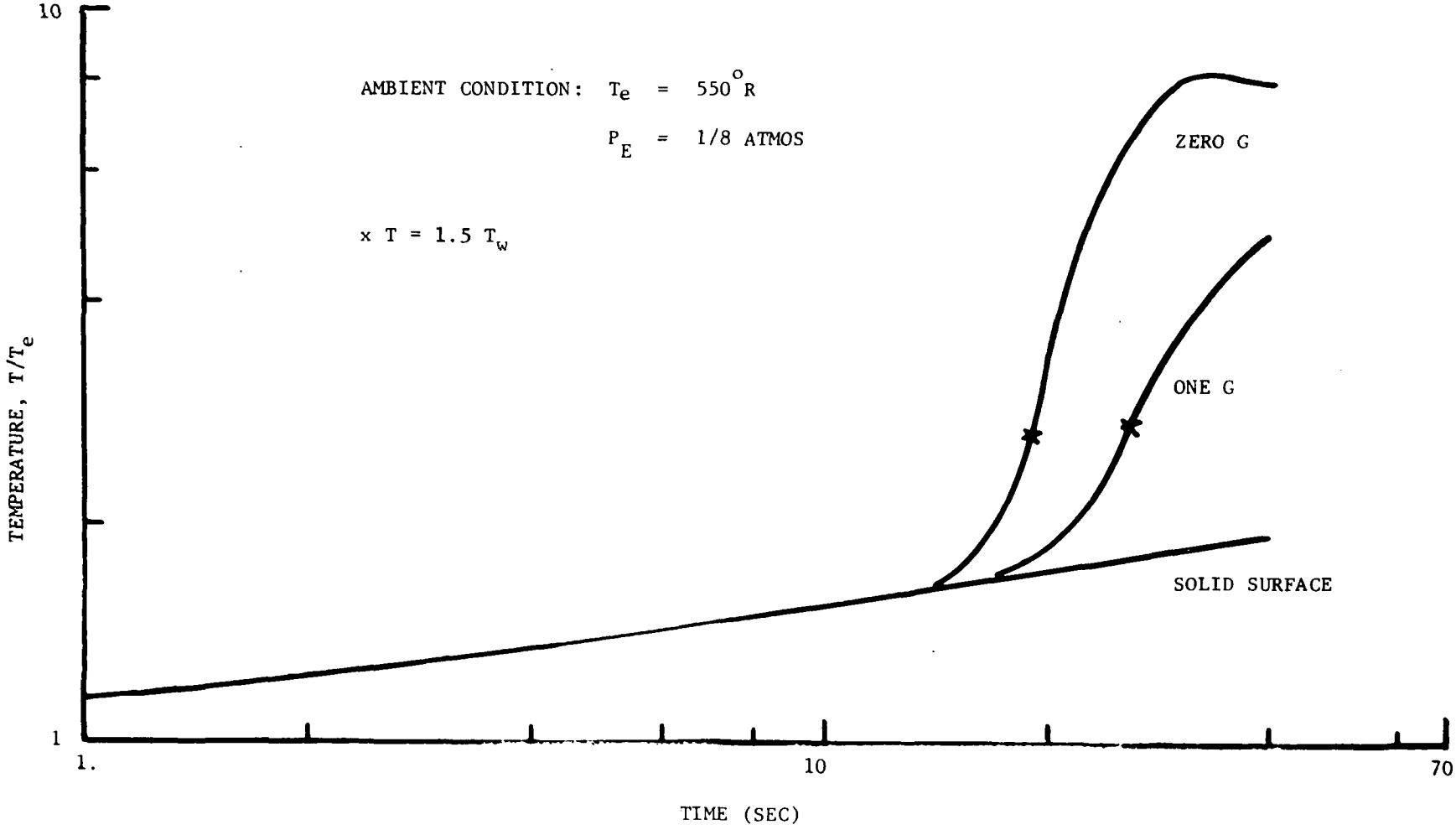

FIGURE 8.1 WALL AND PEAK TEMPERATURE DEVELOPMENT WITH TIME

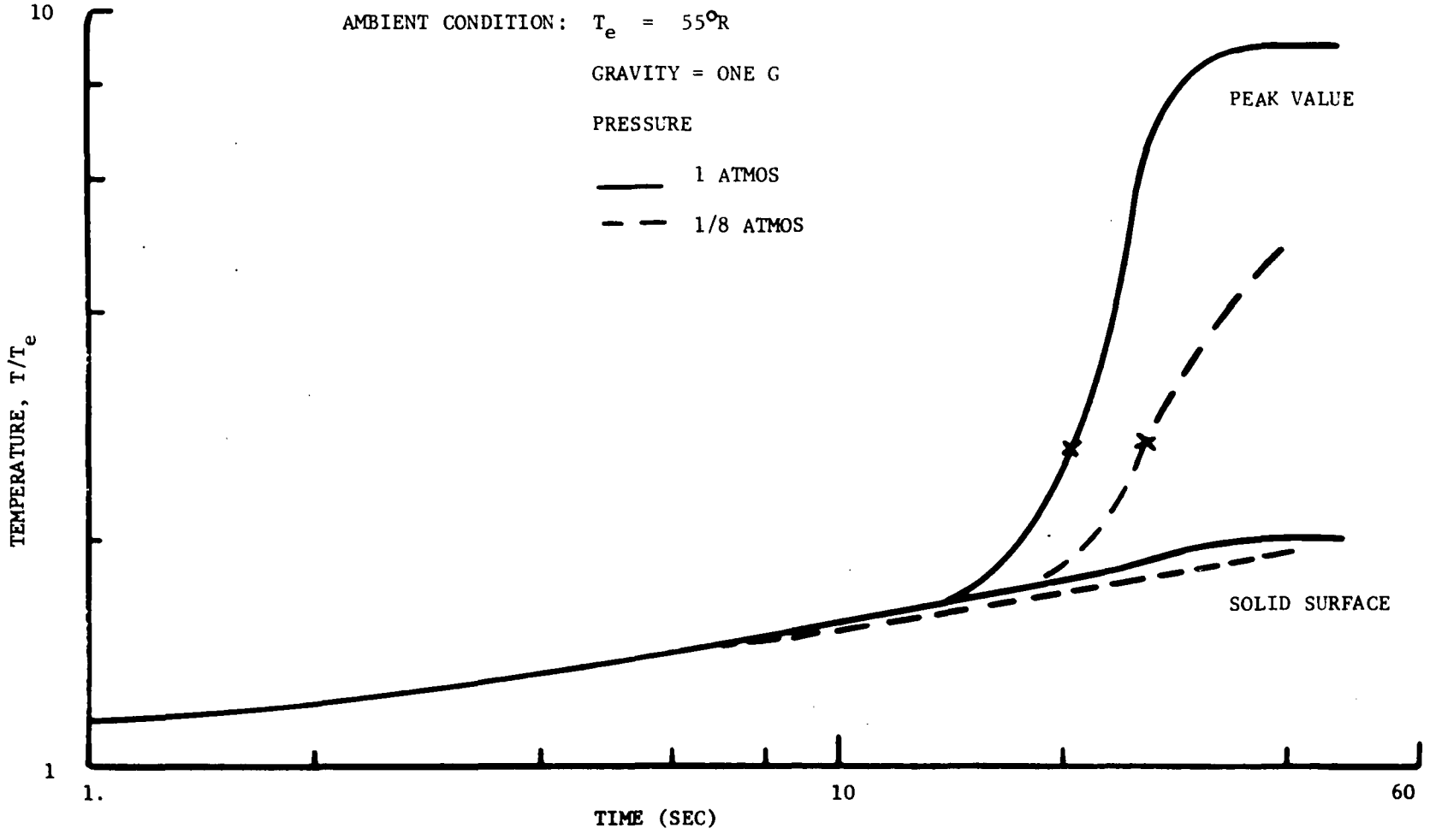

FIGURE 8.2 WALL AND PEAK TEMPERATURE DEVELOPMENT WITH TIME

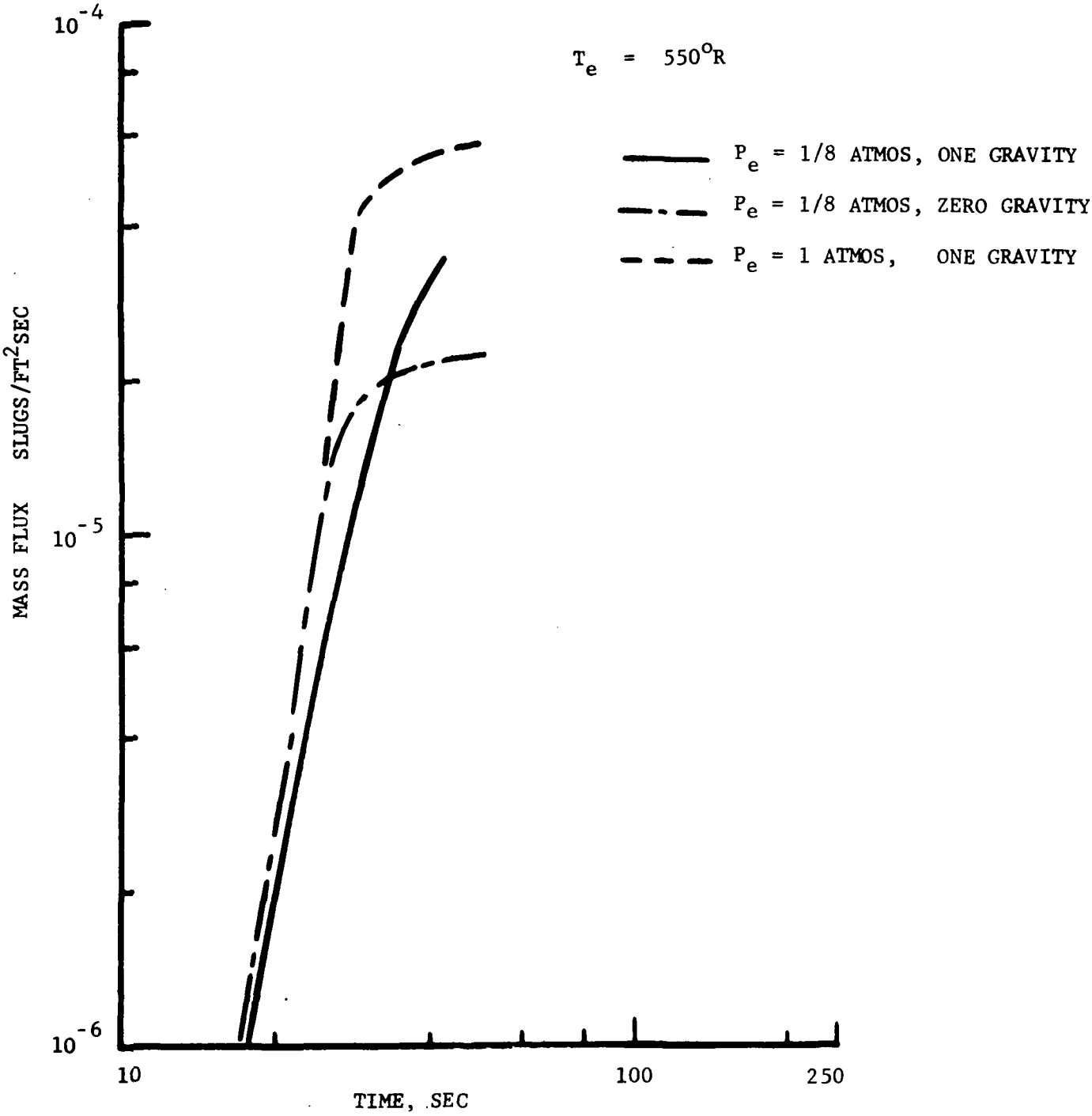

FIGURE 8.3 MASS FLUX OF SOLID INJECTED INTO GAS BY DECOMPOSITION

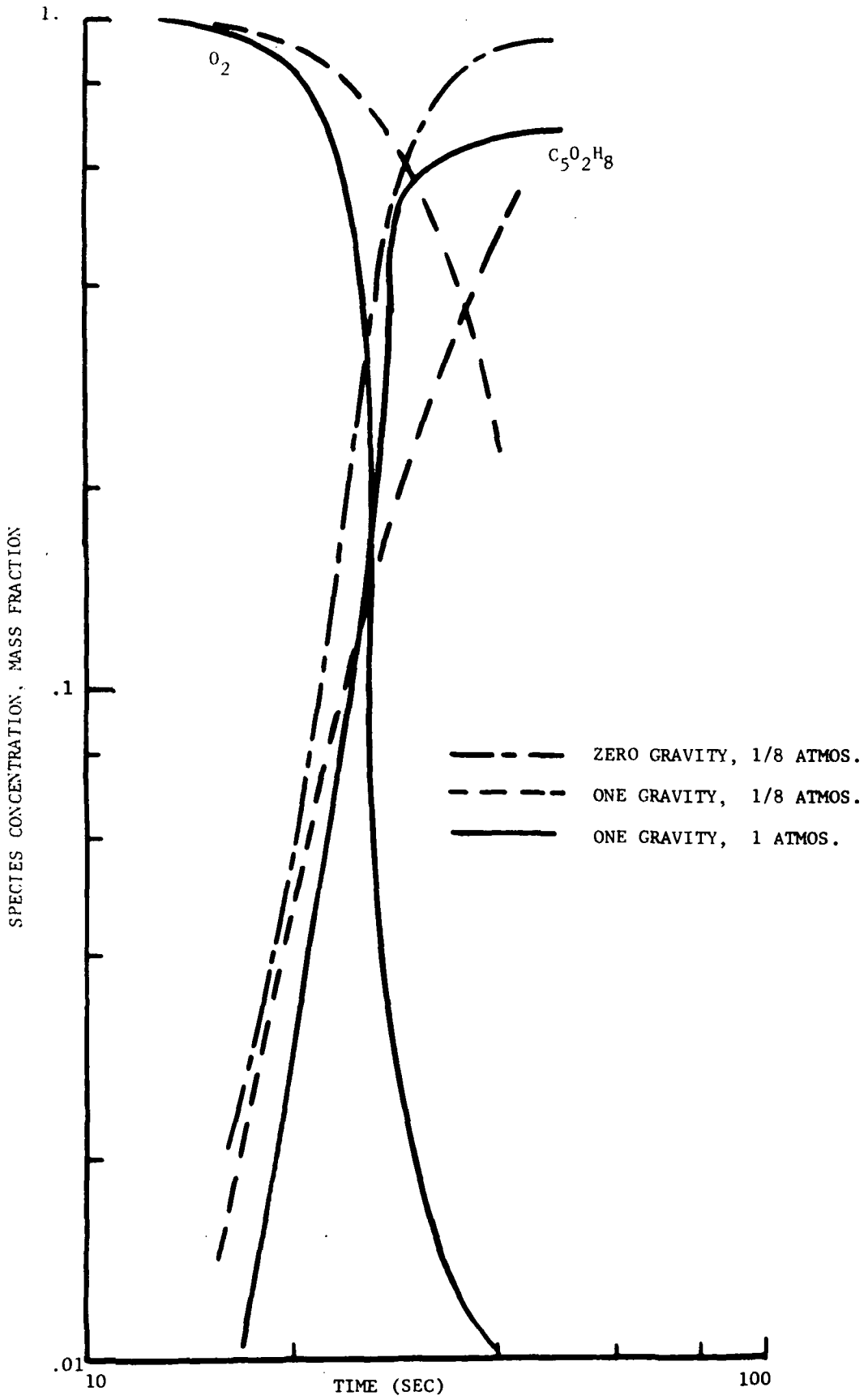

FIGURE 8.4 SURFACE VALUE OF SPECIES CONCENTRATION, MASS FRACTION

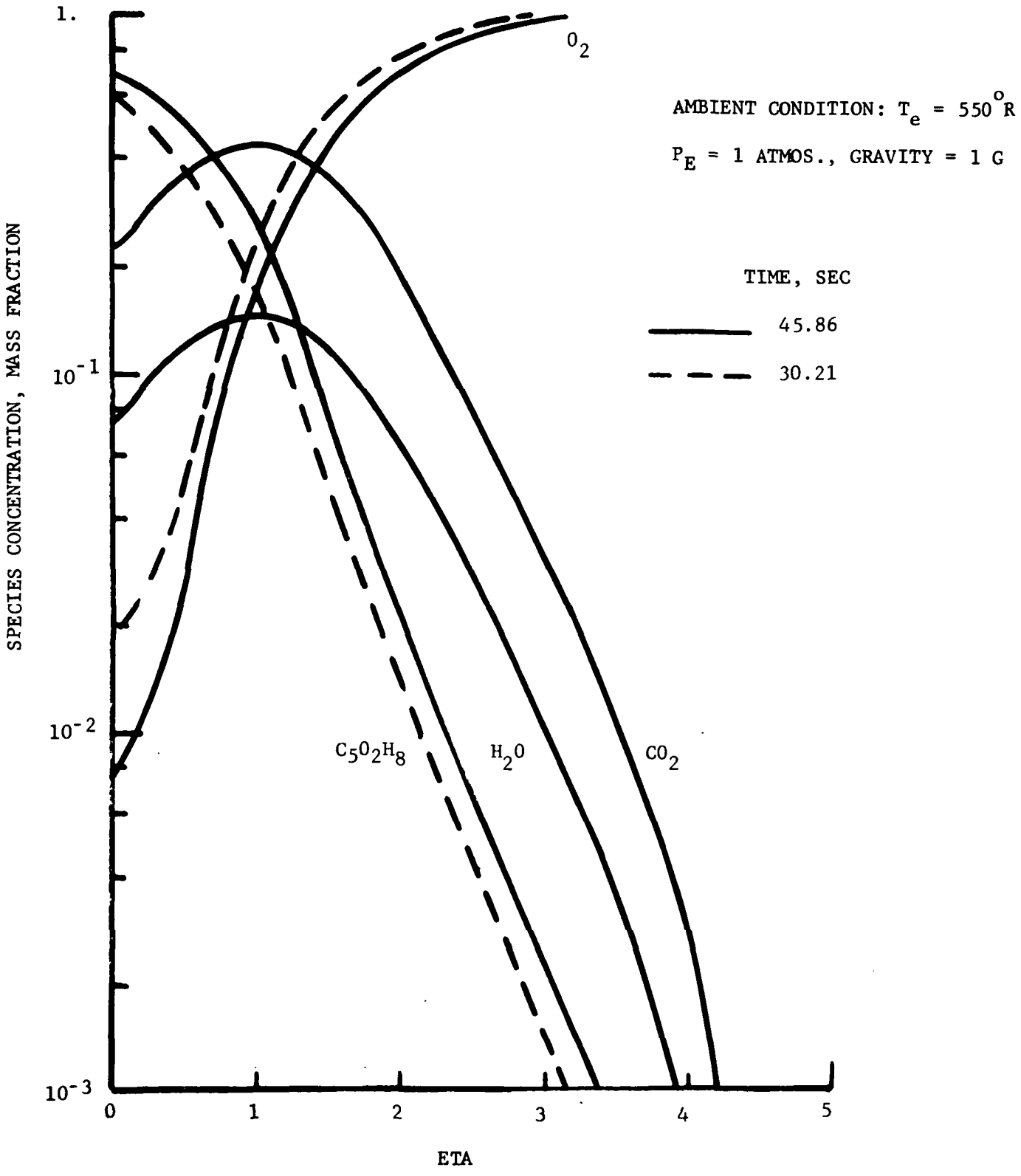

FIGURE 8.5 SPECIES CONCENTRATION DISTRIBUTIONS ACROSS GAS LAYER

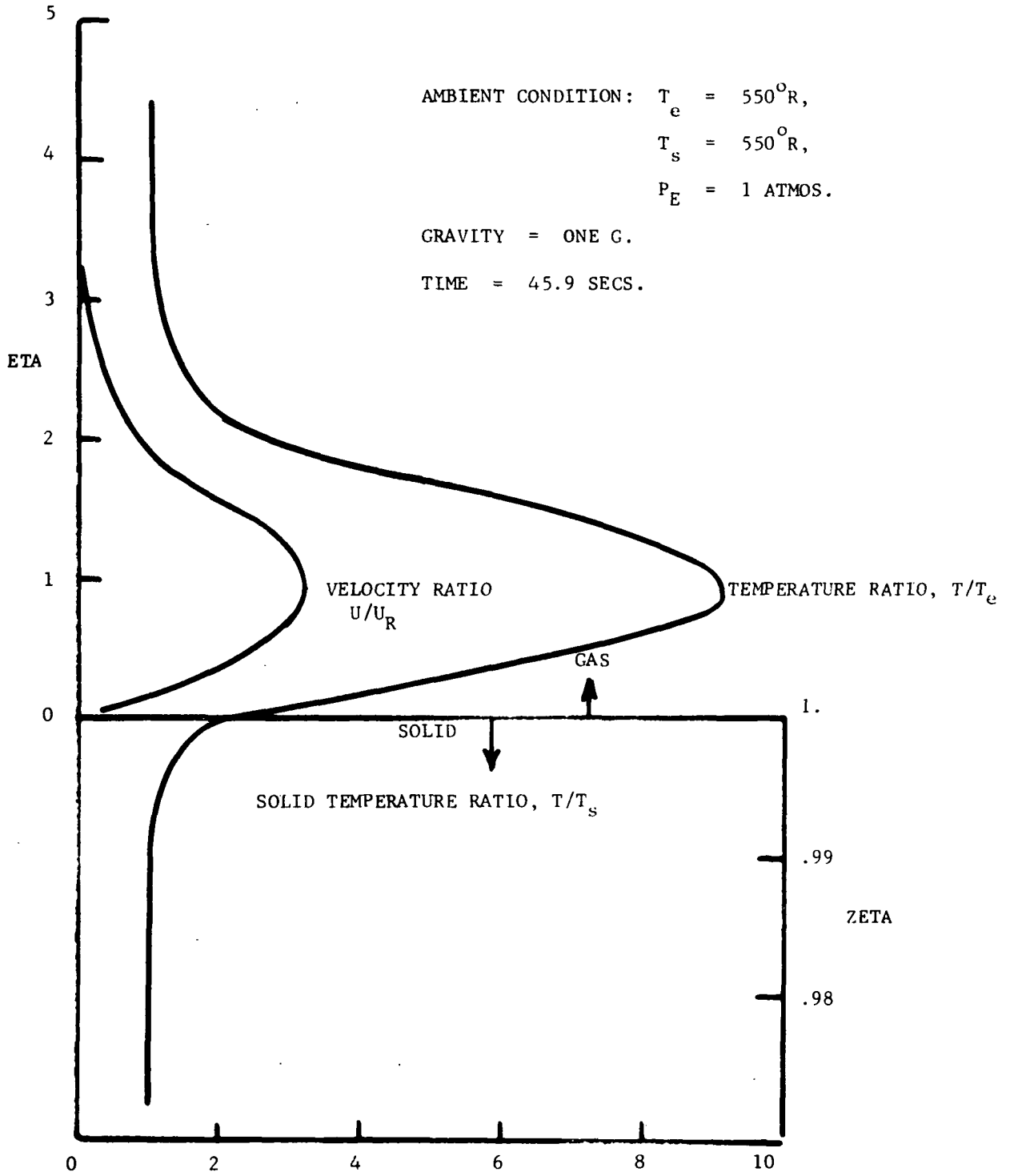

FIGURE 8.6 TEMPERATURE AND FREE CONVECTION VELOCITY DISTRIBUTIONS IN GAS-SOLID SYSTEM

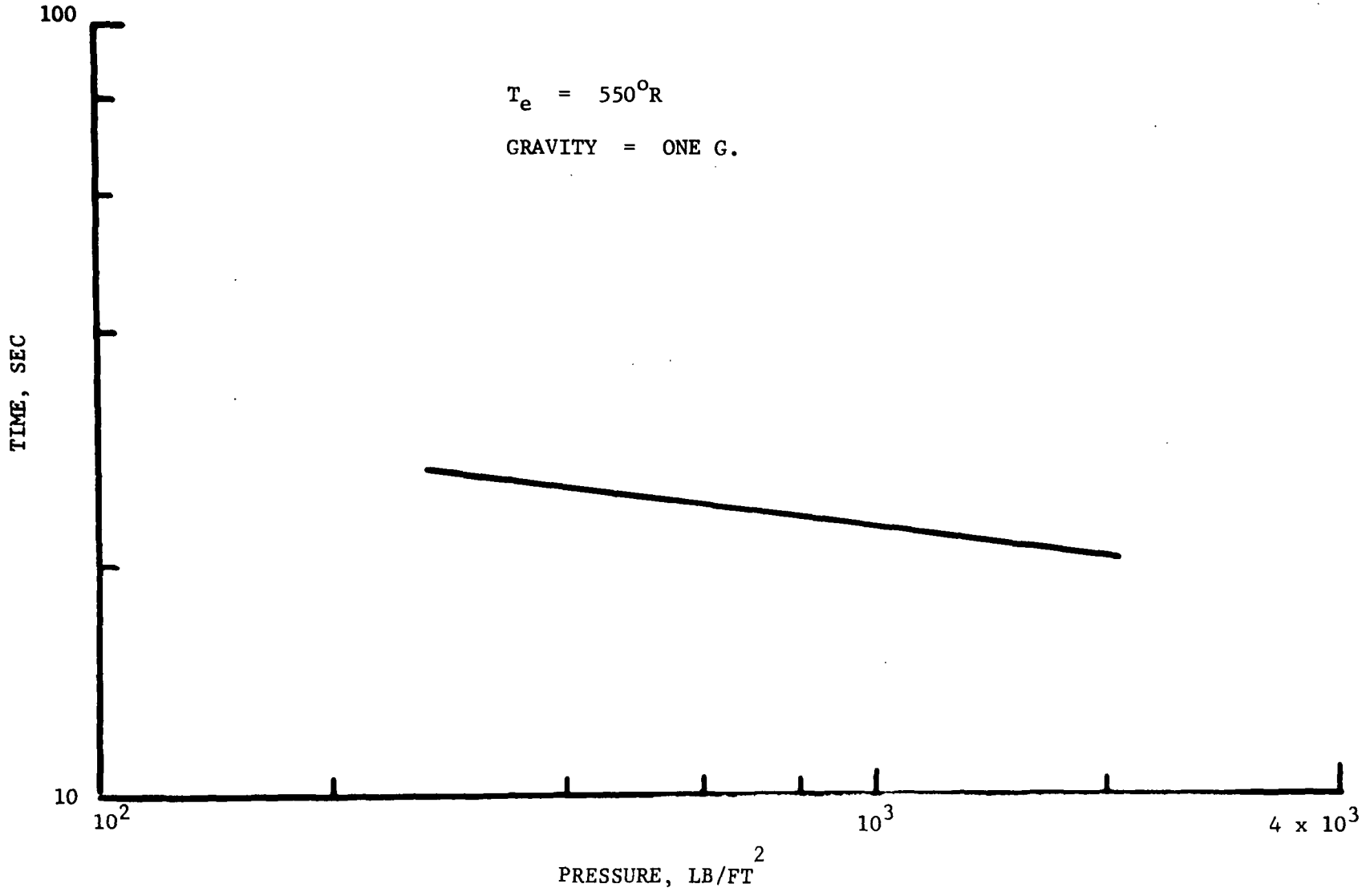

FIGURE 8.7 IGNITION TIME VARIATION WITH PRESSURE

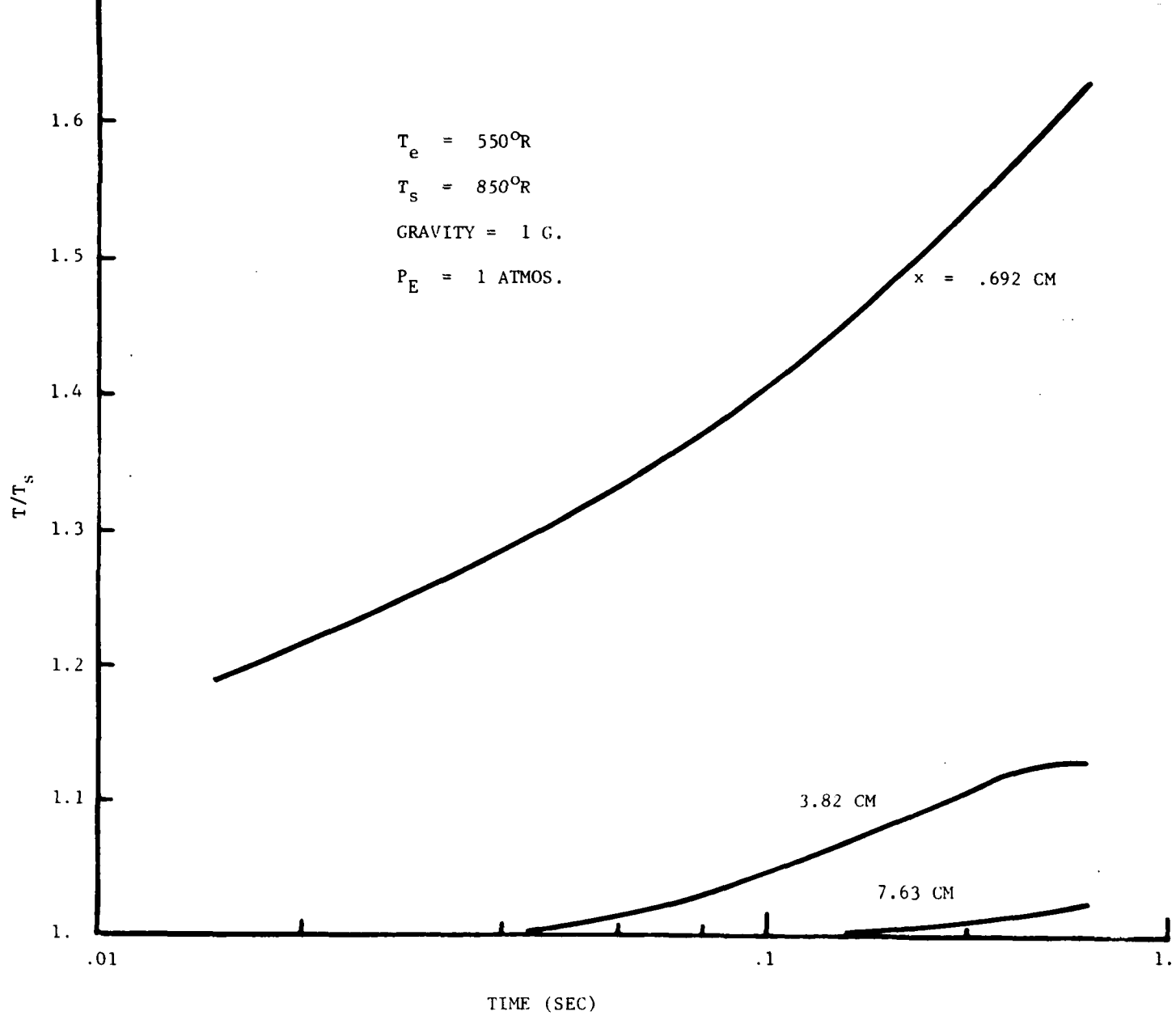

FIGURE 8.8 SURFACE TEMPERATURE VARIATION WITH TIME AT GIVEN LOCATION ON THE SURFACE IN OXYGEN ATMOSPHERE

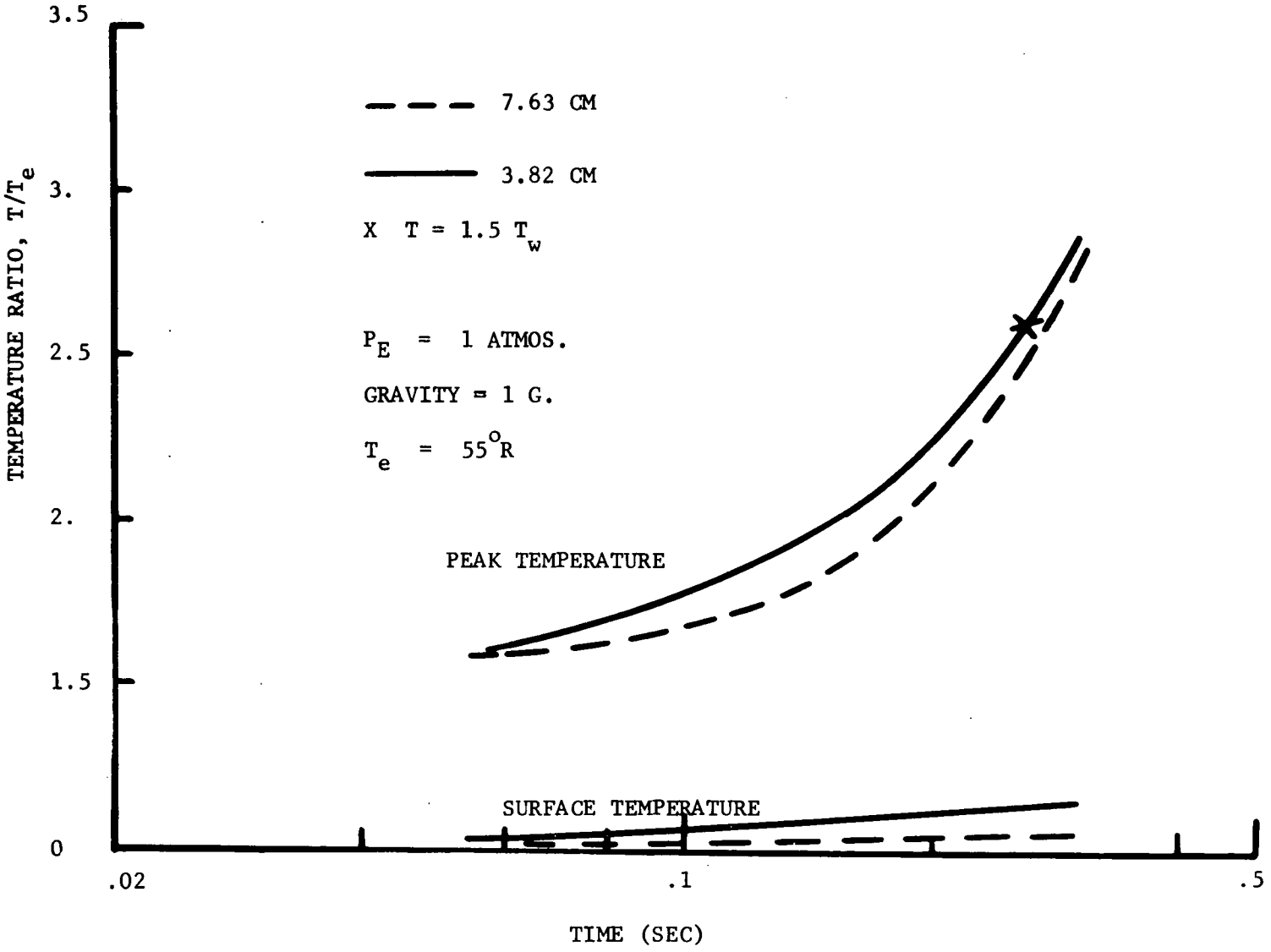

FIGURE 8.9 PEAK TEMPERATURE AND SURFACE TEMPERATURE AT TWO LOCATIONS OF MATERIAL

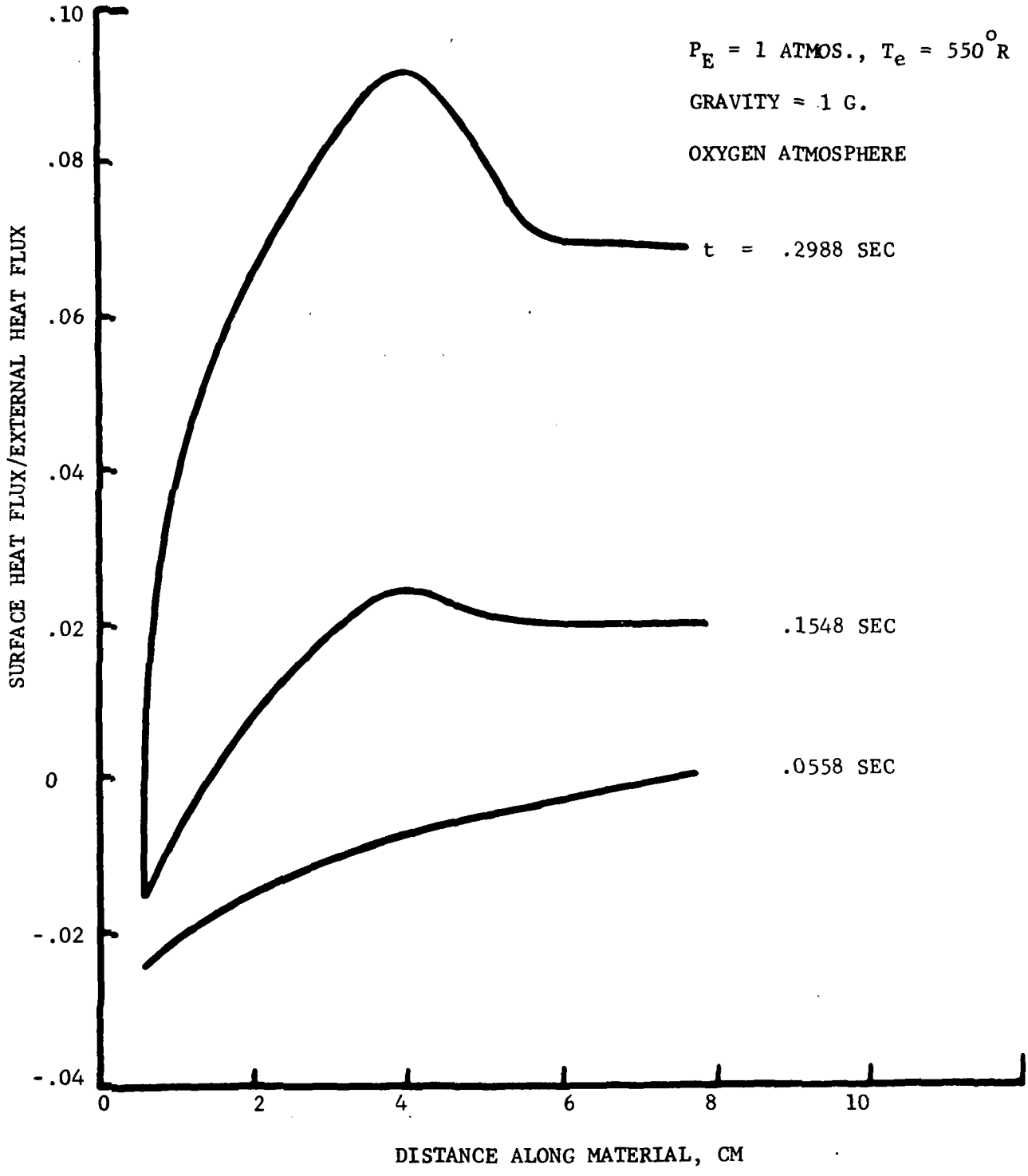

FIGURE 8.10 RATIO OF CONVECTIVE HEAT TRANSFER TO IMPOSED HEAT FLUX

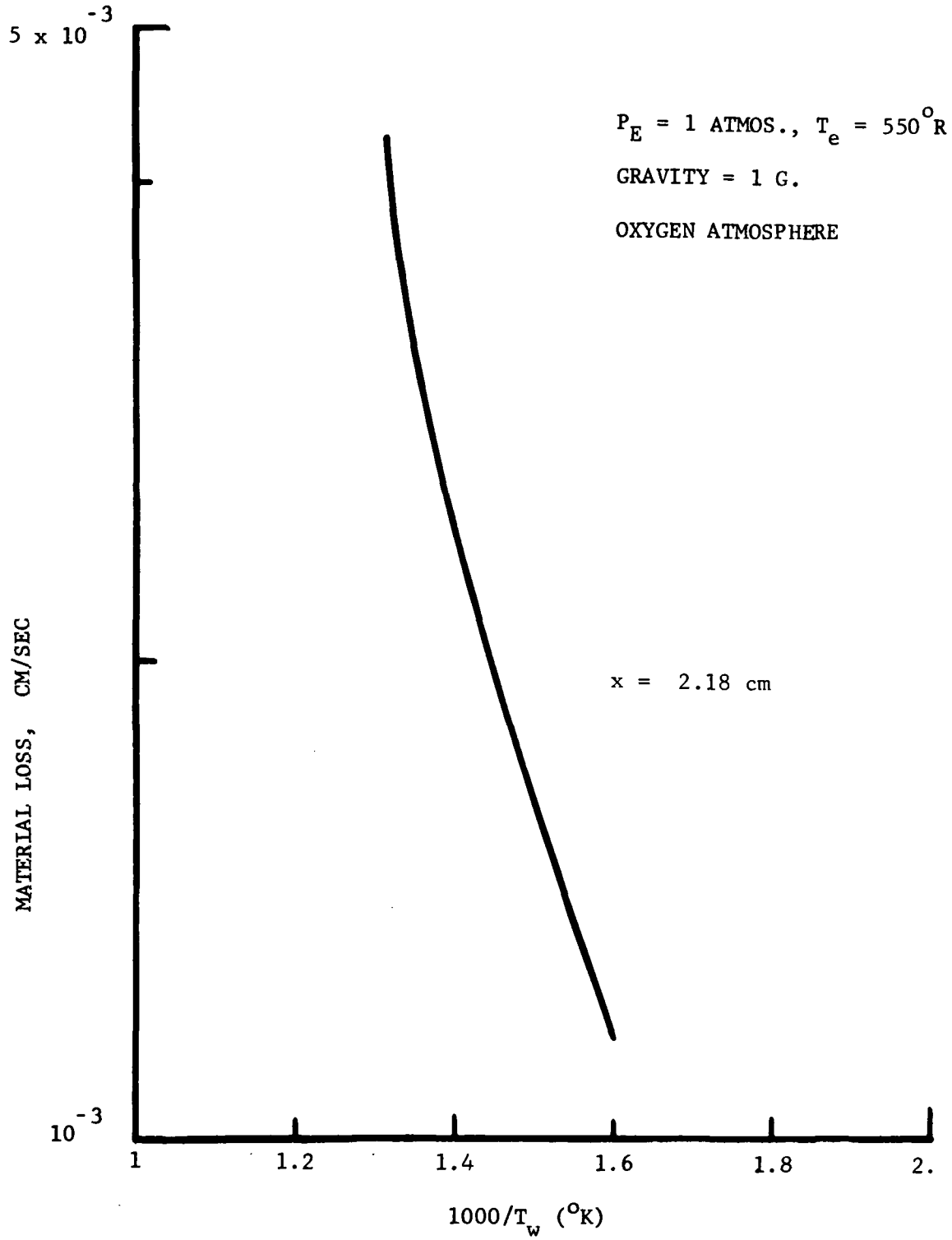

FIGURE 8.11 MATERIAL LOSS AT ONE LOCATION - FUNCTION OF SURFACE TEMPERATURE

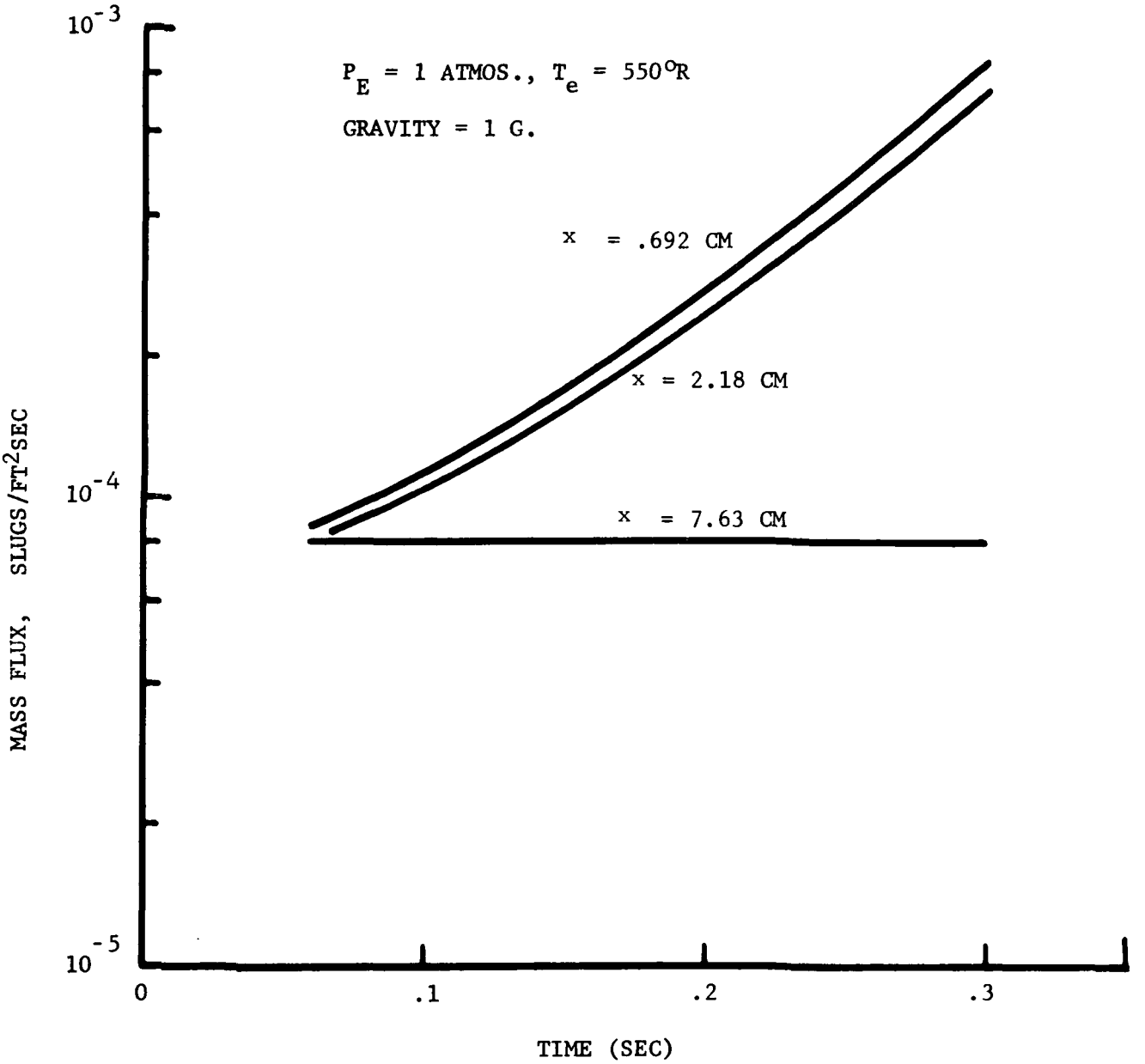

FIGURE 8.12 MASS FLUX OF MATERIAL LOSS

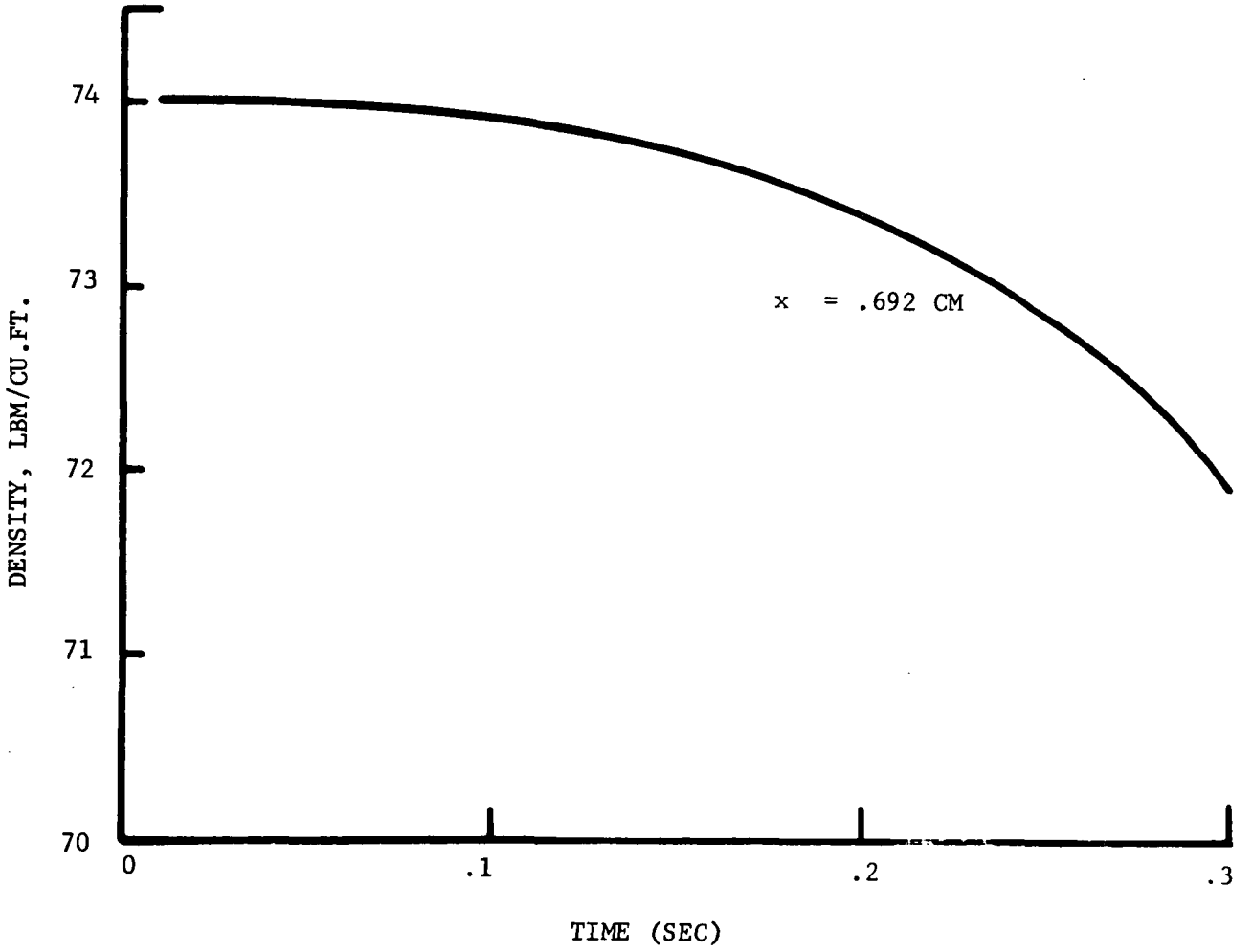

FIGURE 8.13 SURFACE VALUE OF SOLID DENSITY CHANGE DUE TO DEGRADATION

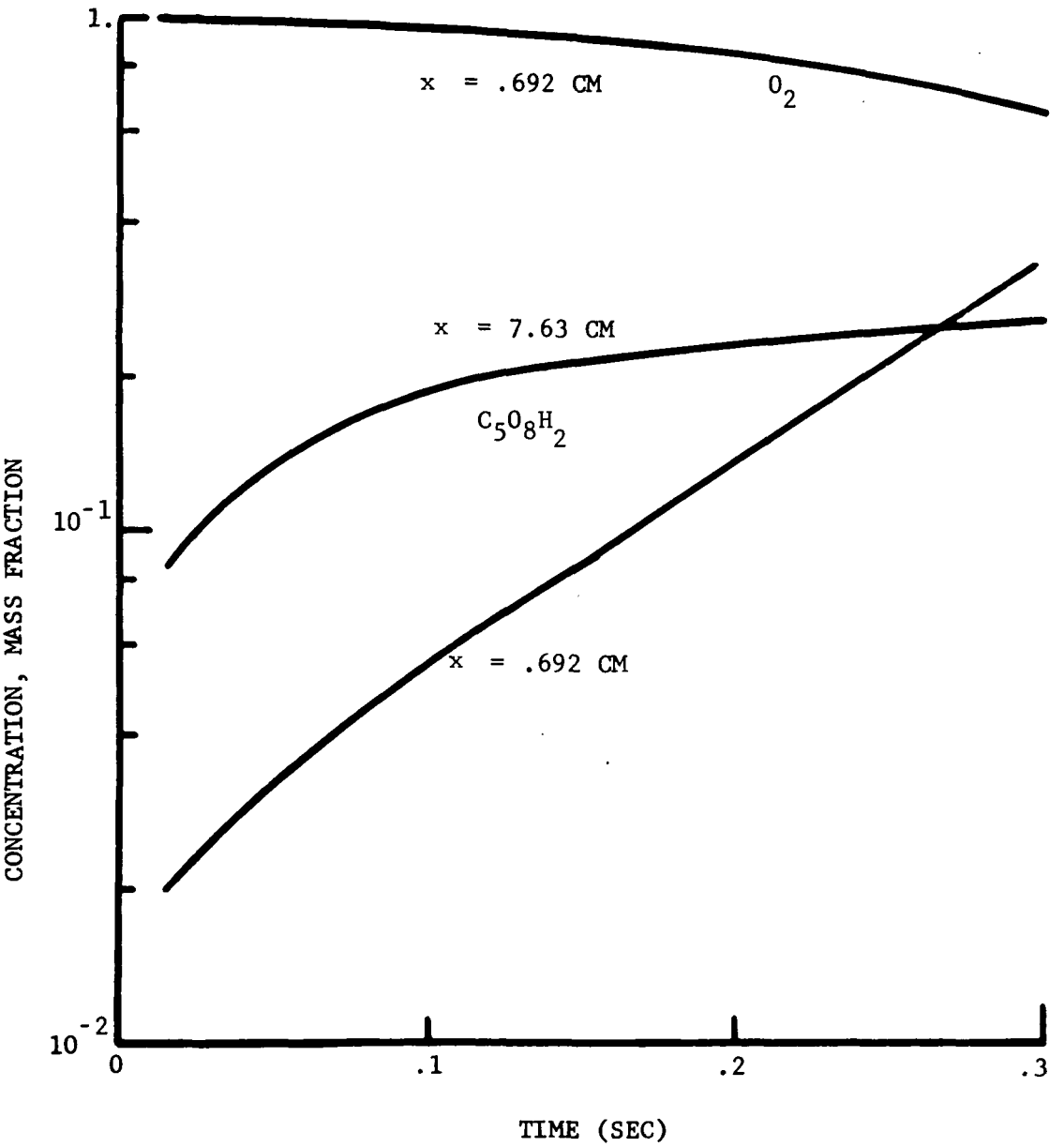

FIGURE 8.14 SURFACE SPECIES CONCENTRATION VARIATION WITH TIME ALONG MATERIAL

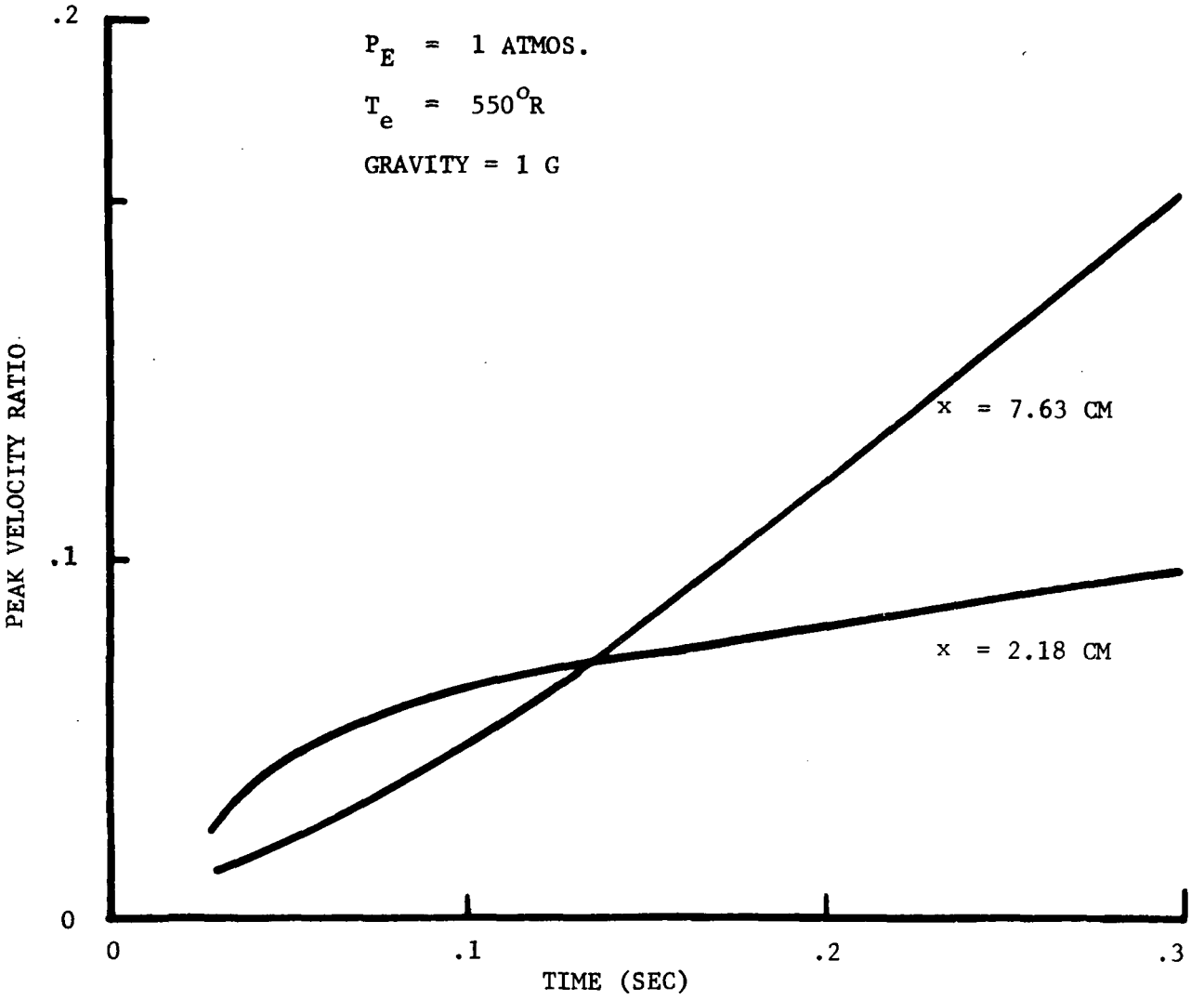

FIGURE 8.15 GROWTH OF PEAK CONVECTION VELOCITY RATIO IN GAS PHASE